A PALAEOMAGNETIC, GEOCHRONOLOGICAL AND PALAEOENVIRONMENTAL INVESTIGATION OF LATE AND POST GLACIAL MAAR LAKE SEDIMENTS FROM NW-EUROPE.

HAZEL A. BROWN

DOCTOR OF PHILOSOPHY
UNIVERSITY OF EDINBURGH
1991

DECLARATION

I hereby declare that the work presented in this thesis is my own, unless otherwise stated in the text. The thesis has been composed by myself.

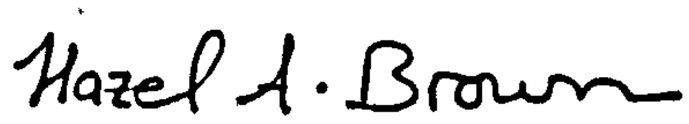

Hazel A. Brown

ABSTRACT

This is a multi-disciplinary study on six Quaternary lake sediment cores, up to 22m in length, obtained with a modified Livingston corer, from Meerfelder Maar (S.Eifel) Germany.

The main emphasis has been on the natural remanent magnetisation and establishing the identity and stability of the magnetic minerals. The carriers of the NRM are dominantly from the titanomagnetite series with a minor element of magnetisation carried by hematite. These minerals carry a stable primary remanence with a weak viscous component and, in some sections, remanence superimposed by the coring process. The NRM records geomagnetic secular variations in declination, inclination and intensity back to approximately 20,000 years BP.

The development of a thermoluminescence dating facility for lake sediments is described, including sample preparation procedures, TL measurements and dose rate measurements. The reliability of TL dating for this, as yet, unestablished application has been assessed by comparison with the excellent time control from varvometric dating (ZOLITSCHKA 1988).

Analysis of the stacked palaeomagnetic data includes the delineation of VGP paths and spectral analysis. Some similarities of the MFM data with the established Lac du Bouchet palaeomagnetic record are revealed; the palaeomagnetic inclination features ξπρσ τ are clearly seen at MFM and improvement to the LDB time transform has been made on the basis of correlation of these features between MFM and LDB.

The influence of organic carbon in degrading the Post Glacial palaeomagnetic signal has been investigated by consideration of a number of organic indicators including total organic carbon, pollen data (USINGER 1984) and organic carbon isotopic data. The carbon isotope data reveals major shifts in the $^{13}C/^{12}C$ ratio of organic matter deposited in MFM over the last 20,000 years which appear mainly dependent on changes in the composition of organic matter entering the maar from its catchment zone in response to changing climate over this period.

ACKNOWLEDGEMENTS

This project was funded by the Natural Environment Research Council. My thanks to Prof.K.M.Creer for initiating this research and guiding me through the intricacies of lake sediment palaeomagnetism, Dr.R.B.Galloway for supervision in the thermoluminescence work and to Dr.P.A.Eakin and Dr.A.E.Fallick for their help and inspiration with the carbon isotope work at SURRC East Kilbride.

Technical assistance in the departments of Geophysics, Physics, Geology and the computing service was much needed and gratefully received, thankyou to all the technical staff in these departments for invaluable and excellent support, especially A.Pike, A.Jackson and C.Grandison without whom work and my motorbike would have been considerably less smooth!

Thanks to all the staff and postgraduate students in the department of Geophysics for taking an interest in this work and providing much useful discussion and other input over the years.

My sanity remains intact due to the influence of the Edinburgh Triathletes and the gorgeous Calum.

This work has also been supported by the European Community Stimulation Activity Programme (STJ-128), "GEOMAAR 1".

CONTENTS

LIST OF ABBREVIATIONS

AF	alternating field
ARM	anhysteretic remanent magnetisation
BP	before present
Bq	becquerels
C_{org}	organic carbon
CAM	crassulacean acid metabolism
CCL	cryogenic consultants limited
cm	centimetres
CRM	chemical remanent magnetisation
^{o}C	degrees centigrade
D	dose rate
Dec	declination
DRM	detrital remanent magnetisation
ED	equivalent dose
FFT	fast Fourier transform
Fig	figure
g	grammes
Gy	grays
Inc	inclination
Int	intensity
IRM	isothermal remanent magnetisation
ka	thousand years before present
kg	kilogrammes
LBT	Laachersee Bimms Tuff
LDB	Lac du Bouchet
LDJ	Lac de Joux
m	metres
ma	million years before present
mA	milliamperes
MDF	median destructive field
MFM	Meerfelder Maar
mg	milligrammes
min	minutes

mm	millimetres
NRM	natural remanent magnetisation
PDB	Pee Dee belemnite
PDRM	post depositional remanent magnetisation
PSV	palaeosecular variation
SEM	scanning electron microscope
SIRM	saturated isothermal remanent magnetisation
SQUID	superconducting quantum interference device
SURRC	Scottish Universities Research and Reactor Centre
Susc	magnetic susceptibility
T	tesla
TL	thermoluminescence
TOC	total organic carbon
VGP	virtual geomagnetic pole
VRM	viscous remanent magnetisation
XRD	X-ray diffraction
XRF	X-ray fluorescence
yr	year

CHAPTER ONE.

INTRODUCTION: GEOMAGNETISM, PALAEOMAGNETIC SECULAR VARIATIONS AND MEERFELDER MAAR GEOLOGY.

1.1 INTRODUCTION

As an intrinsic natural global phenomenon, the Earth's magnetic field has been the subject of scientific research for several hundreds of years, commencing with DE MAGNETE by GILBERTE in 1600. Current representation is as a dipole tilted at 11.5^{o} to the rotational axis with a non-dipole component of continent size foci of maxima and minima superimposed (SMITH 1981).

The source of the dipole field is thought to be magnetohydrodynamic action in the outer core, with the non-dipole field originating from a thin sheet of electric current at the boundary between the highly conducting liquid outer core and the mantle (PEDDIE 1979). The driving mechanism producing the observed geomagnetic field is, as yet, poorly understood. The most plausible mechanism is provided by dynamo theory (MOFFATT 1978), although this has not been sufficiently defined to explain all known features of the geomagnetic field and no critical conjectures have been spawned from dynamo theory for verification. In fact, one of the most prominent features of the field, geomagnetic reversals, were not predicted by dynamo theory but were incorporated after becoming an accepted feature of geomagnetic behaviour.

This calls into question the robustness of the theory and indeed POPPER (1963) uses this type of criteria to demarcate between 'science and non-science', suggesting that scientific theories should not only explain all known observable phenomena but also expose themselves to refutation by predicting undiscovered features which could be used to test the theory. One of the most famous scientific observations this century was exactly such a test for Einstein's General Theory

(29th of May 1919 by Eddington). Einstein correctly predicted that the effect of the Sun's gravity on light from a star would make it appear in a different position from that which it was known to occupy (MAGEE 1982).

An important objective of detailed studies of past geomagnetic field variation is to reveal the nature and evolution of processes producing the field. The role of lake sediment palaeosecular variation investigations is to bridge the gap between the record of long-term variation (10^6 years) from the reversal stratigraphy (found in oceanic crust and also fragmentarily in the terrestrial record), and the record of short-term variation (10-100 years) provided by MAGSAT (GUBBINS 1989), observatory and historical records and archaeomagnetic data (BARRACLOUGH 1982). Lacustrine sediments have the capability to provide data covering the periods of the order of thousands of years that are a feature of the non-dipole field (BULLARD et al. 1950).

1.2 PALAEOSECULAR VARIATION FROM LAKE SEDIMENTS

Extending the palaeosecular variation (PSV) record over space and time has been the direction of much effort since the pioneering work on the Lake Windermere sediments of MACKERETH (1971). It has since been realised that PSV is not preserved faithfully in some lake sediments because it can be degraded by a variety of geomorphological, depositional and geochemical processes. Second generation palaeomagnetic studies (CREER 1985 for review) have seen refinement of coring techniques, sampling methodology and measurement techniques to provide more robust palaeomagnetic information.

Lac du Bouchet (LDB) ($45^oN,4^oE$) Velay, France, (FIG 1.1) has yielded the best results in terms of quality, timespan and consistency because the maar crater walls from which the bottom sediments are exclusively derived are composed of basalts and tuffs. Palaeomagnetic profiles correlate well within the lake and stacked records have been produced defining a tight master curve for western Europe,

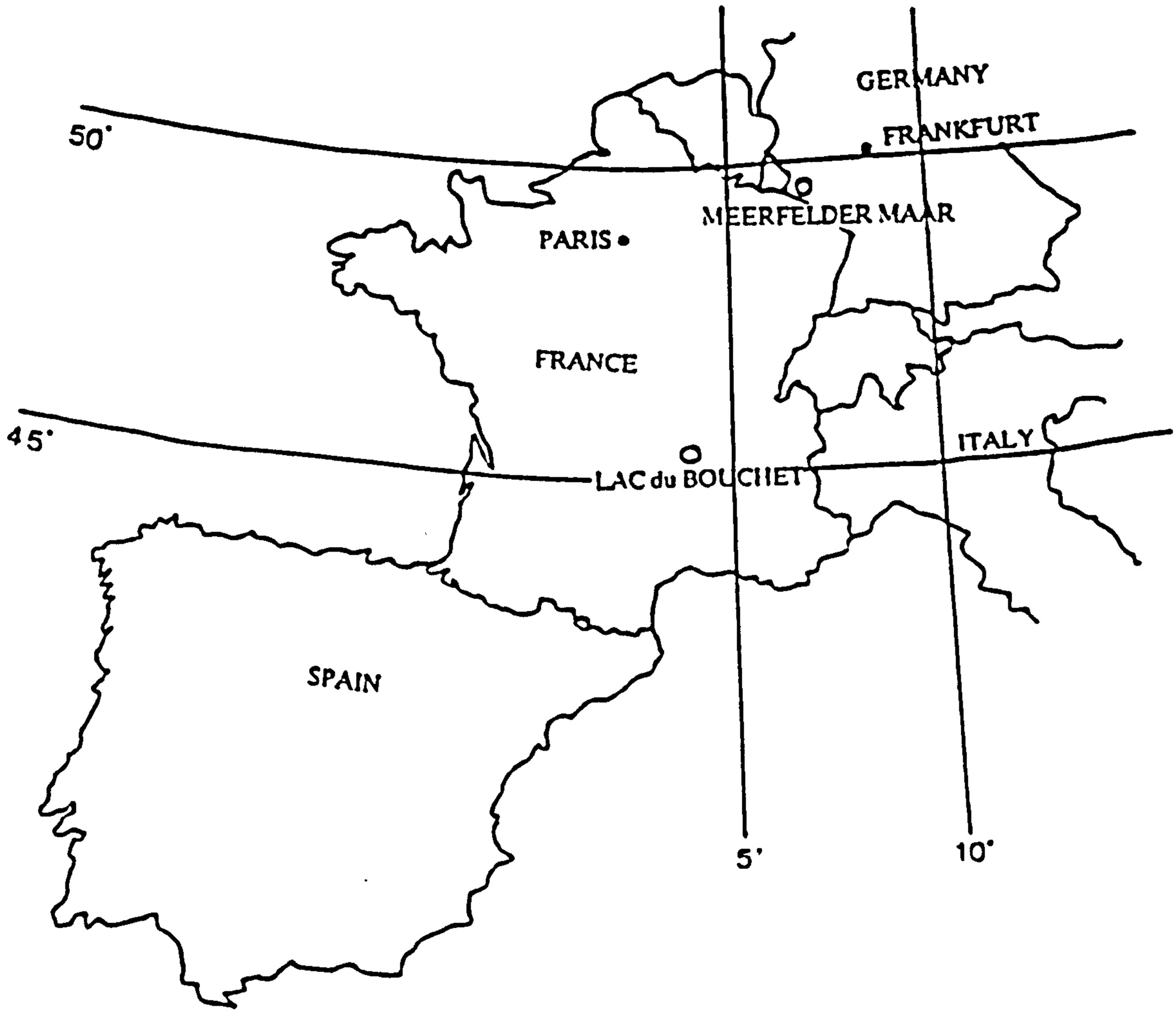

FIG 1.1 LOCATION MAP SHOWING POSITION OF MEERFELDER MAAR AND LAC du BOUCHET IN WESTERN EUROPE.

The type curve is shown in
(FIG 1.2). The present record extends back 120,000 years (THOUVENY et al. 1990).

1.3 SCOPE OF THESIS

To accept this palaeomagnetic variation as an expression of the past geomagnetic field, not an artefact of environmental conditions as has been suggested by, for example, LATHAM (1988), a correlation with other sites must be confirmed.

Meerfelder Maar (MFM) (49^{o}N,7^{o}E) South Eifel, Germany (FIG 1.1), provides a suitable locality where evaluation of the degree of possible correlation between the two sites might indicate the validity of accepting the LDB master curve as a geomagnetic secular variation record.

In addition to tackling a purely palaeomagnetic problem, this thesis has attempted to resolve one of the major obstacles to producing useful geomagnetic secular variation records, that of dating the down-core palaeomagnetic logs to enable time-series analysis of the data. The relatively new technique of thermoluminescence (TL) dating has been developed for application to the maar lake sediments. This work is related in chapters four and five.

Maar lakes also have great potential for recording geochemical information; so providing a valuable continental equivalent to compliment the marine record. Maar lakes provide windows which cover episodes such as the last major climatic change, that of the ice retreat from western Europe. This may have relevance to our understanding of possible anthropogenically-induced climatic variation taking place at present by the study of these similar earlier events of climatic warming and cooling. In chapter seven an isotope geochemistry investigation is presented; chiefly undertaken as a pilot study to distinguish between sources and types of organic carbon in Meerfelder Maar: these potentially provide an insight into part of the carbon cycle over a climatically critical period.

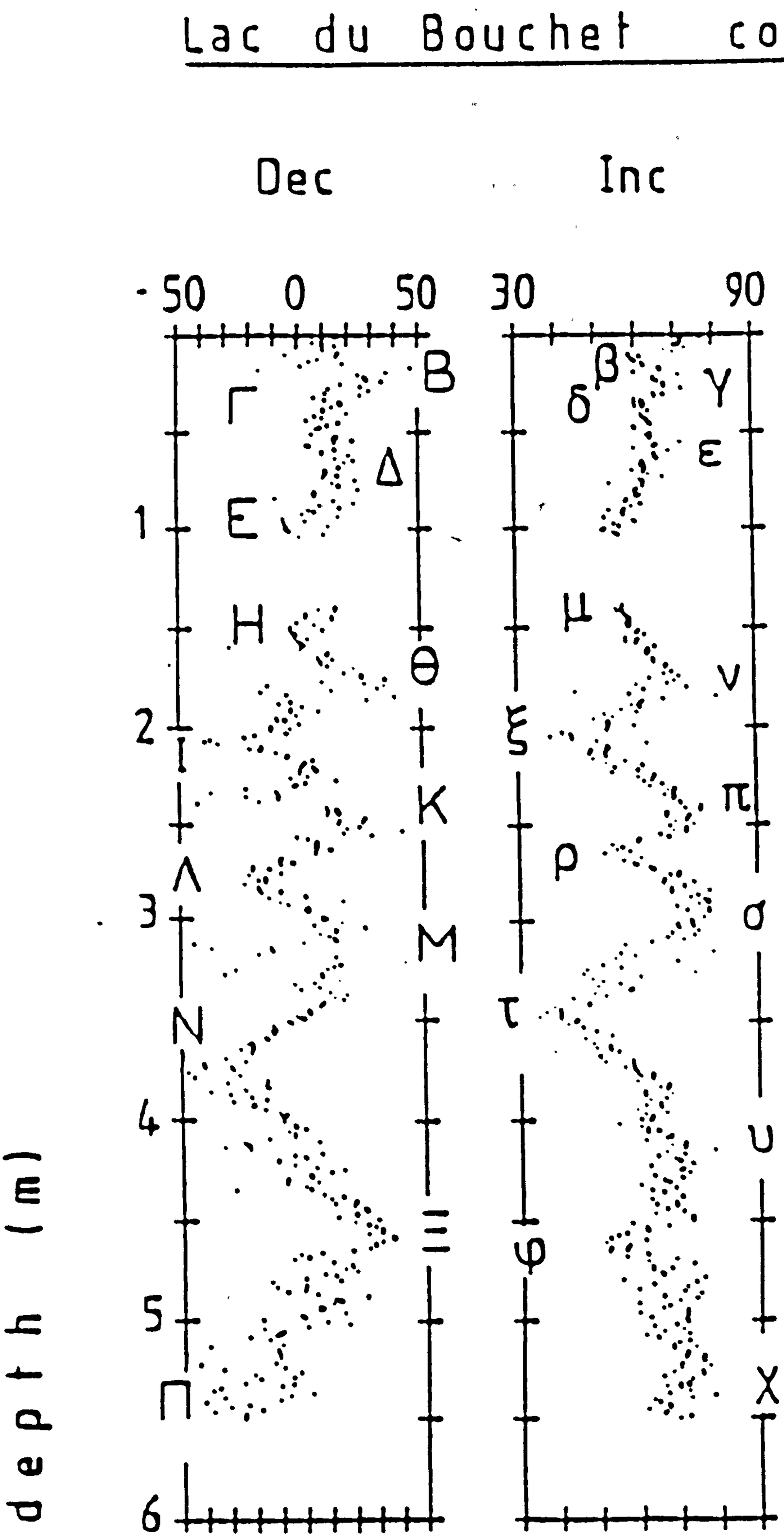

FIG 1.2 LAC DU BOUCHET PALAEOMAGNETICTYPE CURVE FOR WESTERN EUROPE. from CREER et al. (1986)

1.4 GEOLOGICAL SETTING

The quality of the LDB record is largely the product of the geological environment of the lake. It is a maar lake, formed phreatomagmatically, that is, by the explosive interaction of cool groundwater with a source of magmatic heat. The resulting crater lake (maar) is an ideal depositional environment for recording a palaeomagnetic signal as it potentially eliminates hydrodynamical effects, it also has a very slow (<1mm/yr) sedimentation rate due to the restricted nature of the catchment zone.

MFM, was formed in the same manner as LDB. It is the largest of the Quaternary West Eifel volcanic field maars. Groundwater in a hydraulically active zone of structural weakness below the Meerbach valley came into contact with rising olivine nephelinite magma to initiate the phreatomagmatic erruption forming the five Mosenberg scoria cones and the MFM crater (LORENZ 1973).

1.5 MEERFELDER MAAR SEDIMENTOLOGY AND MINERALOGY

Significant differences between MFM and LDB are that the country rock of MFM is Devonian slate and Jurassic Bunter sandstone, while LDB was blasted into olivine basalt with a greater magnetic mineral element producing a more magnetically intense record, also the sedimentation rate at MFM is higher by reason of having a more extensive catchment area due to the crater having been breached by inflows. MFM is approximately circular, 1km diameter with a maximum depth of 18m. Sedimentation has formed a littoral prism with an essentially flat centre from where the cores were taken as the succession is least disturbed here (FIG 1.3). Sediment source is restricted mainly to direct run-off from the crater sides, internal algal bloom and lacustrine plants. This effects an uncomplicated sedimentology at MFM (FIG 1.4).

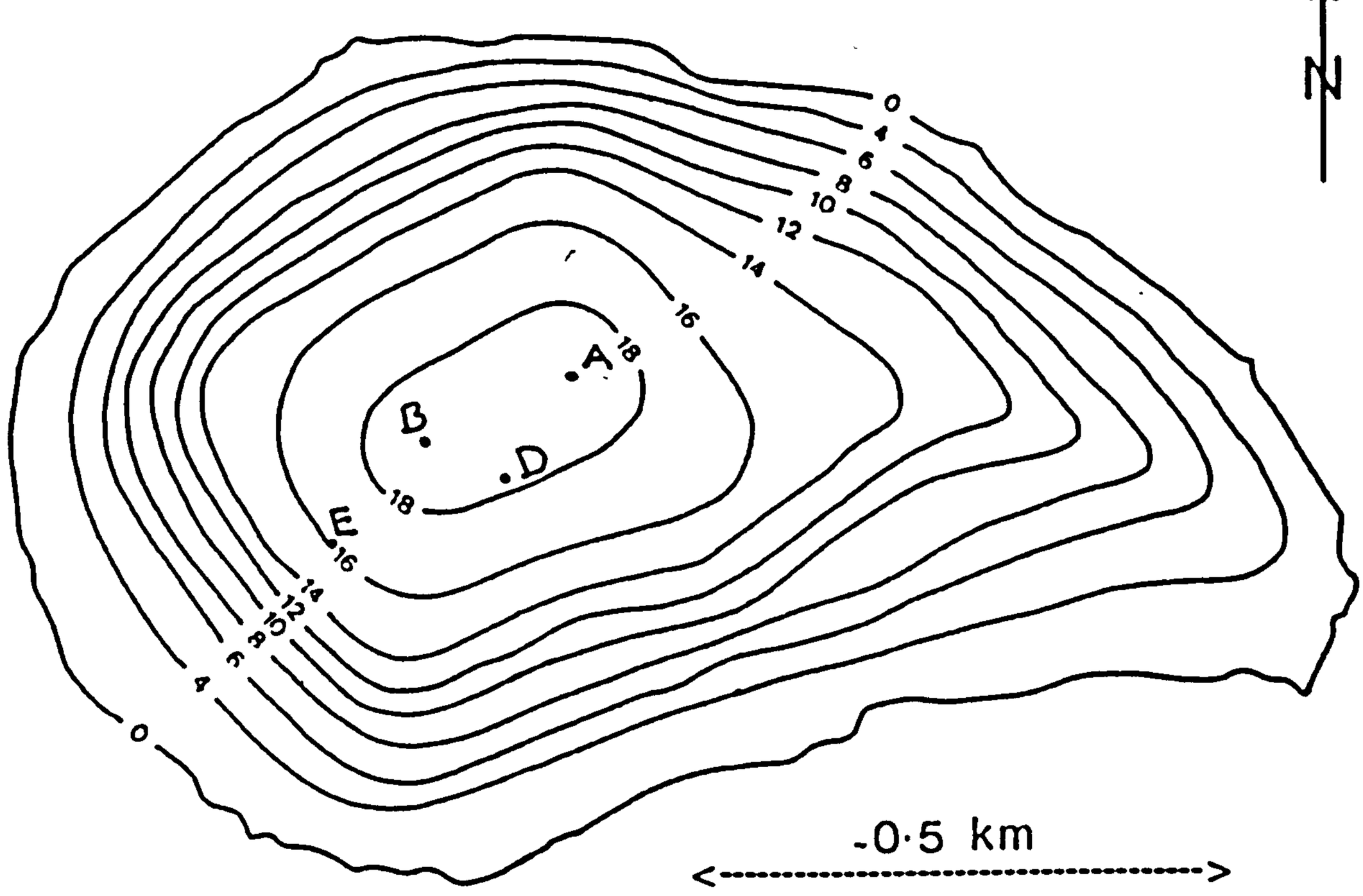

FIG 1.3 MEERFELDER MAAR BATHYMETRY WITH CORE POSITIONS. MFM IS SUB-CIRCULAR OF 1KM DIAMETER WITH A MAXIMUM DEPTH OF 18M. SEDIMENTATION HAS FORMED A LITTORAL PRISM AND A FLAT CENTRE. adapted from IRION and NEGENDANK (1984).

FIG 1.4 A SCHEMATIC SEDIMENTARY LOG FOR MEERFELDER MAAR SHOWING THE FOUR UNITS DESCRIBED IN THE TEXT.

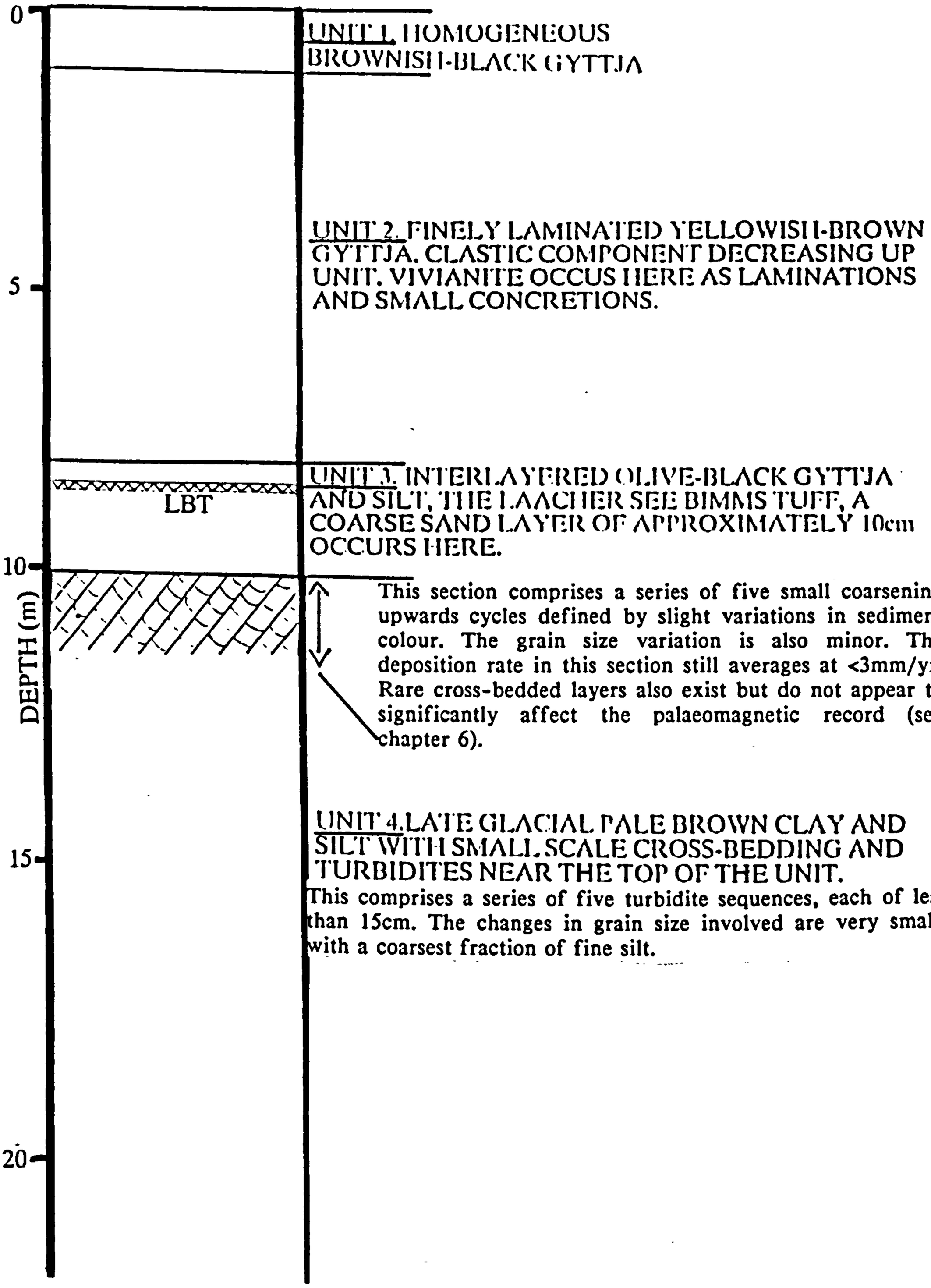

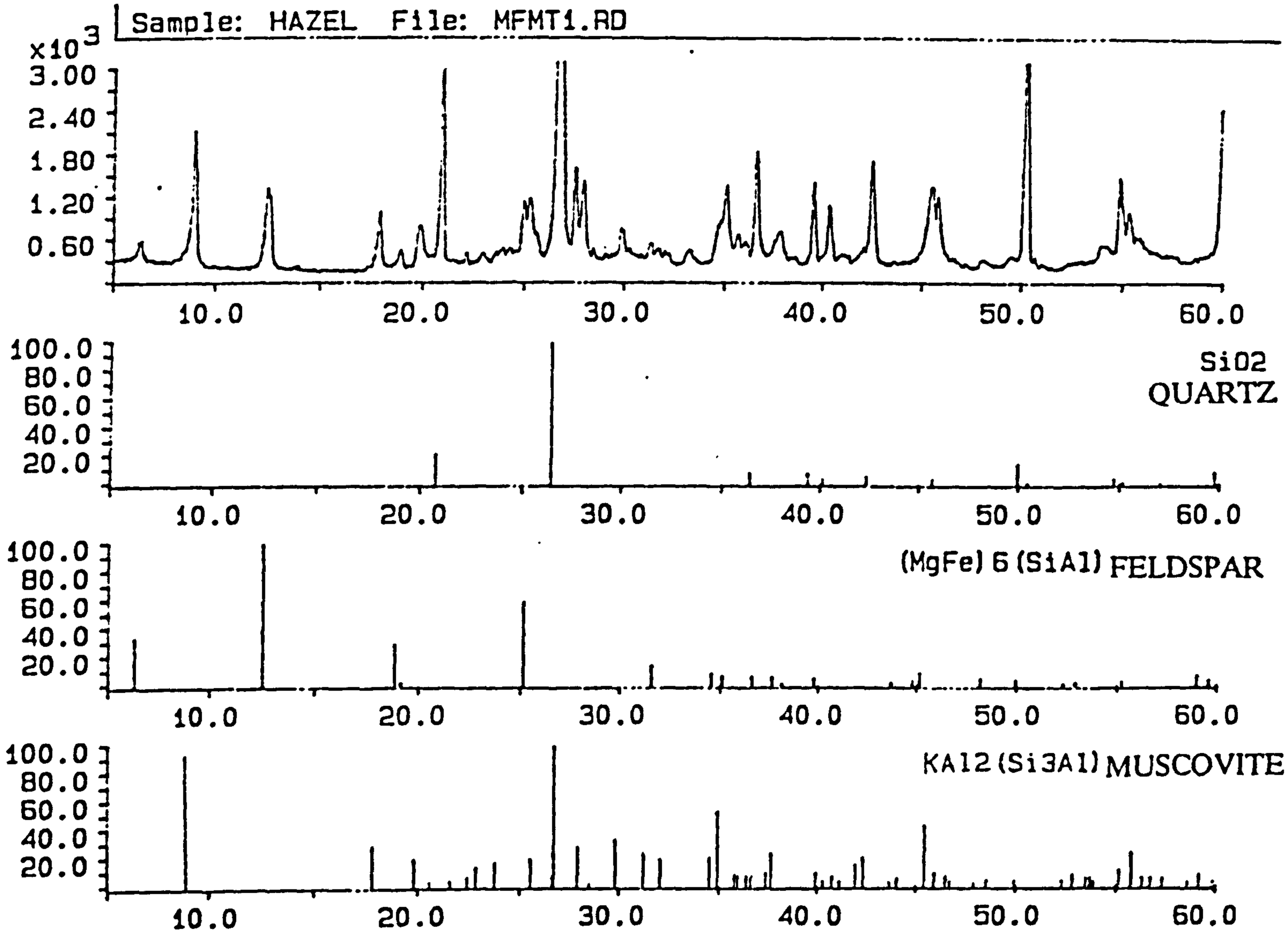

FIG 1.5 X-RAY DIFFRACTION OF WHOLE SEDIMENT FROM MEERFELDER MAAR (UNIT FOUR). THE DOMINANT MINERALS ARE QUARTZ, FELDSPAR AND MUSCOVITE EXCEPT IN UNIT TWO WHERE THE OCCURRENCE OF VIVIANITE IS CONCENTRATED.

Of the six cores from MFM in this study, the longest, core B core extends back approximately 20,000 years (ZOLITSCHKA 1988). The stratigraphy of the lake is described in four units:

0-1m depth interval.
UNIT 1. The most recent sediment is an organic-rich dark ooze composed of homogeneous brownish-black gyttja about 1m thick, with a water content around 75% .

1-8m depth interval.
UNIT 2. This comprises 7m of yellowish-brown gyttja, finely laminated with silt. The water content is around 65%. The organic component visibly decreases with increasing depth. Vivianite, a hydrated iron phosphate occurs as fine laminations and as concretions. In fresh cores the vivianite is white but turns a brilliant blue on a few hours exposure to the atmosphere.

8-10m depth interval.
UNIT 3. This consists of 2m of olive-black gyttja interlayered with silt. The water content is less than 45% and the organic component is low. The distinctive Laacher See Bims Tuff (LBT), 10cm of heavy mineral-rich, coarse sand, pyroclastic debris (LORENZ 1973) occurs within this unit. The base marks the start of Post Glacial deposition.

10-21m depth interval.
UNIT 4. consists of pale brown late glacial clays and silts with a water content of <30% and negligible organic material. A period of higher energy deposition, represented by small scale cross-bedding and a series of turbidites, is evident at the top of the unit. The sediments below are uniformly laminated.

XRD analysis of whole sediment samples indicated that quartz, feldspar and muscovite are dominant (FIG 1.5), except for unit two where vivianite is concentrated.

Seven cores, six from Meerfelder Maar and one from Lac du Bouchet, have been used for this work. An overview of the analyses carried out on each core throughout the the project can be found in appendix A.

The lamination occurring throughout the MFM cores is the result of a seasonally sedimenting algal bloom (ZOLITSCHKA 1989). This feature has been utilised by ZOLITSCHKA to provide an extremely powerful chronological tool in the form of an absolute varve chronology. The seasonal differences in sedimentation take the form of winter clays, spring and summer diatom deposits and autumnal amorphous organic material. The type of diatomaceous material has not yet been defined. It is also noted that vivianite occurs in the autumn cycle of the varve structure (ZOLITSCHKA 1989).

The power of this varve counting as a chronological tool has application to the radiocarbon dating method in the form of independent continuous calibration of the radiocarbon timescale beyond the 9ka limit of dendrochronological dating. This is imposed by the lack of suitable fossil trees. Reccent work by BARD et al (1990) also suggests that uranium-thorium ages obtained by mass spectrometry are suitable for calibration over the last 30,000 years. Radiocarbon data has previously successfully been applied to varved organic sediments as in the case of CALVERT et al (1991) through work on the Black Sea. However, it was concluded in that study that the varves were not of a continuous nature or strictly annual lamina. MFM is a possible locality for attempting a radiocarbon calibration by dating the organic carbon from the organic-rich autumnal layer of the varve using the accelerator method.

CHAPTER TWO.

MAGNETIC CARRIERS: IDENTIFICATION AND STABILITY OF THE REMANENT MAGNETISATION.

2.1 INTRODUCTION

The four cores providing most of the material for this project were recovered from MFM using a modified Livingston corer operated from a raft. The topmost core sections were taken manually by pushing the core tubes into the sediment and then pulling out, to avoid the risk of remagnetisation. Beyond a depth of about 25m the tube diameter must be reduced from 80mm to 55mm and a mechanical hammer had to be used when it became impossible to penetrate the deeper more compacted sediments by manual pushing. The use of the hammer carries the risk of realignment of the magnetic signature due to thixotropic behaviour of the sediment, where it behaves as a solid/liquid system: solid when stationary and liquid when subjected to shearing stresses. As a result the sediment has zero resultant body force and exists in the 'quick condition' (CRAIG 1984). This would obviously 'unlock' a PDRM since the magnetic grains would be free to realign in the present magnetic field direction.

Sections of core were taken in 2m long tubes, made of mild steel which provide a sharp cutting edge through the sediment, but they have to be demagnetised immediately prior to coring to prevent any magnetisation in the steel affecting the sedimentary record. Sections were transported ashore to be extruded and subsampled immediately to minimise distortion of the palaeomagnetic signal which can occur through warping of the sedimentary fabric on drying out or transportation over long distances. Generally this very slow manual coring process produced high quality core sections with millimeter scale laminations undeformed. Each section was continuously sampled in 25mm sided plastic cubes, excluding material from the extreme ends of sections which are disturbed by the coring process.

Having selected maar lakes as the optimum geological setting to circumvent hydrodynamical effects and having adopted coring techniques designed to prevent distortion of the microfabric and consequent remagnetisation, the major remaining uncertainty concerns the stability of the recorded remanent magnetisation. Is the measured remanenent magnetisation the primary one, does it represent a PDRM carried by detrital grains or a subsequent CRM carried by diagenetic minerals?

2.2 METHODS

The following analyses were carried out to determine the stability and origin of the magnetic remanence and to identify the magnetic minerals carrying the remanence.

1. Step-wise alternating field demagnetisation of the natural remanent magnetisation (NRM) was accomplished using a motorised variac-type unit designed by Dr. L Molyneux. The peak operating field is 99.5mT adjustable in 0.5mT increments. Operating principles are covered by AS (1967). Magnetisations were then measured on a CCL cryogenic magnetometer (chapter 3).

2. Thermomagnetic analysis using a Curie Balance, the electronics for which were constructed by Humphrey Instruments, interfaced with a BBC microcomputer. The principles are covered in COLLINSON (1983).

3. SEM analysis of magnetic extracts, using a Cambridge Stereoscan 250.

4. Step-wise AF demagnetisation of ARM's induced in peak fields of 40, 60 and 80 mT, (chapter 3).

5. XRD analysis of magnetic extracts on a Philips PW 1800 X-ray Diffractometer.

6. Step-wise IRM aquisition. Fields up to 1 Tesla were provided by electromagnets. Higher fields (up to 2 Tesla) were produced with a Trilec pulse

magnetiser. The resulting IRM's were measured on a Molspin portable fluxgate magnetometer, calibrated with a magnetic tape standard of known intensity. Noise levels were of the order of 1×10^{-6} Am^2.

7. Partial demagnetisation of SIRM. Magnetisation was achieved using electromagnets and measurement on a Molspin magnetometer.

2.3 RESULTS AND DISCUSSION

Step-wise AF demagnetisation of at least 10% of the samples from every core was carried out in steps up to a peak field of 60mT. Three orthogonal sample positions were used, followed by a reversal of the third position at half the field strength to reduce the effect of ARM's. Two components (FIG 2.1), viz a weak viscous component affecting grains with very short relaxation times (NÉEL 1955), removed on application of a 10mT peak alternating field (AF), and a dominant primary magnetisation remaining stable in the maxiumum field of 60mT were identified. The very weak sample D090 (MDF< 10mT), demonstrates the presence of some low coercivity remanence carriers with an inclination error which is progressively demagnetised to recover true inclination in the later stages of treatment.

The normalised intensity plotted against demagnetising field strength gives an indication of the coercivity spectrum of the magnetic carriers and allows comparison between samples of different magnetic mineral concentrations. The magnetisation is typically carried predominantly by a single mineral but some 'concave-up' plots suggest the presence of small quantities of a 'harder' mineral. Stereographic plots of directional changes during demagnetisation typically show a shift of a few degrees between the initial NRM and the 10mT demagnetised directions. Thereafter the direction remains up to 60mT which was the maximum demagnetising field. Alternatively the demagnetisation data may be presented as two plots of two of the three cartesian coordinates during demagnetisation. (ZIJDERVELD 1967). Typically these show a steady linear trend towards zero intensity.

It was concluded that optimum estimates of the primary remanence was obtained after AF 'cleaning' in a peak field of 10mT. Median destructive field (MDF)

FIG 2.1 INCREMENTAL ALTERNATING FIELD DEMAGNETISATIONS: INTENSITY VARIATION WITH INCREASING FIELD, STEREONET PROJECTION AND ZIJDERVELD PLOTS.

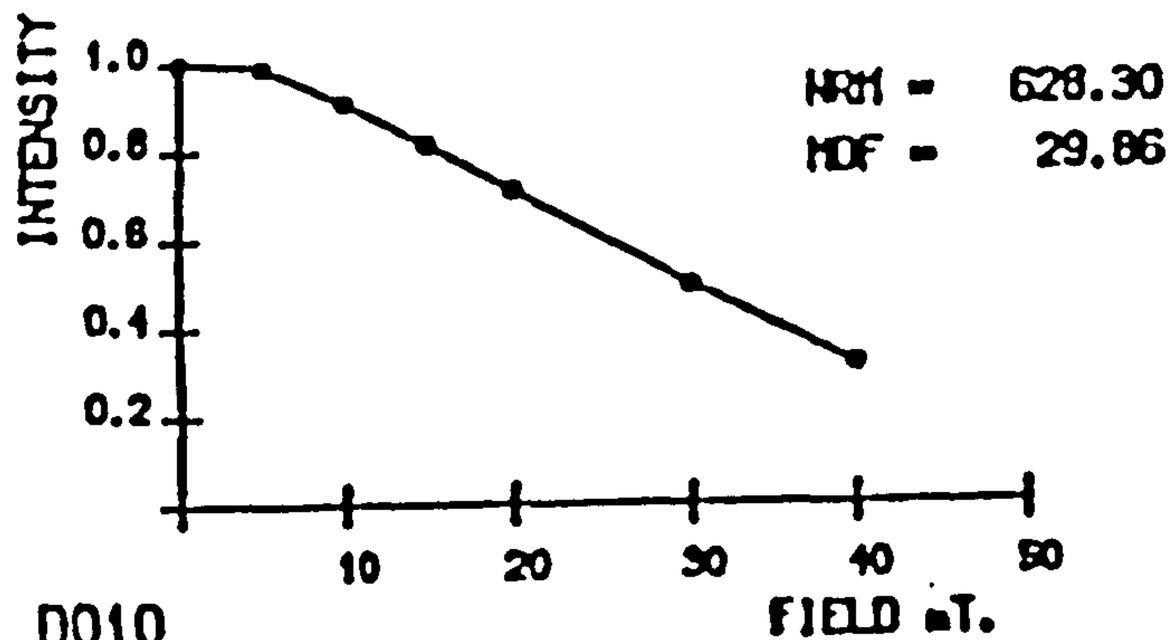

D010
Field only

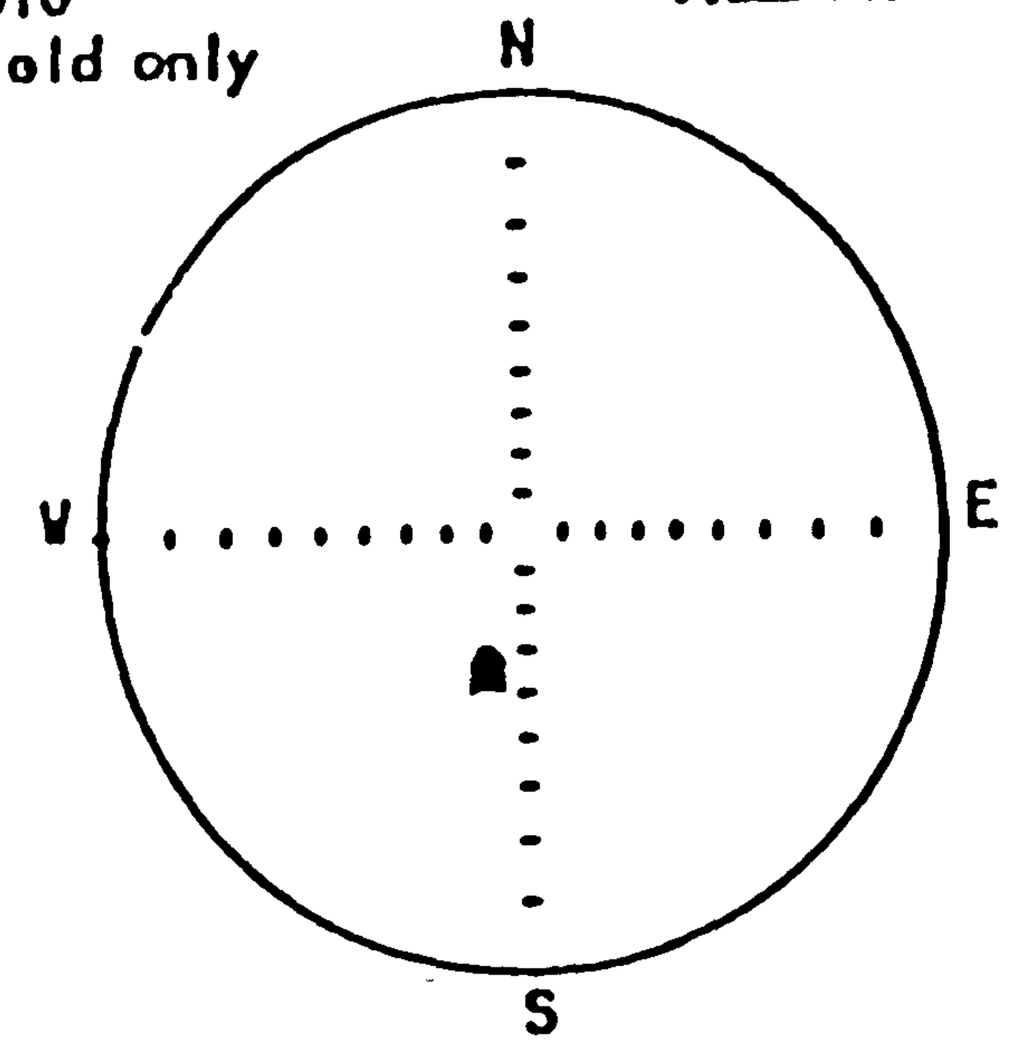

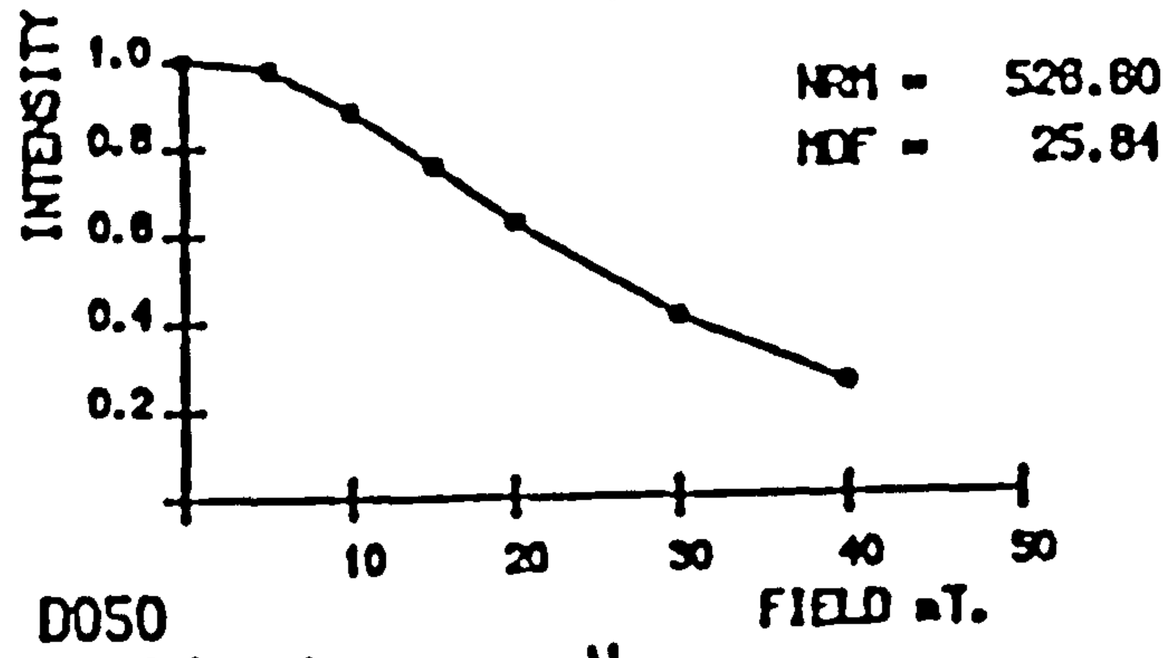

D050
Field only

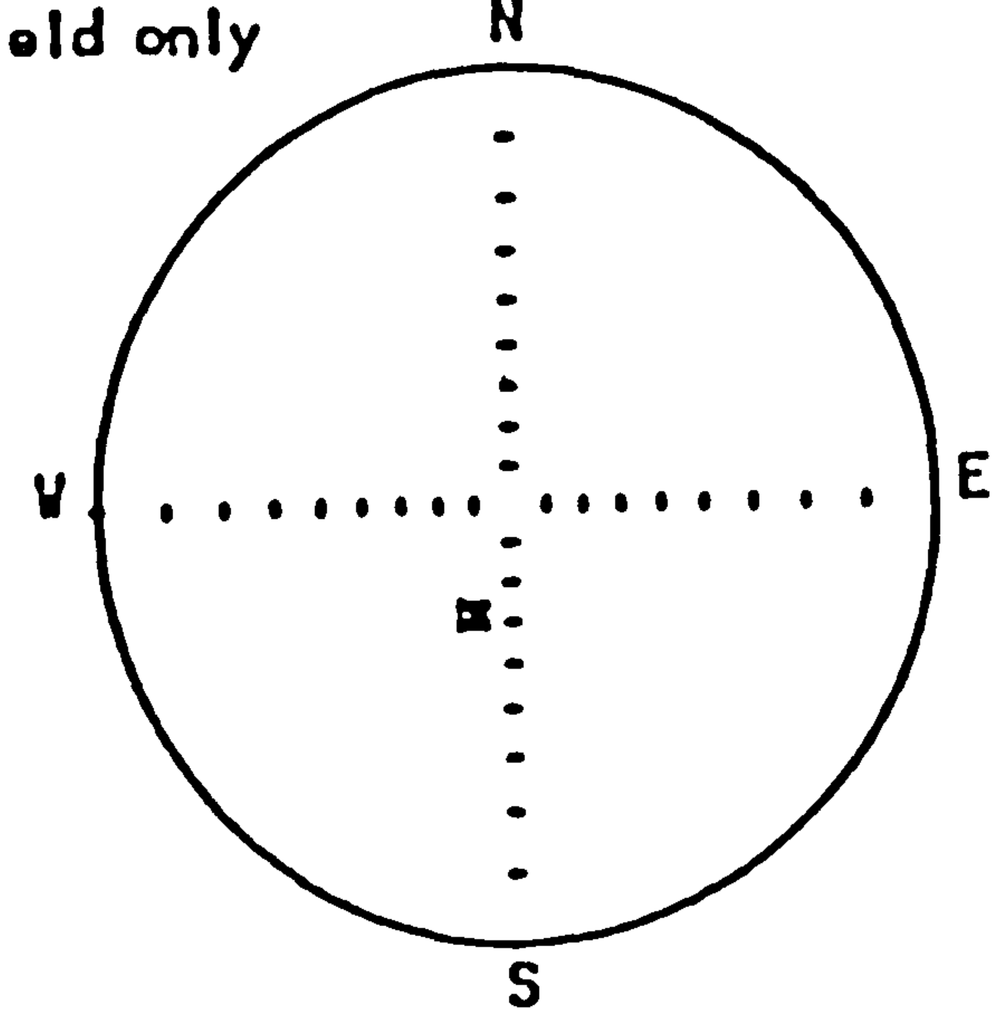

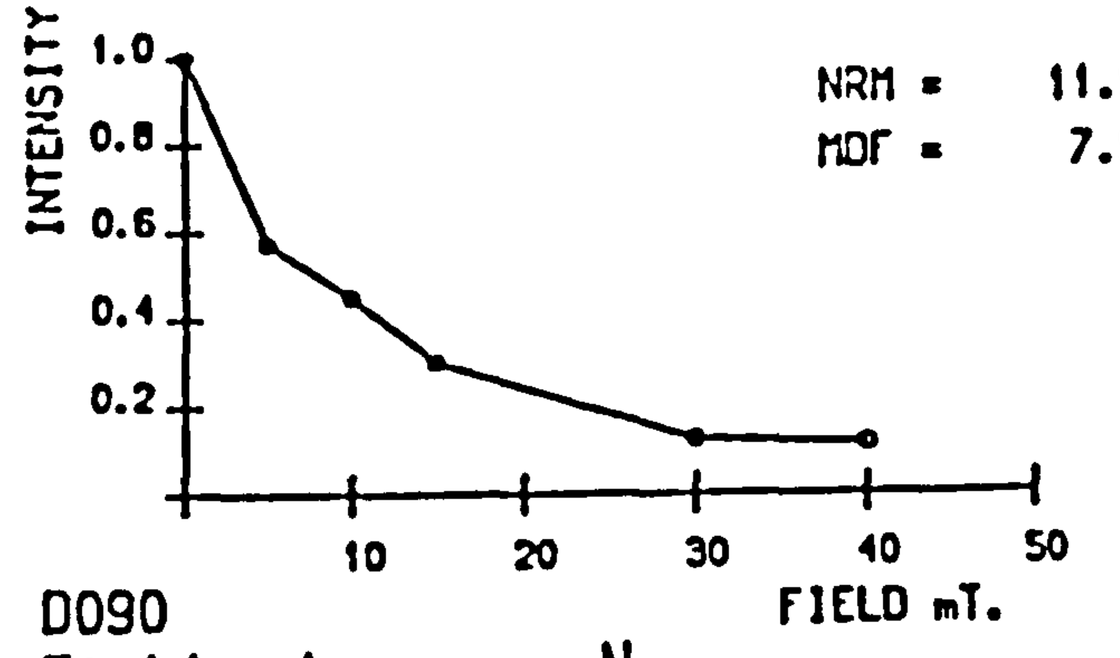

D090
Field only

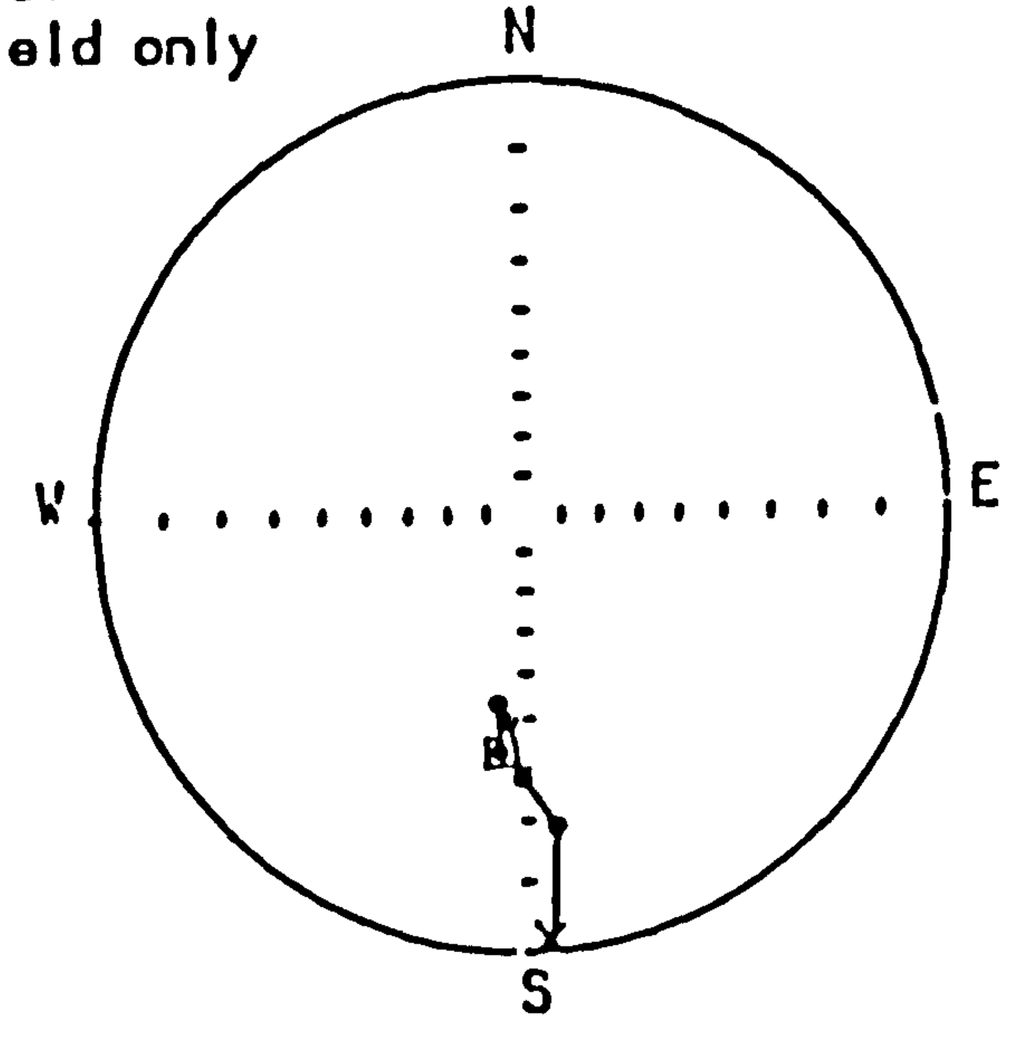

FIG 2.1contd.

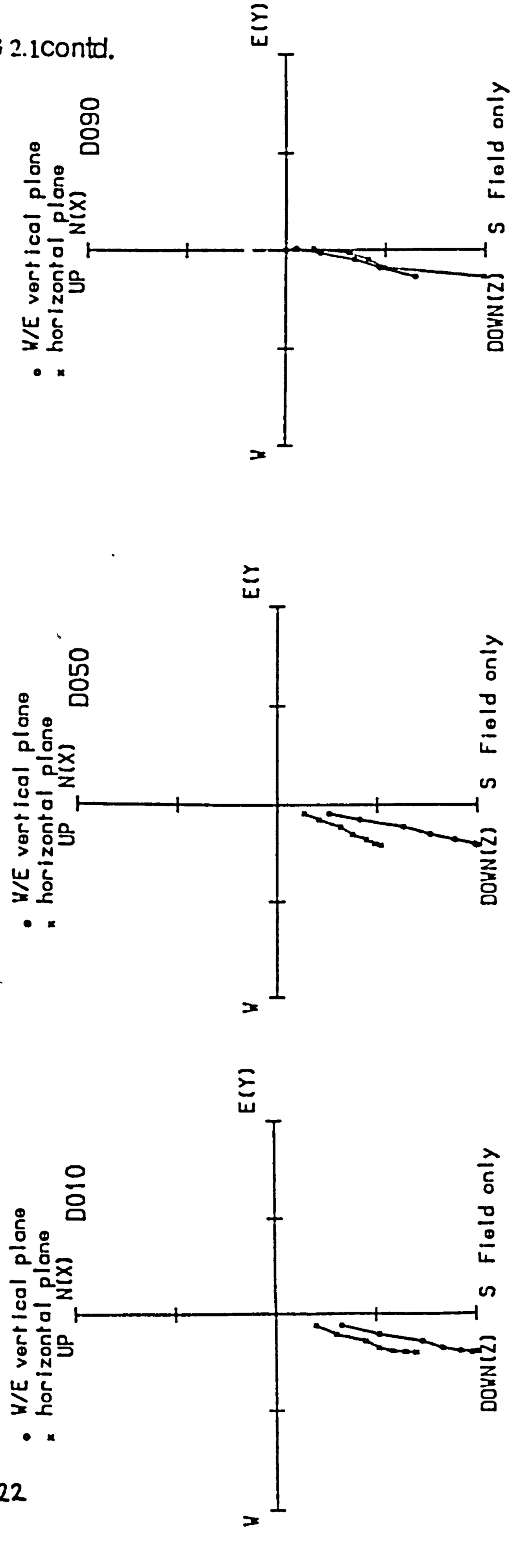
W/E vertical plane
horizontal plane
UP
N(X)
D090
E(Y)
S Field only
DOWN(Z)
W
W/E vertical plane
horizontal plane
UP
N(X)
D050
E(Y)
W
S Field only
DOWN(Z)
W/E vertical plane
horizontal plane
UP
N(X)
D010
E(Y)
W
S Field only
DOWN(Z)

TABLE 2.1 MEDIAN DESTRUCTIVE FIELD VALUES FOR CORE D. THIS COERCIVITY SPECTRUM INDICATES A MULTI-DOMAIN MAGNETITE CARRIER, (COLLINSON 1983).

DEPTH (cm)	MDF (mT)
30	29.9
175	34.3
220	25.8
265	19.4
311	8.0
358	15.3
406	25.9
452	26.0
497	19.8
543	18.9
588	30.1
680	19.8
727	36.6
773	26.5
819	26.7
865	32.6
915	28.3
961	39.5
1007	41.6
1032	26.4

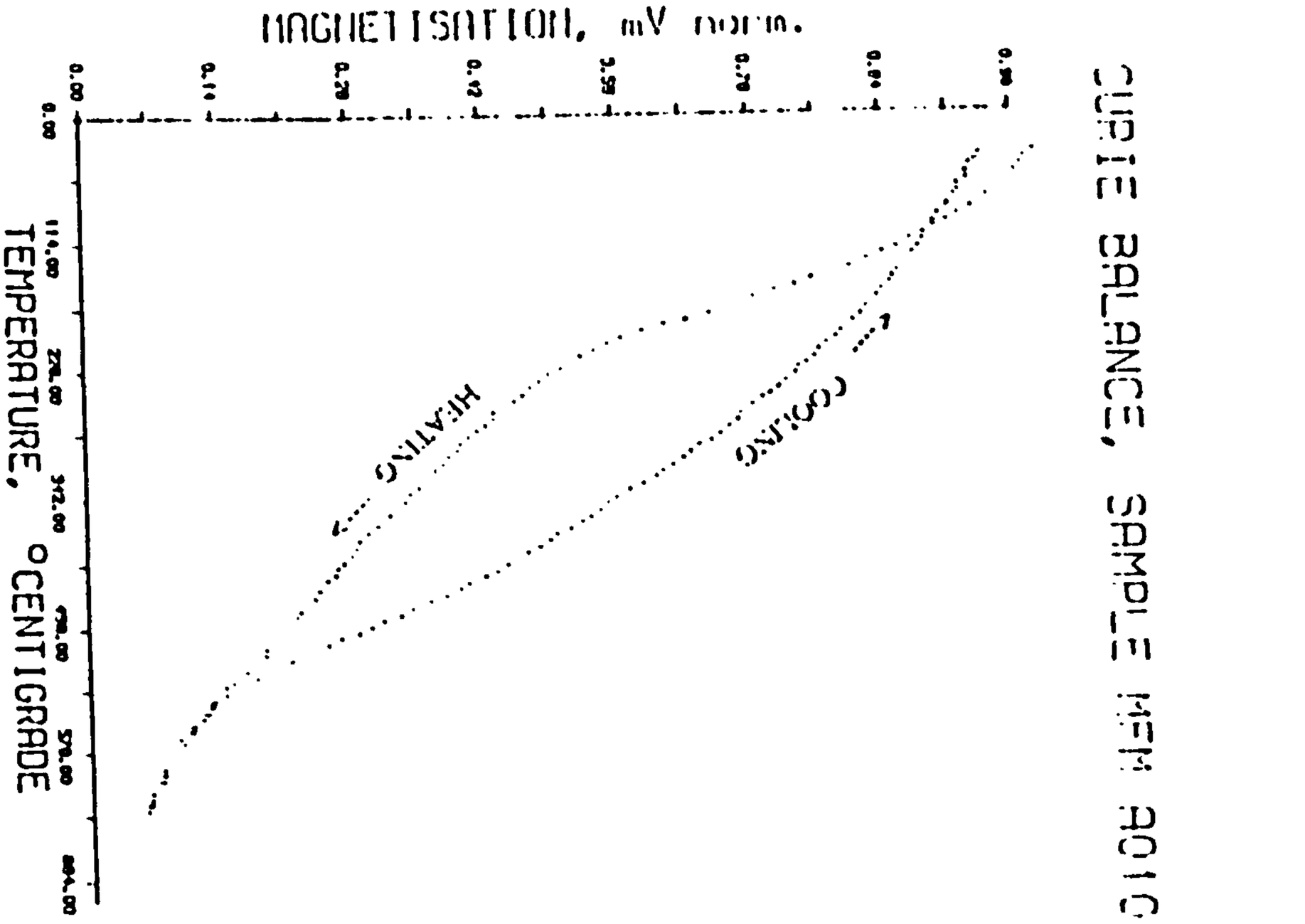

FIG 2.2A THERMOMAGNETIC BEHAVIOUR OF SAMPLE MFM A010

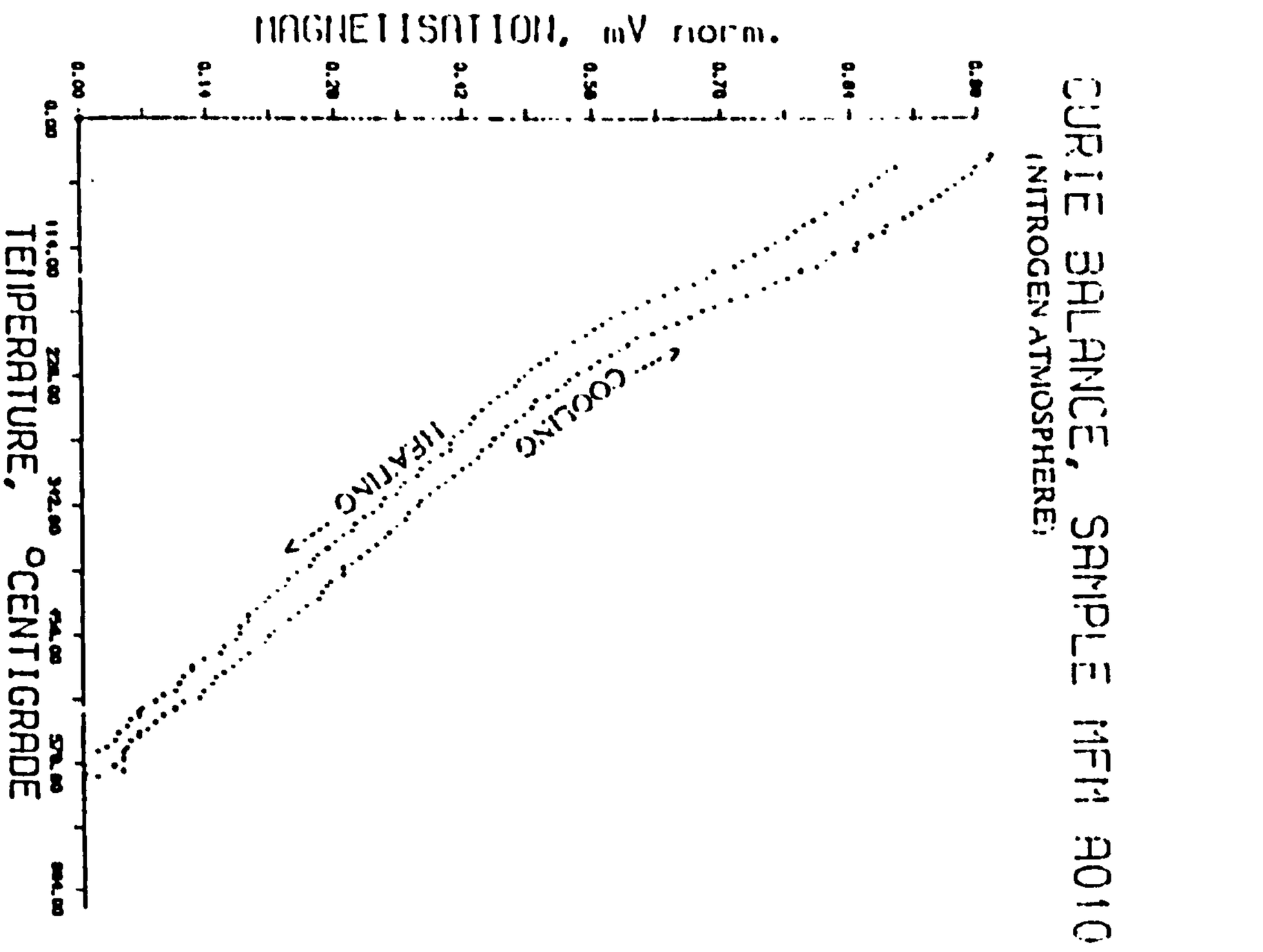

FIG 2.2B THERMOMAGNETIC BEHAVIOUR OF SAMPLE MFM A010 IN A NITROGEN ATMOSPHERE.

FIG 2.3 ARM DEMAG. MDF's with sedimentary units, (see FIG 1.4)

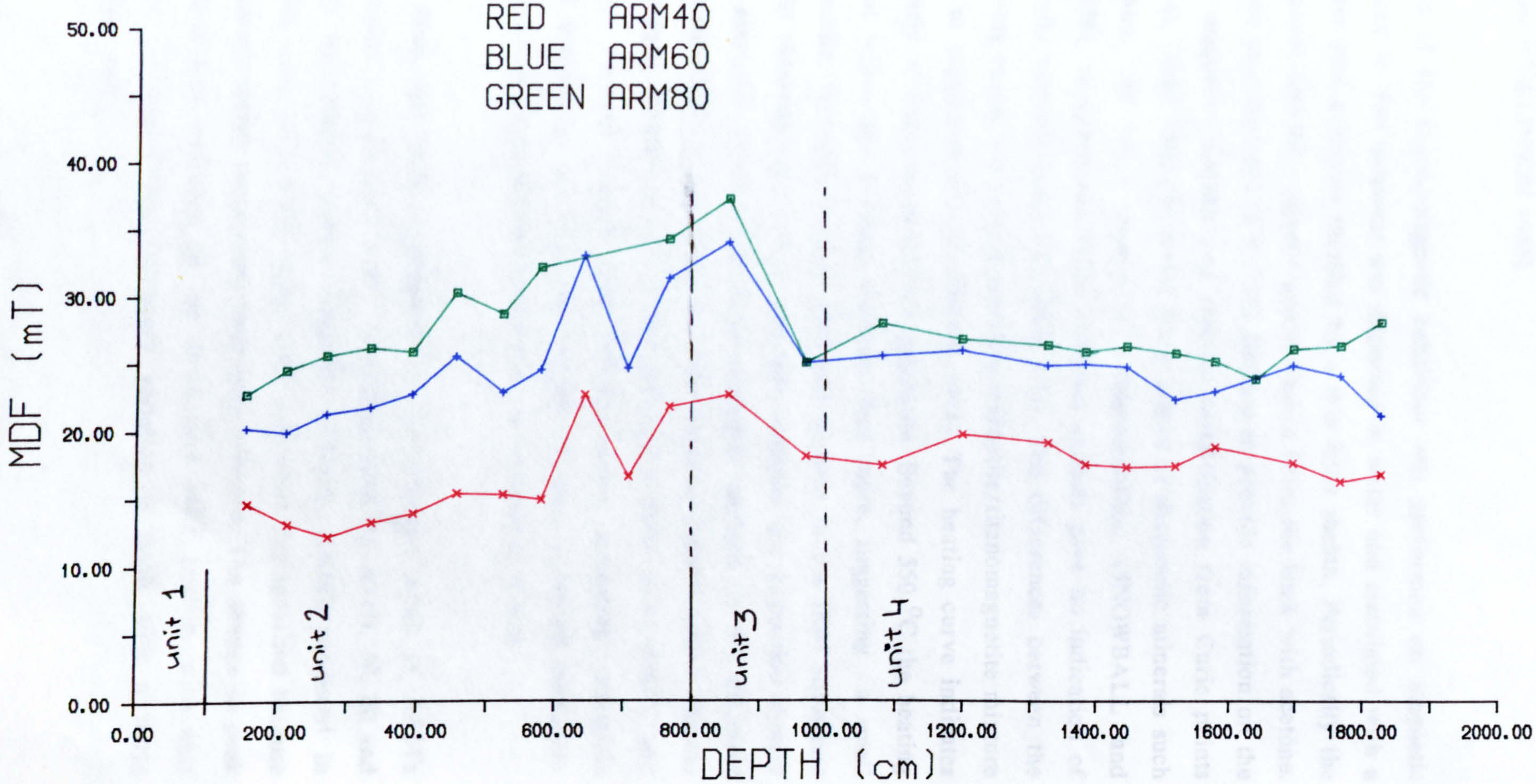

values for the demagnetisations from core D range from 8.0 to 41.6mT, with a mean of 24.1mT (TABLE 2.1), suggesting that multi-domain magnetite is the remanence carrier (COLLINSON 1983).

An investigation of the thermomagnetic behaviour was performed on magnetic extracts from core A. The sediment was dispersed in water and circulated with a mechanical stirrer past a magnet shielded by a thin latex sheath. Periodically the magnet was removed and the magnetic grains washed from the latex with acetone. The extracts were then analysed in a Curie Balance to provide information on the stability of the magnetic minerals and possible identification from Curie points (HOUSDEN et al. 1988). This can reveal the presence of diagenetic minerals such as greigite which can be a source of remagnetisation, (SNOWBALL and THOMPSON 1988). However, the MFM magnetic extracts gave no indication of unusual chemically unstable behaviour (FIG 2.2a). The differences between the heating and cooling curves are consistent with a magnetite/titanomagnetite mixture or may be due to exsolution effects (CREER 1971). The heating curve indicates the presence firstly of titanomagnetite then magnetite. Beyond 550 ^{o}C the heating curve has a tail where the gradient shallows once more, suggesting a small quantity of hematite. Hematite is more obviously present in the IRM aquisition curves (FIG 2.5) obtained from whole sediment analysis, the extraction system separating the magnetic extracts for thermomagnetic analysis is not efficient enough to separate hematite out from the non-magnetic matrix grains. Repeat analysis in a nitrogen atmosphere (FIG 2.2b) produced a Curie point <600^{o}C and better agreement between heating and cooling curves indicating negligible alteration. SEM analysis of the magnetic extract revealed unaltered magnetite crystals (PLATE 2.1) without diagenetic alteration or dissolution effects.

The coercivity range has been investigated by the demagnetisation of ARM's aquired in a constant bias field of 0.1mT with three peak AF levels, 40, 60 and 80mT, to affect increasingly 'harder' magnetic minerals. ARM's produced in higher peak fields have larger MDF values (FIG 2.3) when demagnetised because grains of increasingly higher coercivities have been affected. The change in peak field has no significant influence on the down core MDF profile, with near faithful mimicry between levels. Downcore variation is small with a range typically less than 5mT.

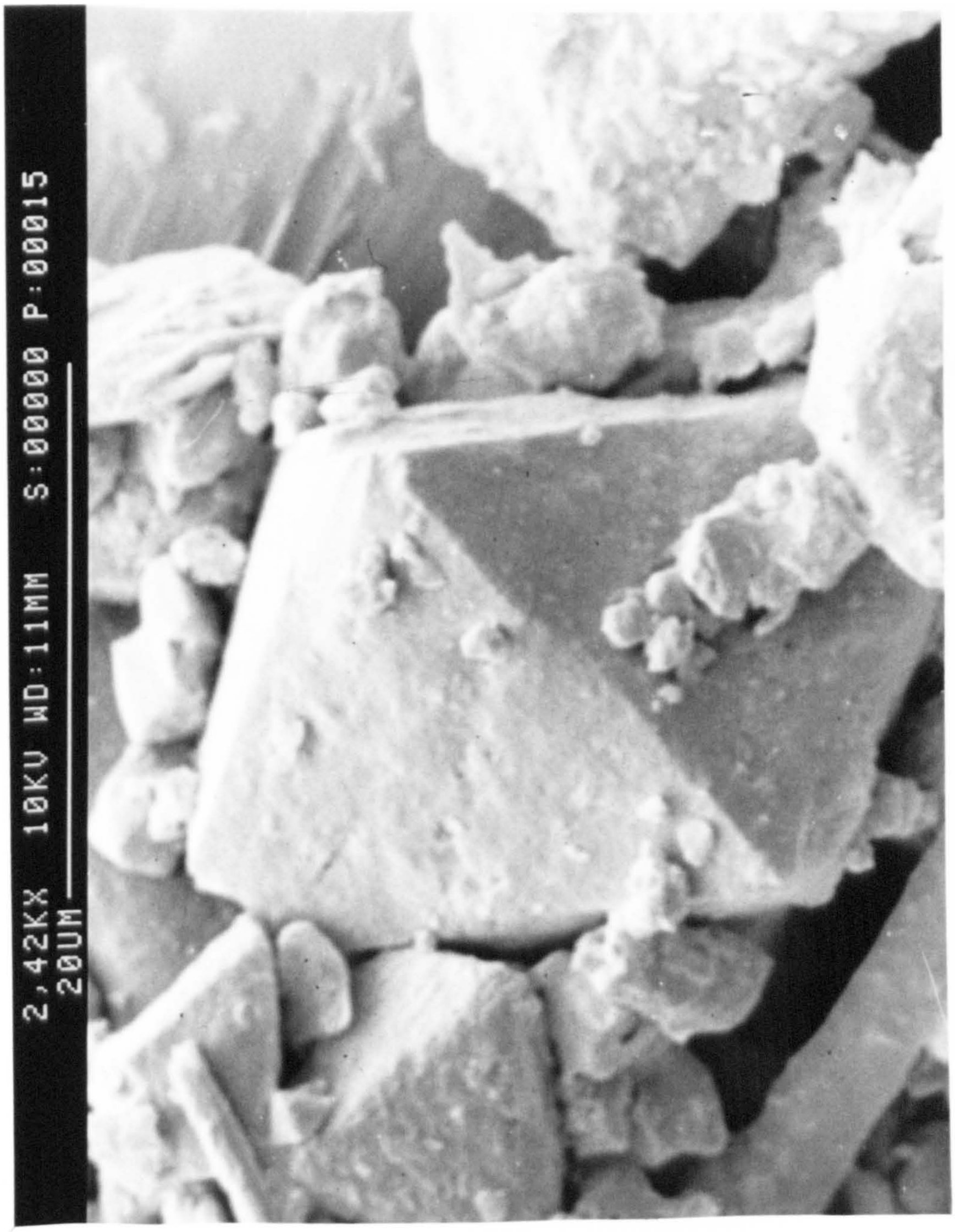

PLATE 2.1 SEM VEIW OF MAGNETIC EXTRACT FROM MFM A CORE, FEATURING A WELL FORMED MAGNETITE CRYSTAL.

Increasing MDF values between 0 and 8·5m have two possible explanations; firstly it could be caused by a decrease in grain size (LOWRIE and FULLER 1971, DUNLOP 1981), or alternatively it could be a result of an increase in the ratio of hard:soft magnetic minerals. The latter possibility is refuted by the model produced in FIG 2.6 where the intensity of magnetisation of the 'softer' component has been isolated. If the hard:soft ratio were the controlling factor for MDF values, we would expect a decrease in the percentage magnetisation from the soft magnetic mineral components to correlate with the increased MDF values. This is not so, concluding that the elevated MDF values are most likely to be the result of a reduction in grain size.

Comparison of average MDF values for each peak field: 40mT (14.4mT), 60mT (24.7mT) and 80mT (27.3mT) with that for NRM demagnetisations (24.1mT), suggests that ARM's produced in a peak field of approximately 60mT most closely match the coercivity spectrum of the NRM carriers. It is therefore the ARM intensity values produced at 60mT peak field which could be used to normalise the NRM intensities to obtain palaeointensity estimations, (LEVI and BANERJEE 1976). Other intensity normalising methods include the technique of laboratory redepositions (TUCKER 1981). This was found to be more accurate in a study by THOUVENY (1987) to recover palaeointensities from maar lake sediments.

In determining the magnetic mineralogy of the maar sediment two further methods of approach were used. The first was XRD analysis of the magnetic extract to estimate the nature of the magnetic minerals present either as individual grains or as inclusions, results are shown in FIG 2.4 . Secondly, IRM aquisition curves were constructed for whole sediment to provide information on the coercive spectrum of the magnetic minerals present and to indicate the saturation points of different minerals detected by a change in slope as the applied field was incrementally increased from 100 to 2000mT. In all samples two components were present (FIG 2.5), the first 'softer' mineral saturating below 100mT and a 'harder' mineral which remained unsaturated at the peak field of 2 T.

The softer component is probably the magnetite/titanomagnetite detected on the

FIG 2.4 XRD OF
MAGNETIC EXTRACT (SAMPLE MFM A010)

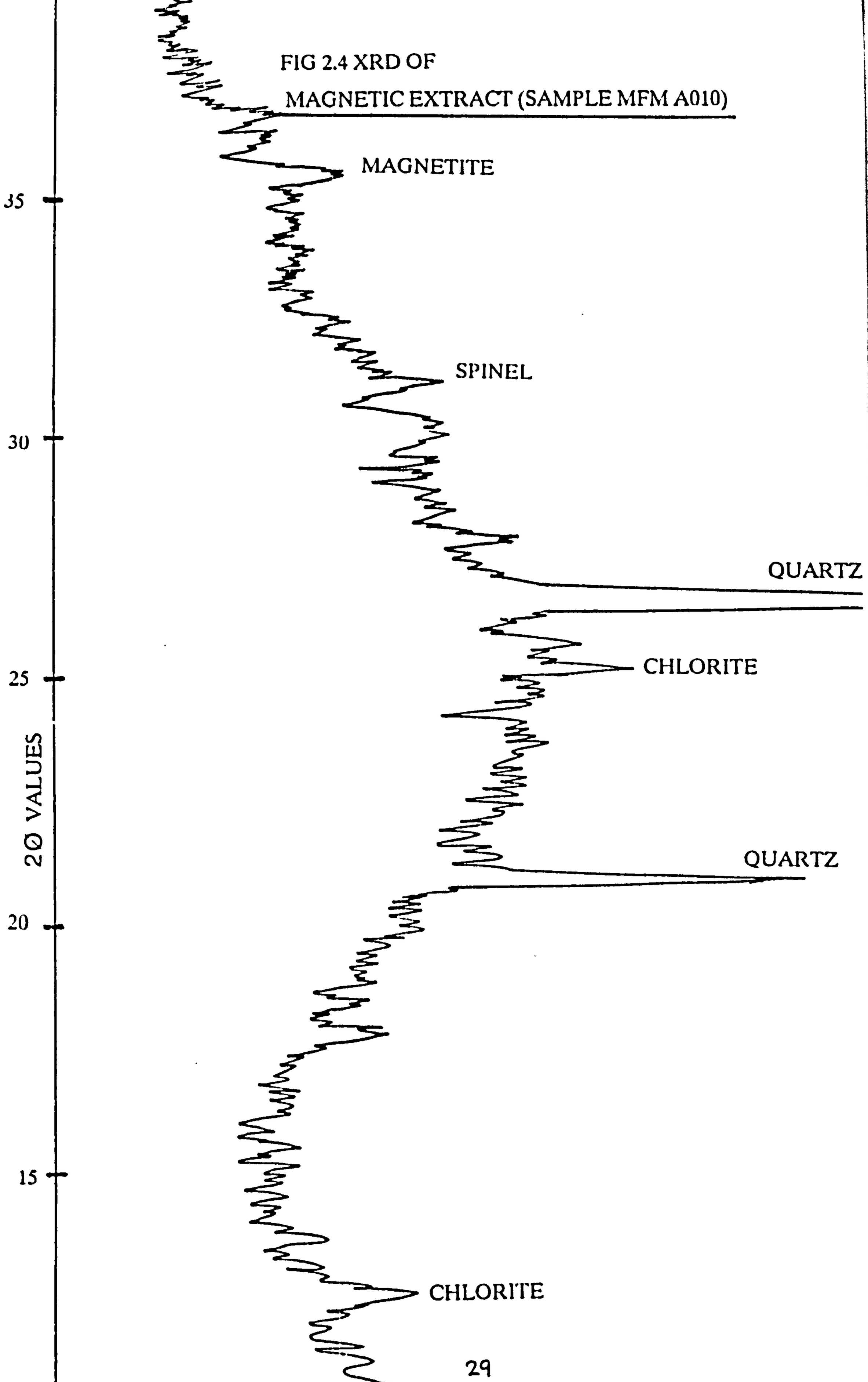

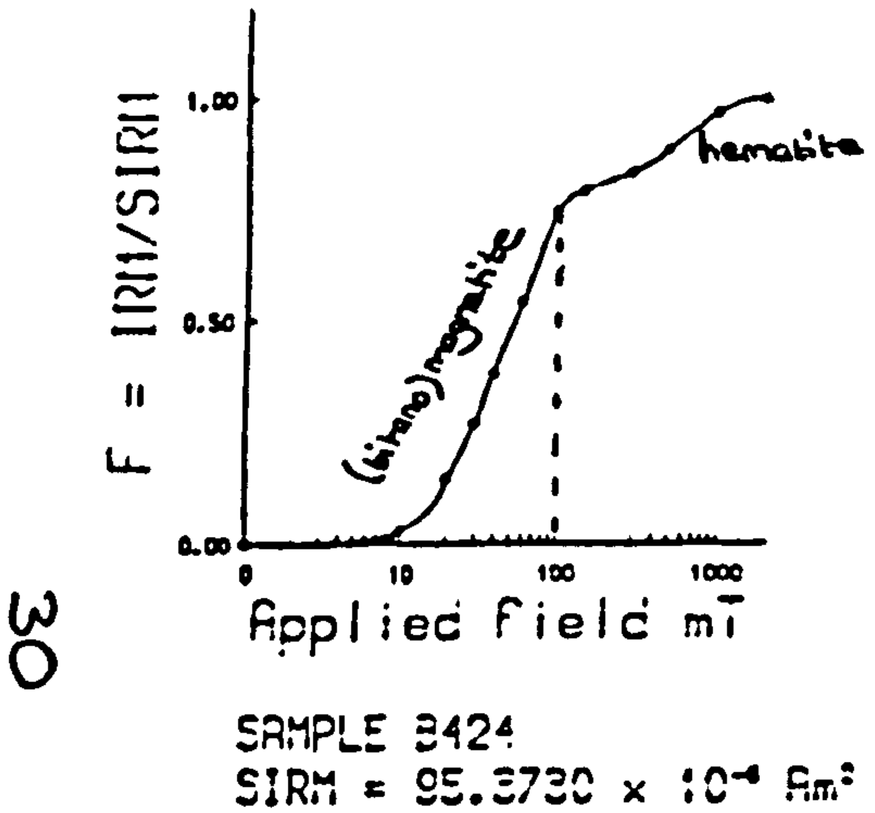

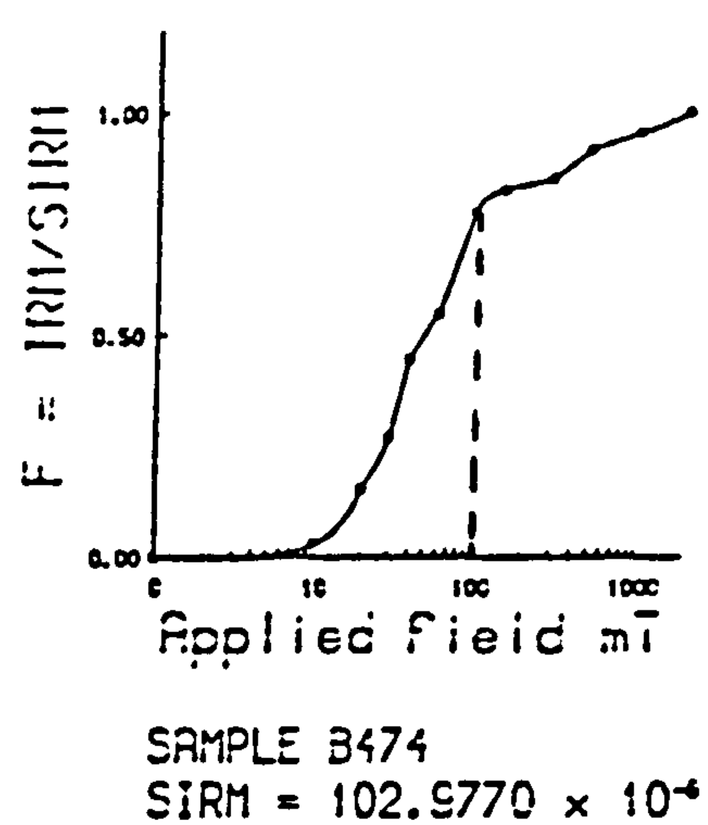

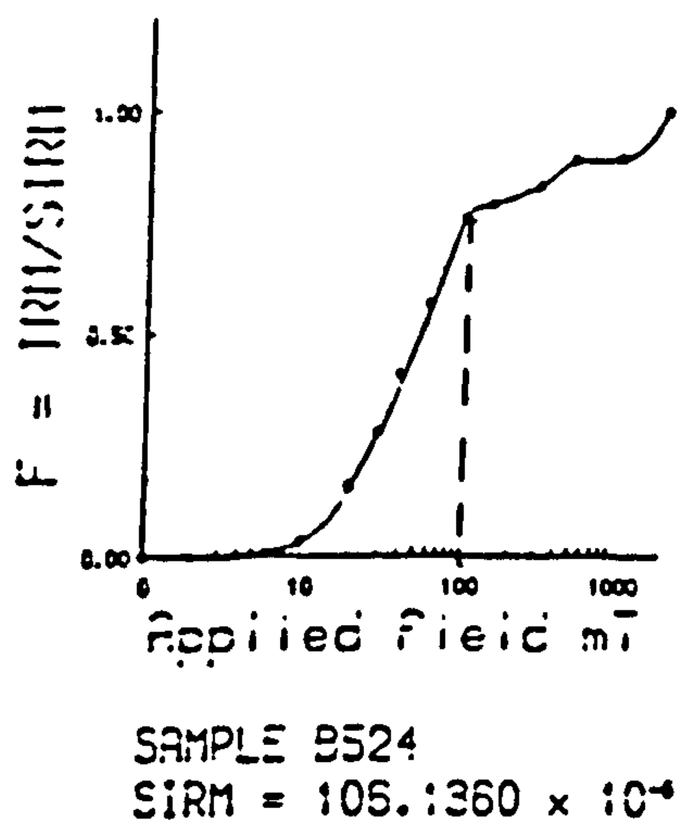

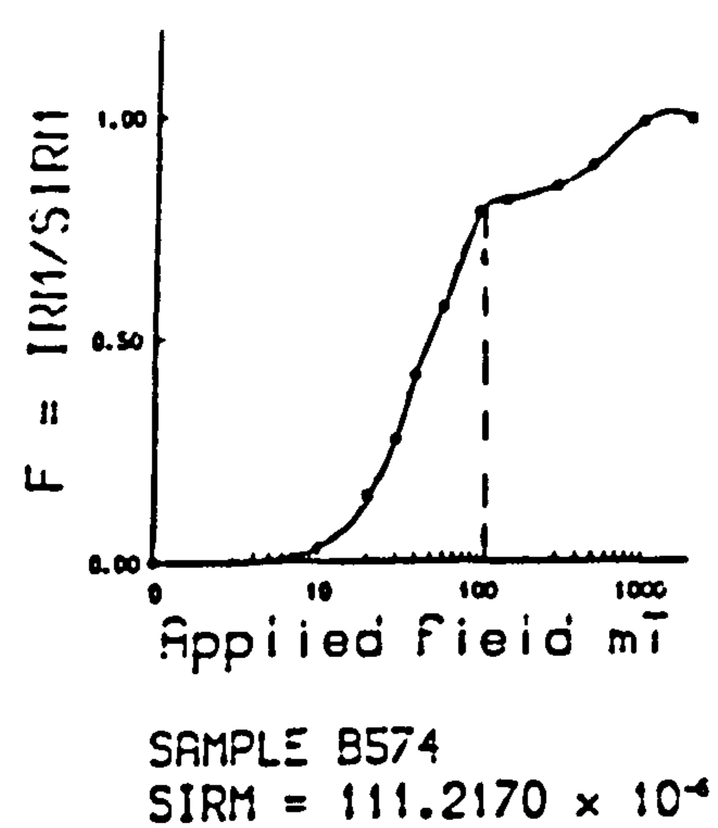

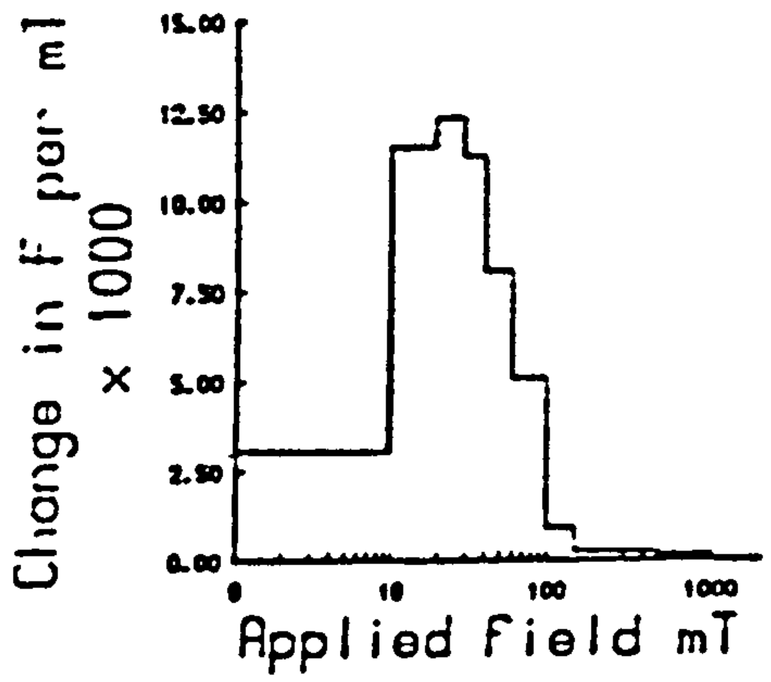

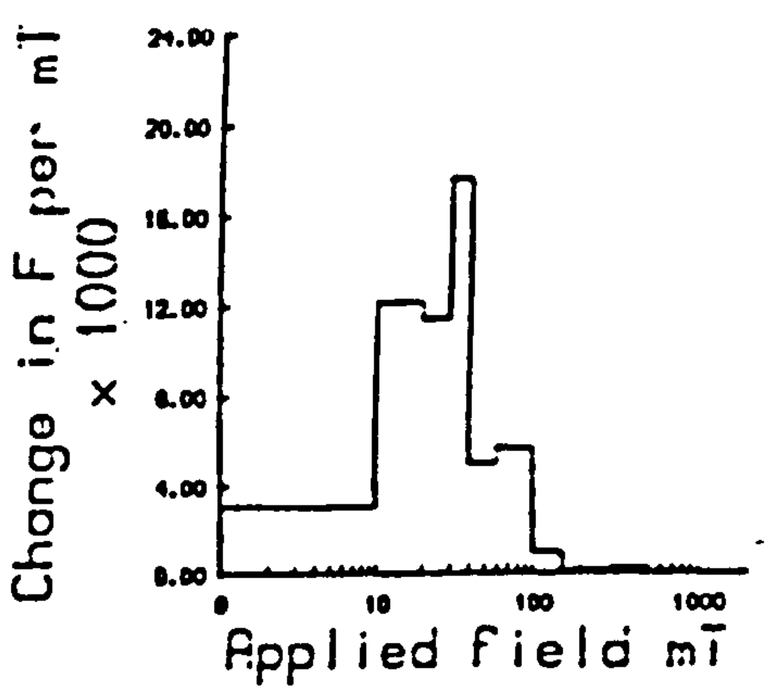

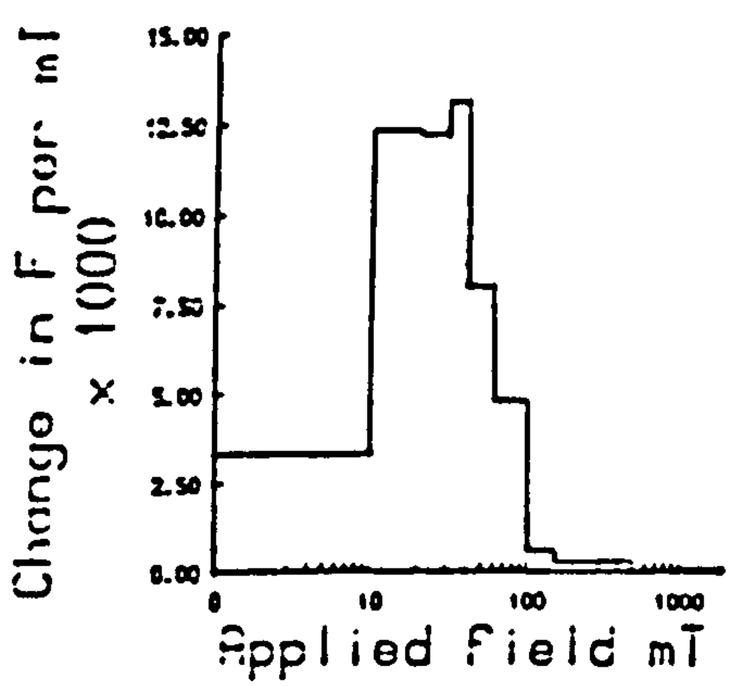

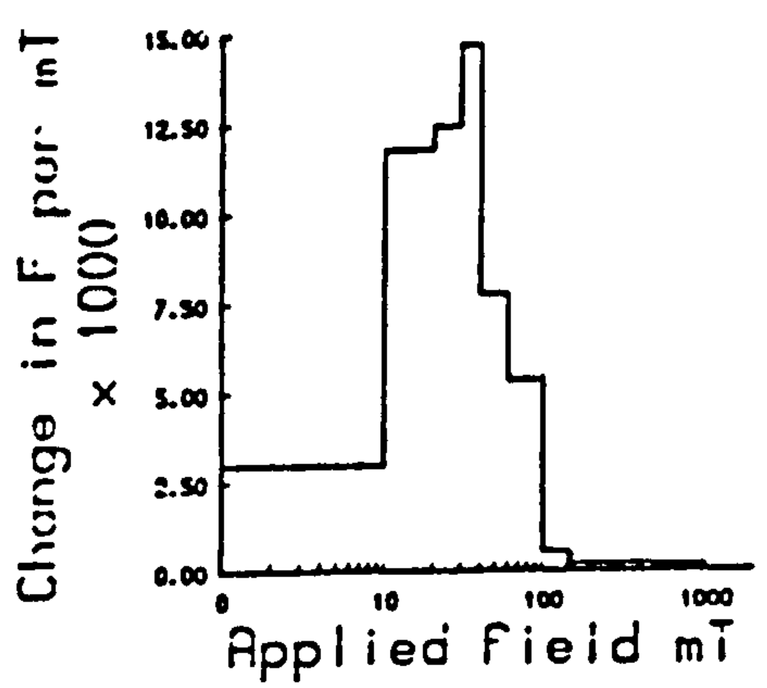

FIG 2.5 IRM AQUISITION CURVES FOR WHOLE SEDIMENT PROVIDING INFORMATION ON THE COERCIVE SPECTRUM AND THE SATURATION MAGNETISATIONS OF THE MAGNETIC CARRIERS.

FIG 2.6 COMPONENT OF MAGNETISATION FROM 'SOFT' MAGNETIC MINERAL IN EXTRACT. THIS PARAMETER IS RELATED TO THE 'S' RATIO (STOBER & THOMPSON 1979) BY DIVIDING BY 100.

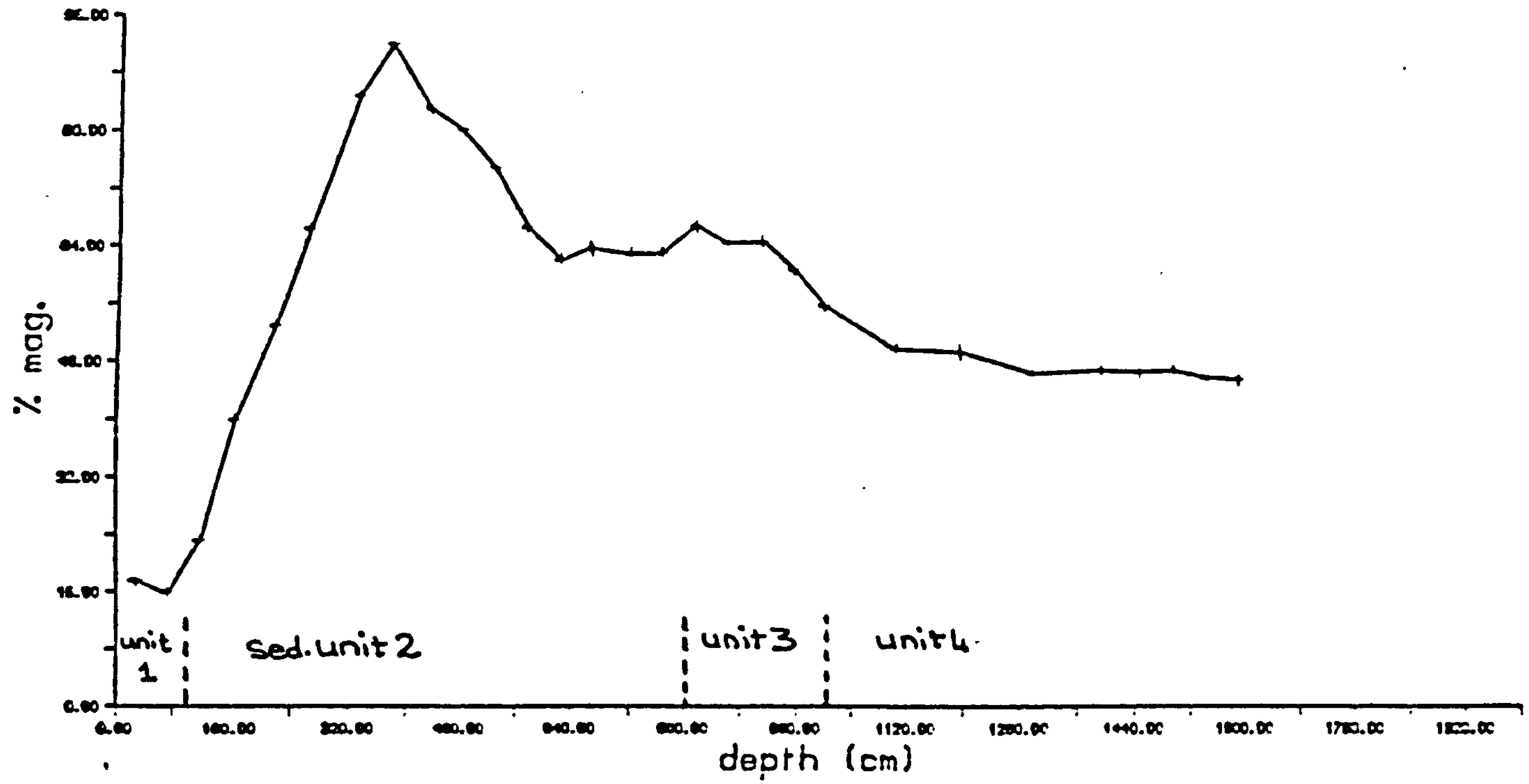

Curie balance. The harder one is probably hematite although this mineral was not evident in the extract by reason of the lack of sensitivity of the extraction system. To identify how the relative amounts of soft and hard minerals have varied downcore, a series of measurements were conducted where the sample intensity was measured after 'saturation' to 1T and remeasured after application of an opposing field of 100mT designed to remove the effect of the softer component. The ratio of intensities was plotted as the magnetite/titanomagnetite element of magnetisation (FIG 2.6). It can be seen that after rising steeply to 95% of the magnetisation between 50cm and 4m, the magnetisation from magnetite decreases at first steeply then more slowly, to plateau at approximately 45% .

2.4 CONCLUSIONS

From the results of the series of magnetic mineral analyses we can make some conclusions about the magnetic mineralogy of the MFM sediments and the stability of the remanence carried.

The NRM is a stable primary remanence with a superimposed component, induced either viscously or by drilling. IRM aquisition by the whole sediment indicates two magnetic mineral components; a soft one saturating below 100mT and a hard one, unsaturated at 2T. The magnetic mineral extract is composed mainly of magnetite and spinel, thermomagnetic analysis of the extract showing a curie point <600^{o}C with the shape of the curve consistent with a magnetite/titanomagnetite mixture. The harder remanence carrier is most likely hematite, although the magnetic extraction system is not efficient enough to separate out this relatively magnetically weak mineral (to assess its thermomagnetic properties).

The range of MDF values on demagnetisation of the NRM's indicates the magnetic carriers to be multi-domain magnetite. NRM coercivity is best reproduced by an ARM implanted by a field of 60mT which could be used to normalise NRM intensities to obtain a palaeointensity profile. The ARM data also indicate a decrease in grain size of the magnetic grains between 0m and 3.5m .

The magnetisation carriers remain stable at temperatures over 600^{o}C and exhibit no signs of chemical change when viewed by SEM. They are therefore likely to be original detrital grains unaffected by dissolution so the magnetic signal must have been acquired during or soon after deposition by alignment of magnetic grains in the Earth's magnetic field of that time.

There is however strong evidence in support of the occurrence of some degree of dissolution when considering the progressive decrease in magnetic mineral grain size between 0m and 8.5m corresponding to the decrease in organic carbon over this interval (FIG 7.2). It is suggested that diagenetic reactions involving magnetic minerals and organic material are taking place. This is probably part of the process resulting in the formation of the hydrated iron phosphate mineral, vivianite, found in MFM.

CHAPTER THREE.

MEASUREMENT OF NARURAL REMANENT MAGNETISATION.

3.1 INTRODUCTION

This chapter deals with the measurement and processing of palaeomagnetic data from MFM. Four cores (A, B, D and E) have been analysed. Cores A and B were taken duing the summer of 1987 and are respectively 16m and 21m long. Cores D and E of lengths 11m and 6m were taken during 1988 for additional Post Glacial coverage. (The full lengths of cores A and B were 40 and 45m respectively).

3.2 METHODS

The NRM and then the magnetisations cleaned in 10mT were measured on a cryogenic magnetometer after storage in 'zero' field, produced by Helmholz coils, for a week to reduce the effect of VRM. The cryogenic magnetometer (Cryogenic Consultants Ltd.) operation is based on SQUID (superconducting quantum interference device) technology (GOREE and FULLER 1976). Noise levels for this machine were in the order of 0.1 mA m^{-1} (MORRIS 1990). Operation was via an extensive and flexible control program written and developed by SMITH (1985) for a Sirius microcomputer. For much of the period of measurment only one SQUID was operational, this necessitated measurement in four orientations (FIG 3.1), (two automated measurements in each orientation) to obtain at least two values for each component of magnetic intensity, north, east and down. The control program allowed the automatic removal of the sample holder magnetisation based on several measurements prior to sample measurement at each session. Component data were transferred to the main frame computer to calculate declinations, inclinations and intensities via a series of Fortran programs to manipulate and process the cryogenic output.

As a result of the modified Livingston coring technique, each 2m core section is randomly oriented in the horizontal plane. Relative declination data are first

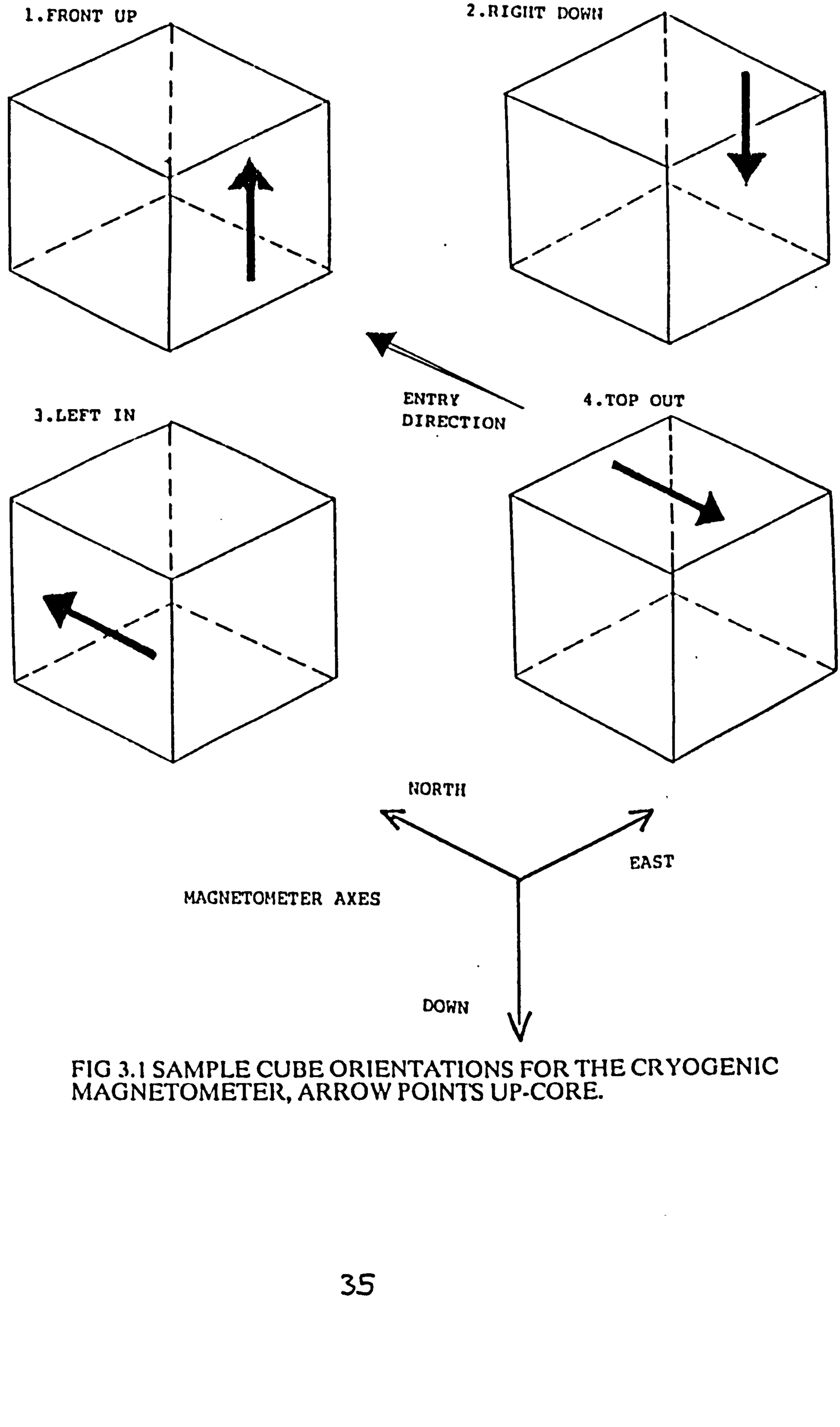

FIG 3.1 SAMPLE CUBE ORIENTATIONS FOR THE CRYOGENIC MAGNETOMETER, ARROW POINTS UP-CORE.

arbitrarily recovered by setting the average declination for each section to zero. This result was then improved by rotating individual sections to match trends visibly out of alignment across section boundaries. Inclinations have not been adjusted because misalignments of the core tube axis from the vertical were not measured during coring and in any case are thought to be small.

A Bartington Susceptibility Bridge was used to measure the magnetic susceptibility of all samples from all cores in the palaeomagnetic study. Susceptibility, in conjunction with intensity data from the cryogenic magnetometer, can contribute knowledge on the past geomagnetic intensity. The susceptibility, which reflects the amount and type of magnetic minerals present and hence the ability of the sediment to record the field intensity, can be used to normalise the NRM intensities.

Conversion of cores A, B, D and E to a common depth scale to allow for variations in sedimentation rate over the lake and enable direct comparison of the directional data has been achieved on the basis of intensity correlations. Core B has been used as the standard since it was the longest (FIG 3.2).

3.3 RESULTS

The NRM intensity data exhibit three phases: firstly, the upper 1.5m where the intensity is high (up to 1000 mA m^{-1}); secondly a phase of very low intensity, below 50 mA m^{-1} between 1.5 and 5.5m, and finally a phase with intensity fluctuating around approximately 500 mA m^{-1} in a series of irregular spikes.

The magnetic susceptibility records (FIG 3.3) have a similar form to the intensity records. High values above 1.5m, then a section of very low values extending down to approximately 6m, and then a gradual increase to fluctuate around 65m^3 kg^{-1}. FIG 3.3a highlights the variation in intensity and susceptibility where these are relatively low, by plotting as log(int) and log(susc).

Declinations have a range of less than 100^o (FIG 3.4). The scatter is considerable

FIG 3.2 MFM NRM INTENSITY PROFILES FOR CORES A, B, D AND E. CORRELATION BETWEEN THESE WAS USED TO CONVERT TO A COMMONDEPTH SCALE BASED ON CORE B. (with sed. units marked)

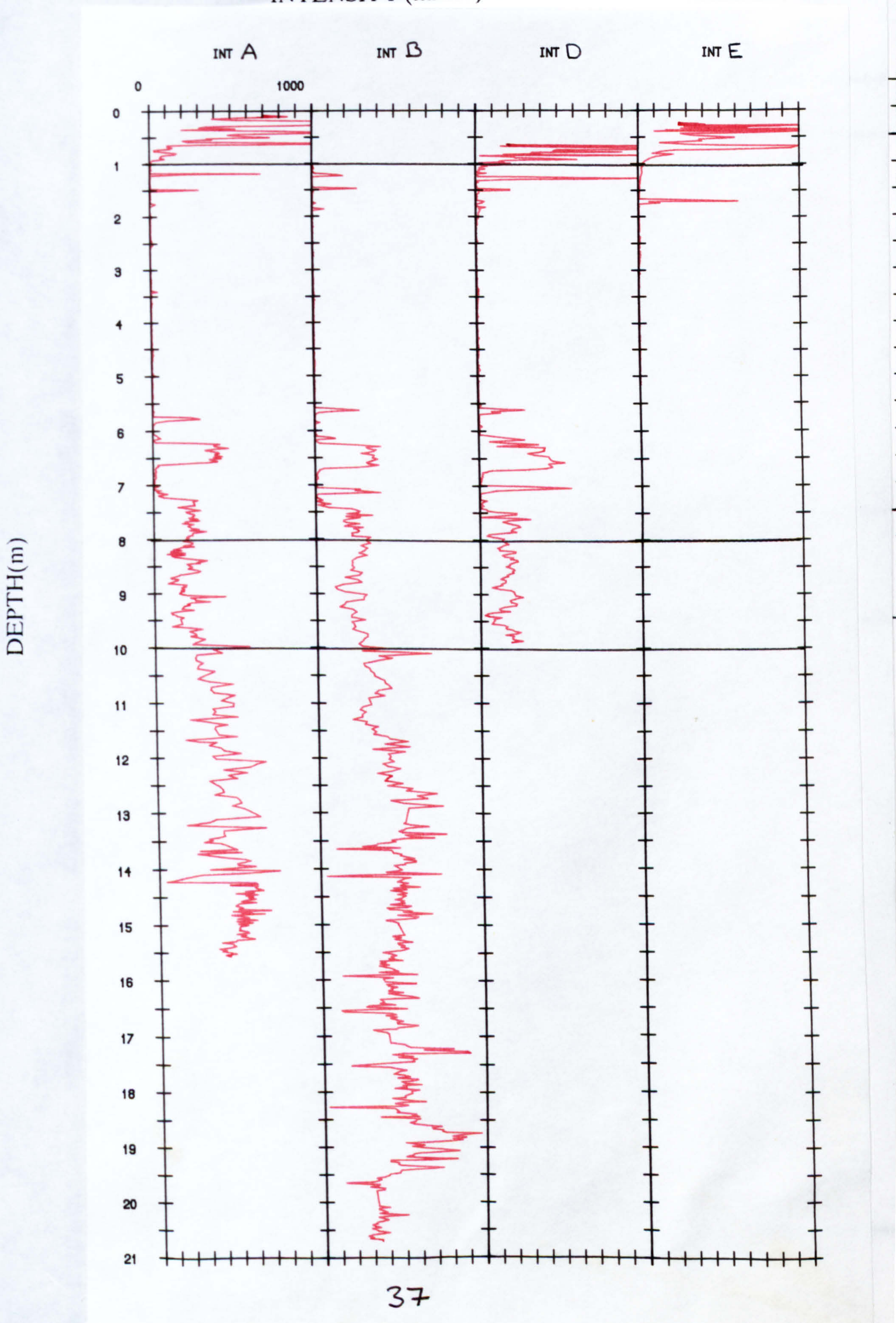

FIG 3.3 MFM MAGNETIC SUSCEPTIBILITY PROFILES FOR CORES A, B AND D. (with sedimentary units marked)

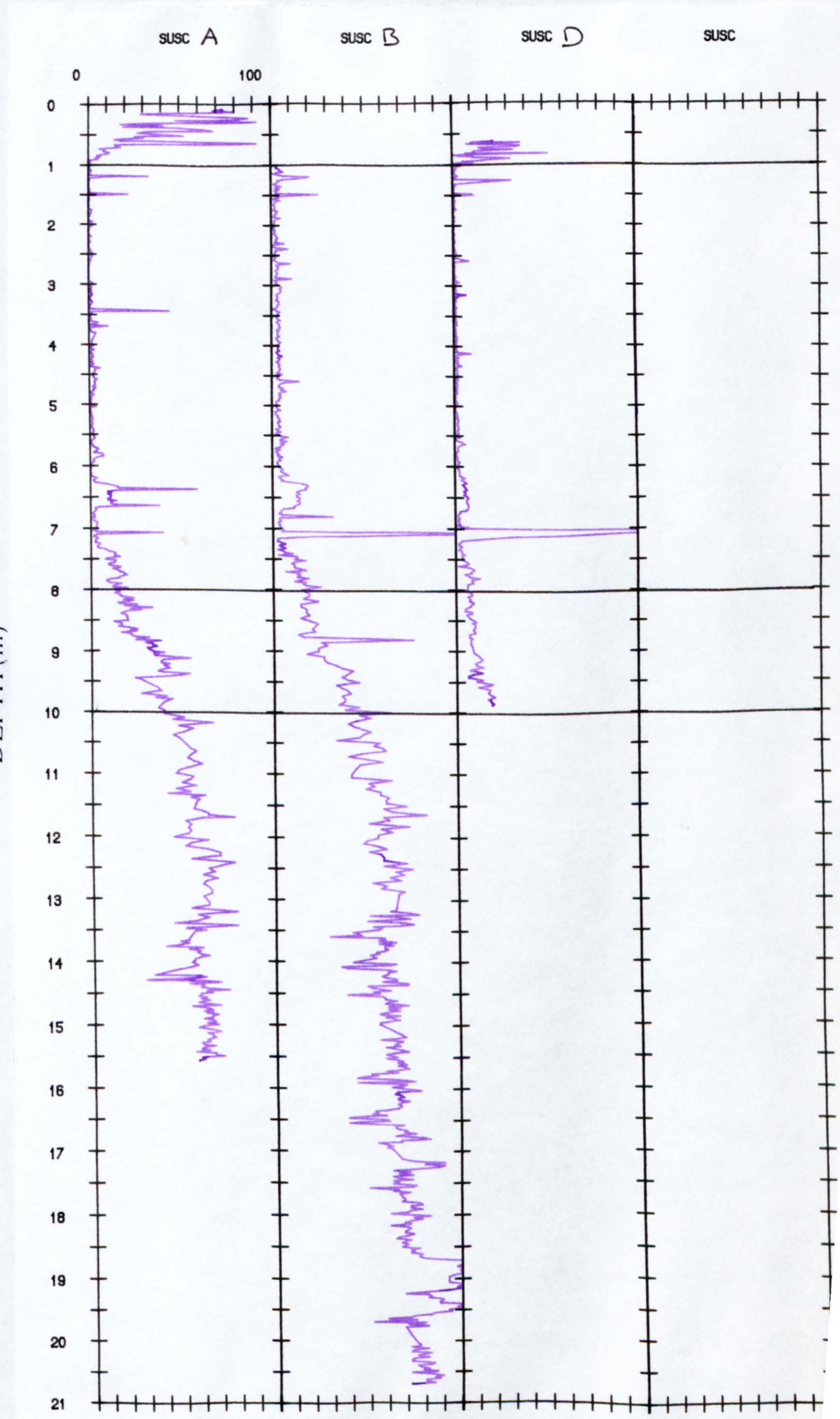

SUSCEPTIBILITY ($m^3 kg^{-1}$)

FIG 3.3a THE VARIATION OF LOG(INTENSITY) AND LOG(SUSCEPTIBILITY) WITH DEPTH FOR CORE B. THIS HIGHLIGHTS THE VARIATION WHERE INTENSITY AND SUSCEPTIBILITY ARE RELATIVELY LOW.

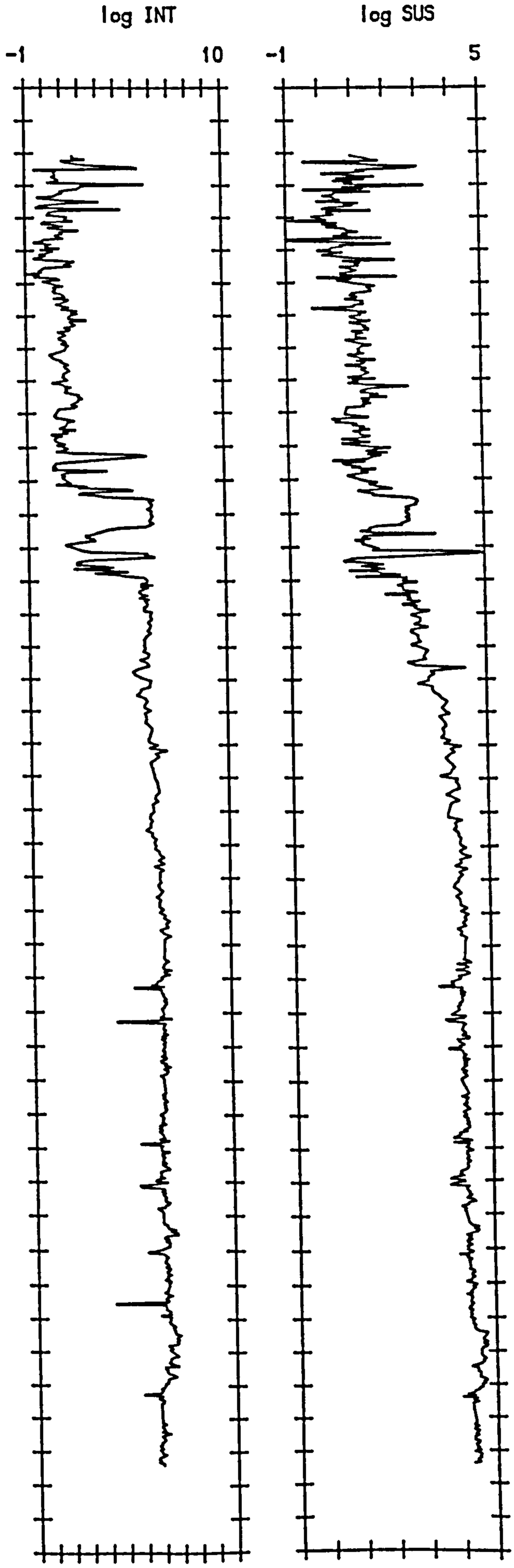

(standard deviation over a 10cm depth window is typically 9.1°) in the top 6m failing to define any coherent variation. Below 6m the data are less scattered (standard deviation over 10cm depth window typically 4.7°), developing a distinct though discontinuous record. Continuity between the cores also emerges. Further improvement in data quality occurs below 15m where the standard deviation over a 10cm depth window reduces to typically 3.3°.

Variation of inclination with depth (FIG 3.5) has a range between 30 and 80°, similarly to the declination record, the scatter is pronounced (standard deviation over a 10cm depth window 8.1°). Only below 14m does the data improve sufficiently to exhibit a tight continuous variation (standard deviation over a 10cm depth window 2.0°).

3.4 DISCUSSION

Removal of the softest components by 10mT alternating field demagnetisation resulted in a decrease of the NRM intensity by approximately 20%. The declination and inclination records do not exhibit any systematic shifts, suggesting that the weak magnetic overprint removed by cleaning is randomly directed, possibly a drilling remanence. There is a decrease in scatter on cleaning.

The decrease (going up core) of both the intensity and susceptibility at approximately 6m is associated with the increase in the proportion of organic material (CHAPTER 1) and consequent dilution of magnetic grains which are part of the clastic component (CHAPTER 7). The unexpectedly high intensity and susceptibility values for the top 1.5m is probably an anthropogenic effect from the burning of soil for agriculture to form magnetite, a strongly magnetic mineral, from hematite a weakly magnetic mineral (THOMPSON and OLDFIELD 1986). The general similarity of the susceptibility to the intensity record deteriorates when considering the data on a smaller scale, this is to be expected since the susceptibility is a product only of the magnetic mineralogy, where as the intensity is additionally influenced by the geomagnetic intensity at the time of magnetisation.

FIG 3.4 MFM DECLINATION RECORDS FROM CORES A, B, D AND E. (with sed. units marked)

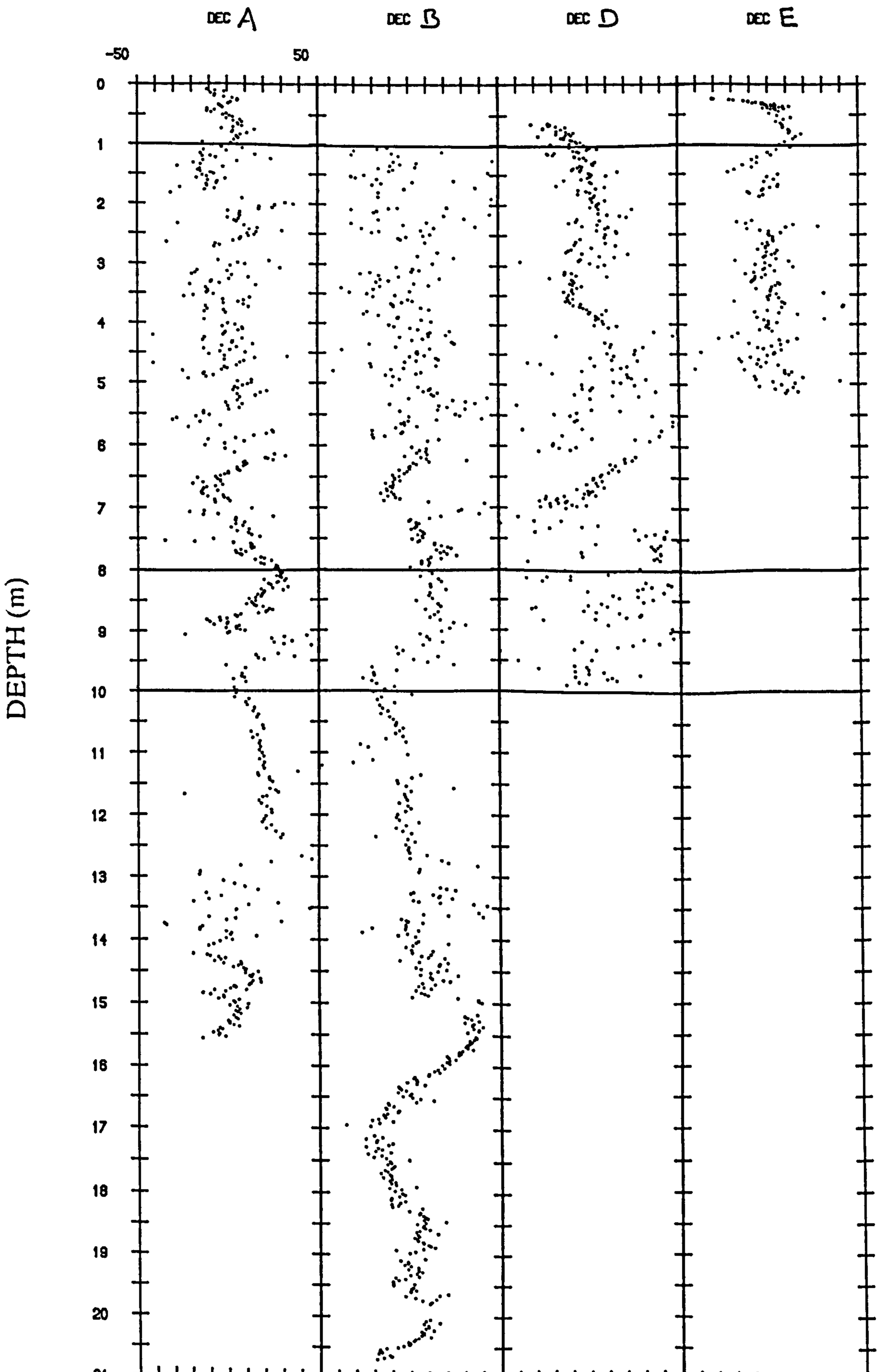

FIG 3.5 MFM INCLINATION RECORD FROM CORES A, B, D AND E. (with sed. units marked)

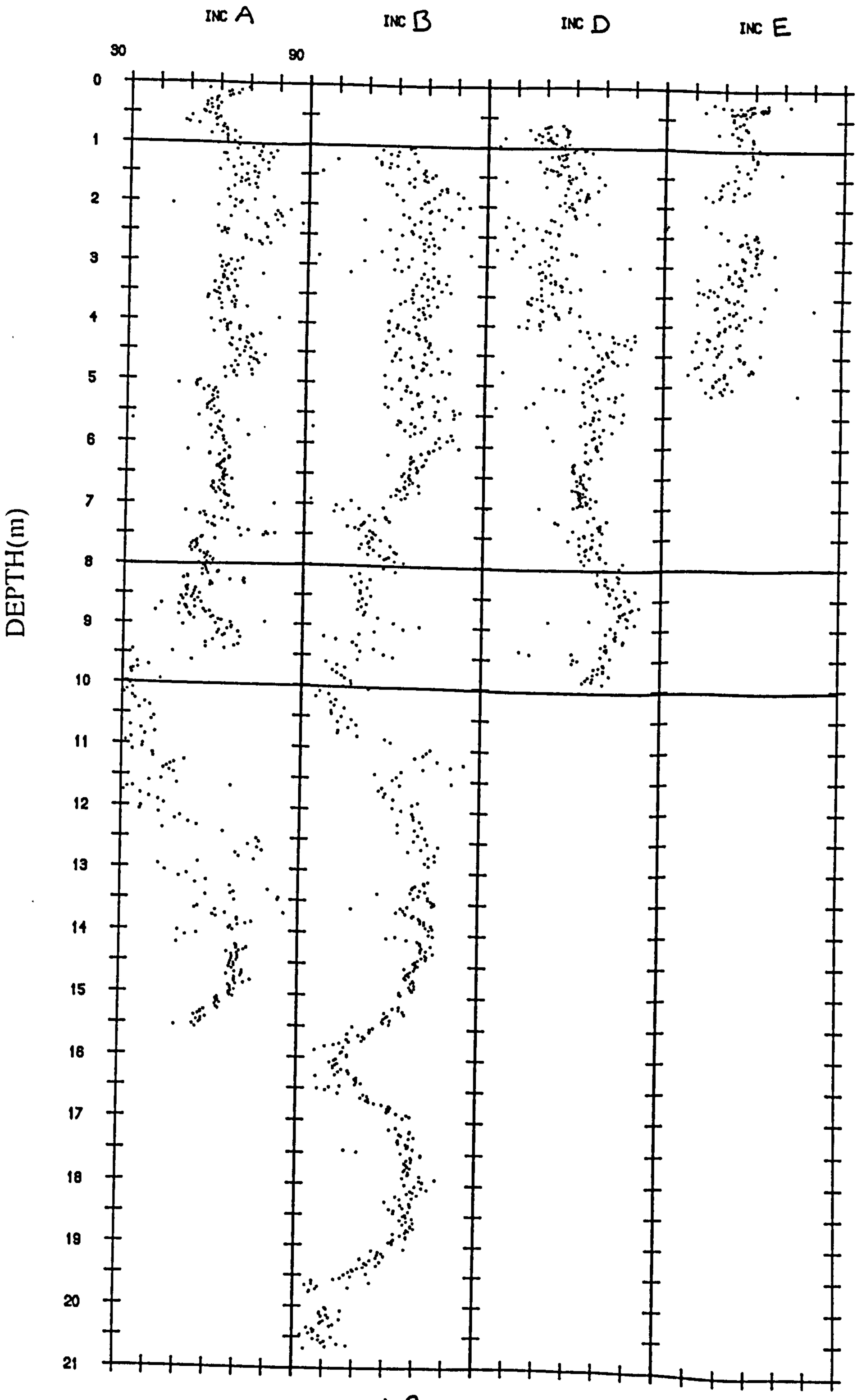

Correlation between inclination records although not as good as for intensity and susceptibility, is better than that for declination which is not affected by the inaccuracies involved in section realignment. The changes in quality of the directional data are visibly coincident with sedimentological variations, indicating some degree of control over the palaeomagnetic record by the sedimentology. The high scatter of the Post Glacial period directional data is probably the consequence of the high organic content, up to 20%, which in addition to diluting the magnetic mineral concentrations may also distort the palaeomagnetic signal. The record immediately below the Post Glacial boundary must be influenced by the presence of turbidites and cross-bedding structure revealed by the sedimentological study (CHAPTER 1).

3.5 SUMMARY

Palaeomagnetic measurements by cryogenic magnetometer and susceptibility bridge of AF cleaned A, B, D and E core and their conversion to a common depth scale based on magnetic intensity correlations has produced comparable directional data for four MFM cores. The quality of declination and inclination data, based on the visual scatter and correlation between cores, varies greatly, this appears to be linked to the sedimentology. The best directional data is found below 14m, however, only MFM B core extends significantly beyond this level.

In order to interpret these results fully and allow inter-maar comparison with Lac du Bouchet, it is necessary to transform the common depth scale to a time scale, this is the subject of the following chapters.

CHAPTER FOUR.

THERMOLUMINESCENCE DATING OF LAKE SEDIMENTS.

4.1 TIMESCALING

Creating a good depth to time transform function is a critical step in the processing of palaeomagnetic data. It has also been one of the more elusive requirements to fulfil (CREER 1985). Interpretation of a palaeomagnetic signal as past geomagnetic behaviour can only be appropriate if the data is a time-series.

MFM, with its seasonally sedimenting algal bloom provides a varve framework from which a chronology has been constructed by careful microscopic counting of the individual varve layers by B.ZOLITSCHKA at Trier university (Germany). This has been produced from work on MFMB core and has been directly related to the log(susceptibility). Hence, by plotting the log(susc) profile for MFMB core, spikes labelled and dated on the original, may be distinguished and therefore given an age. In addition, the marker horizon LBT (Laacher see Bimms Tuff) layer can be given an age of 10,950 yrs BP (LORENZ 1973). The depth to time transform based on this data is shown in FIG 4.1 . Application of this function to the palaeomagnetic data has the effect of squashing and stretching the signal into true proportion. After 11,000 yrs BP the average sedimentation rate was on average less than 1mm/yr, before this a rate of 2.5mm/yr characterises the period of cross-bedding and turbidites, below this a slower rate of approximately 1mm/yr prevails into the Late Glacial.

Most lakes do not have the possibility for constructing a varve chronology and other dating techniques must be used. MFM with its ready made varve chronology (ZOLITSCHKA 1989 pers comm) presents the opportunity for testing thermoluminescence as a lake sediment dating technique. Cores MFMC and MFMF were specially sampled for TL to evaluate the ability of the technique in this unestablished application. In the most recent review paper, BERGER (1988)

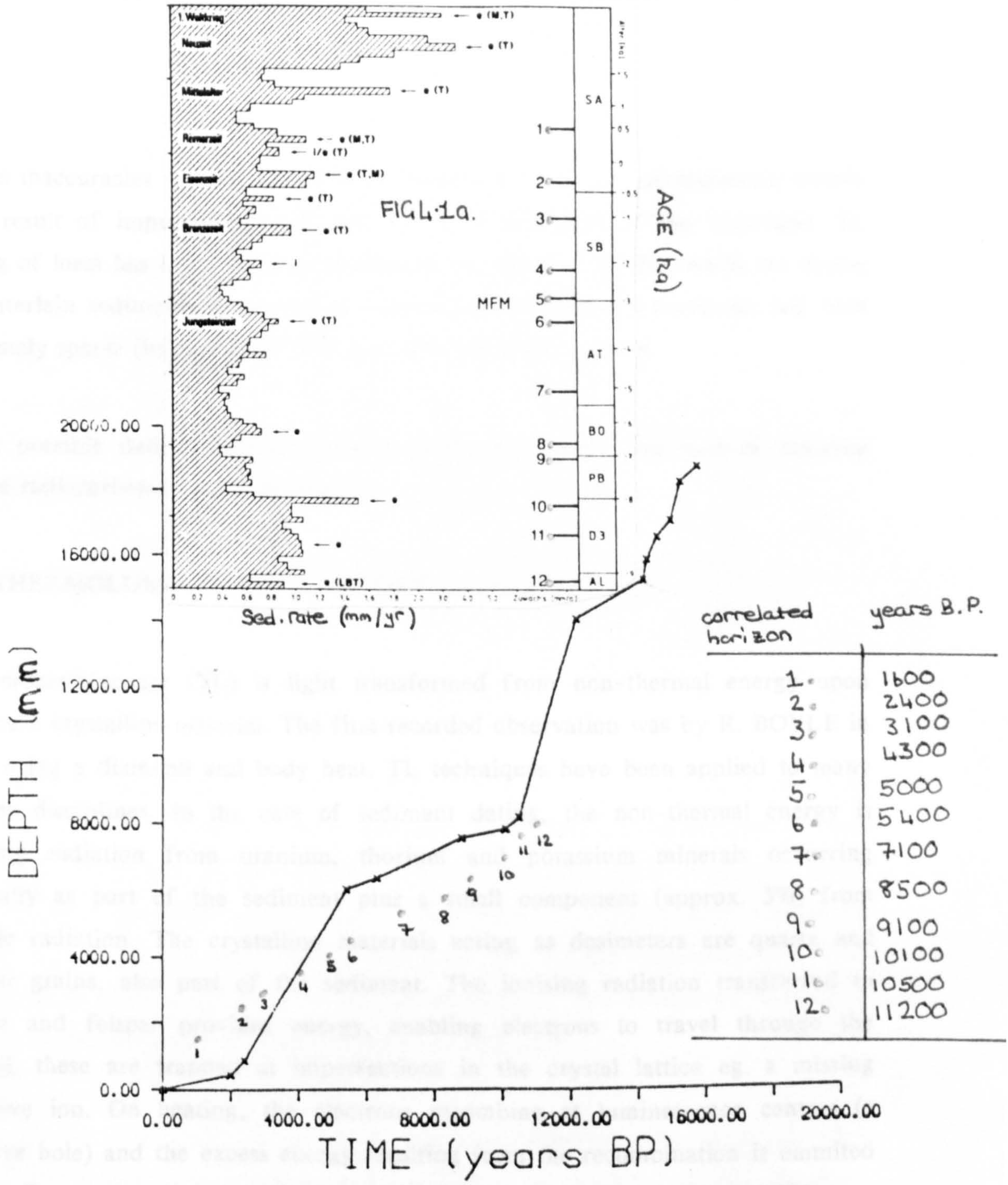

correlated horizon	years B.P.
1	1600
2	2400
3	3100
4	4300
5	5000
6	5400
7	7100
8	8500
9	9100
10	10100
11	10500
12	11200

FIG 4.1 DEPTH TO TIME TRANSFORM FOR MFM BASED ON THE VARVE CHRONOLOGY ACCORDING TO ZOLITSCHKA (1988).

The time transform used in this thesis is based on 14 marker features of the log susceptibility profile, which is consistent between cores MFM A and B, and tied to varve ages. The varve chronology itself comprises more than 100 ages. These have been utilised by NEGENDANK et al (1990) see FIG 4.1a, to produce a more sophisticated transform which exhibits some differences to the one presented in this thesis (the main 12 features constraining the improved Holocene transform are overprinted in green). Had this data been available, it would have altered to some degree the time scaled palaeomagnetic data presented in chapter 6, influencing the Fourier and correlation analyses as well as the organic carbon geochemical data described in chapter 7.

quotes inaccuracies greater than 50% as common for TL ages of sediments mainly as a result of improper methods and not as a limitation of the technique. TL dating of loess has been the most successful eg. WINTLE (1981), while the dating of waterlain sediments in general and lacustrine sediments in particular has been extremely sparse (but see BERGER et al 1987) and inconsistent.

Other possible dating methods suitable to the age range and type of material maybe radiocarbon or potassium-argon.

4.2 THERMOLUMINESCENCE THEORY

Thermoluminescence (TL) is light transformed from non-thermal energy upon heating a crystalline material. The first recorded observation was by R. BOYLE in 1663 using a diamond and body heat. TL techniques have been applied to many diverse disciplines. In the case of sediment dating, the non-thermal energy is ionising radiation from uranium, thorium and potassium minerals occurring naturally as part of the sediment plus a small component (approx. 5%) from cosmic radiation. The crystalline materials acting as dosimeters are quartz and felspar grains, also part of the sediment. The ionising radiation transferred to quartz and felspar provides energy, enabling electrons to travel through the crystal; these are trapped at imperfections in the crystal lattice eg. a missing negative ion. On heating, the electrons recombine at luminescence centres (a positive hole) and the excess energy resulting from the recombination is emmited as TL. For a comprehensive background to TL theory see McKEEVER (1985).

Unheated sediment dating by TL was proposed by WINTLE and HUNTLEY (1979), who established the technique as an absolute dating device through work on deep sea cores. Previous TL dating was limited to baked archaeological specimen (FLEMING 1970, ZIMMERMAN 1971). The critical knowledge in the use of TL for sediment dating is the fact that TL is reduced to zero or some residual level by exposure to sunlight during weathering and erosion by a process of optical bleaching (WINTLE and HUNTLEY 1979). On deposition, the sediment grains acting as weak dosimeters, accumulating TL with time by reason of exposure

to natural background radiation. This is generally linear up to a saturation point (SINGHVI and MEJDAHL 1985) and therefore reflects the time since deposition (the most reccent zeroing event (GEMMELL 1985)).

Apart from the palaeodose of radiation absorbed by the natural dosimeters, the other parameter required before calculating an age is the dose rate. This is the level at which the quartz and felspars have been exposed to ionising radiation. This enables us to solve the simplest form of the age equation (MEJDAHL 1986):

AGE = PALAEODOSE / ANNUAL DOSE

4.3 THE TL UNIT

Our system for measuring TL (the palaeodose) consists of a controlled heater in an evacuable chamber capable of being nitrogen filled, with a photomultiplier placed above to record the TL glow curve. The photomultiplier is removable to be replaced by a radiation source, and a microcomputer used to both control the heater and record the temperature dependent TL via the photomultiplier (FIG 4.2). A full account of the TL unit constructed in the Edinburgh University Physics Department can be found in GALLOWAY (1990).

The radiation source, a Sr-90, 3.7 GBq type, was calibrated using predosed quartz sand (9.97+-0.30 Gy) provided by V.MEJDAHL from the Riso TL lab, Denmark. This was divided into a suite of identical samples which were given a range of additional doses from the Sr-90 source. The resulting TL levels measured (the methodology for TL measurement is covered in section 4.7). The series of TL values formed a straight line (correlation coefficient 0.998) which intersected the X-axis at -1.86 minutes added dose (FIG 4.3). This equates to a dose rate from the source of 89.3+-0.6 mGy/s or 5.36+-0.036 Gy/min.

4.4. THE GAMMA SPECTROMETER

There is a wide range of instruments and methods with which it is possible to

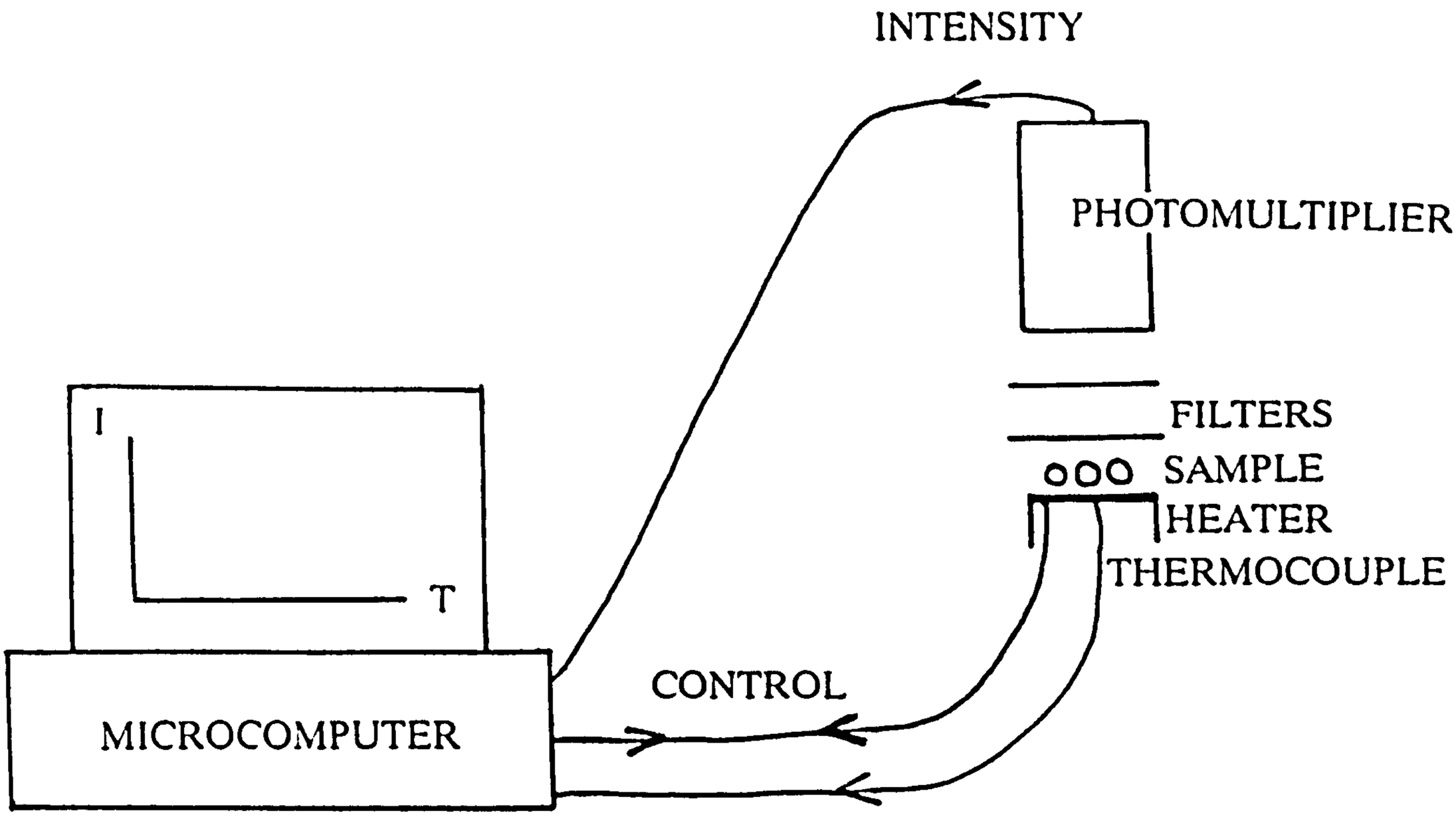

FIG 4.2 A SCHEMATIC OUTLINE OF THE TL UNIT.

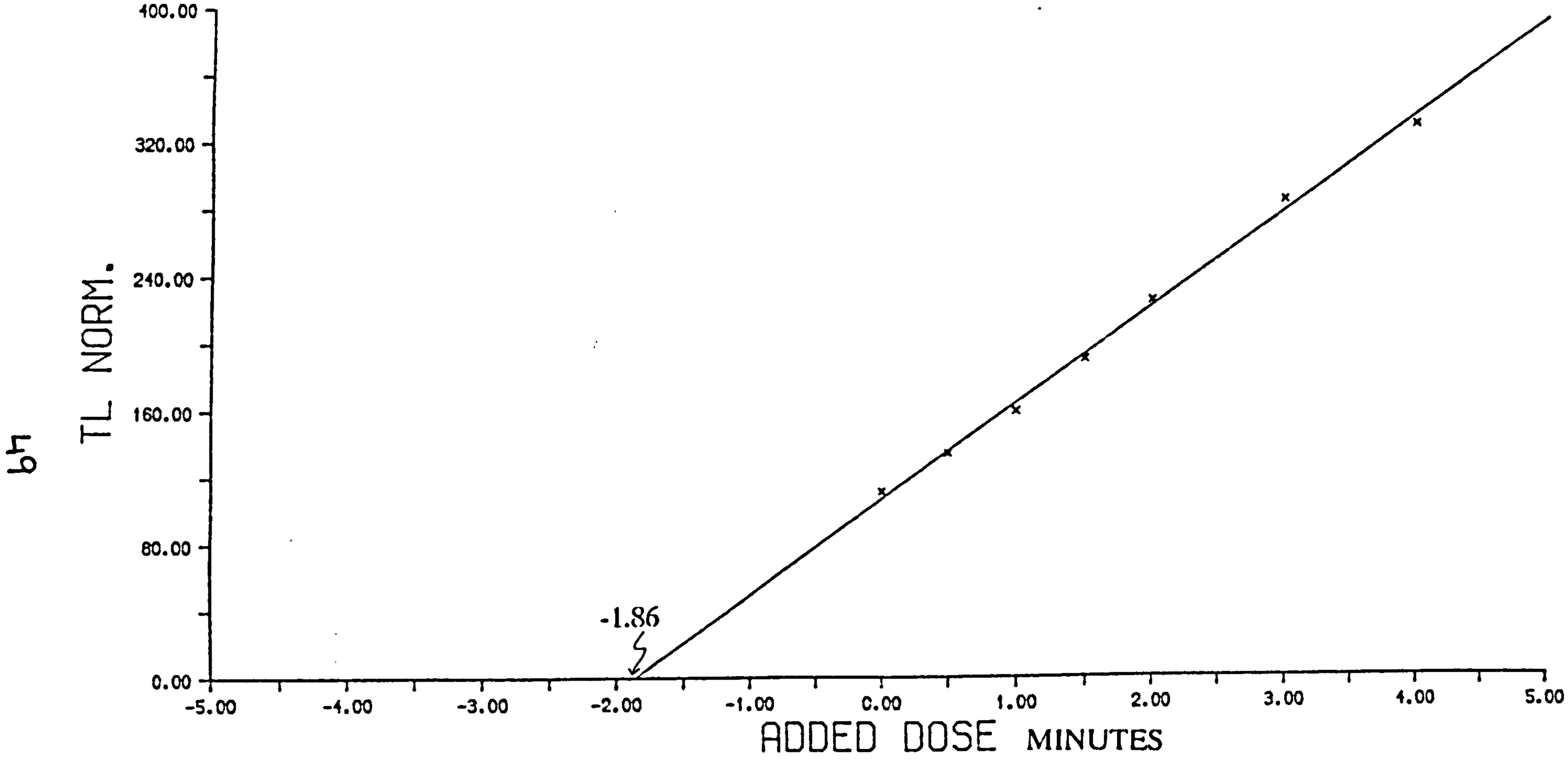

FIG 4.3 CALIBRATION CURVE FOR Sr90 B SOURCE.

measure the dose rate of sediment samples, these include (AITKEN 1979, PERNIKA and WAGNER 1982):

1. alpha counting with flame photommetry

2. TL dosimetry

3. gamma spectro :metry

4. neutron activation

In this study, gamma spectro metry with a high resolution germanium detector was used. This has the advantage of resolving the energy spectrum to the extent that it is possible to look at individual components in the decay series to detect departure from equilibrium. The germanium detector (52mm diameter by 20mm thick) is shielded within 100mm thick lead to exclude natural background radiation and interfaced with a BBC Master micro computer which controls the timed measurements. The 8k channel pulse height spectra are stored on floppy disc and the area under relevant peaks is calculated by integration, using software developed by R.B.GALLOWAY.

Calibration of the system to give the specific activity was based on standard uranium and thorium ores and on potassium salts to calibrate the system for response to potassium-40. In addition, alpha counting using silver doped ZnS screens was carried out as a check on the uranium and thorium contents.

Initially a series of measurements were implemented to determine the spectrometer response to MFM sediment, the geometry of the sample holder was varied to investigate any effect this might cause. The best result was achieved with cylindrical, clear plastic boxes approximately 2cm high and 4cm diameter; peak heights for the first 1000 channels were at least twice the background level. These

containers were then adopted as standard sample holders for all gamma spectrometer measurments. The differing masses of individual sediment samples is taken into account during data processing.

The gamma-spectrometer was calibrated by measuring the emitted gamma spectrum from pitchblende ores with known ratios of uranium and thorium minerals.

4.5 BLEACHING UNIT

For laboratory bleaching, predominantly to determine residual TL levels, a commercial sunlight simulator was used, the HONLE SOL2. This uses a high pressure metal halide lamp and specific filters to produce a close spectral similarity to natural daylight, (FIG 4.4) but at an average of 6.5 times the intensity.

A suite of 12 samples was prepared. Each sample was given an arbitrary 53.6 Gy (10min.) dose with the Sr-90 β source, the samples were then subjected to a range of SOL2 light exposures ranging from zero to 240 minutes. The TL levels were then measured. The resulting decay curve, FIG 4.5 , shows a sharp reduction in TL between 0 and 40 minutes, followed by a more gradual decline. On this basis it was decided to use the TL value after one hour SOL2 exposure as the residual TL level.

Having described the instruments used, the following sections deal with the methodologies involved in the TL age determination.

4.6 SAMPLE COLLECTION AND PREPARATION

Cores for TL analysis were extruded into overlapping tube 'halves' and wrapped in aluminium foil to prevent light penetration and escape of moisture. Sampling was carried out in a 'light safe' laboratory at Trier university. After scraping the surface sediment away, two samples, of approximately 20g weight, were taken side

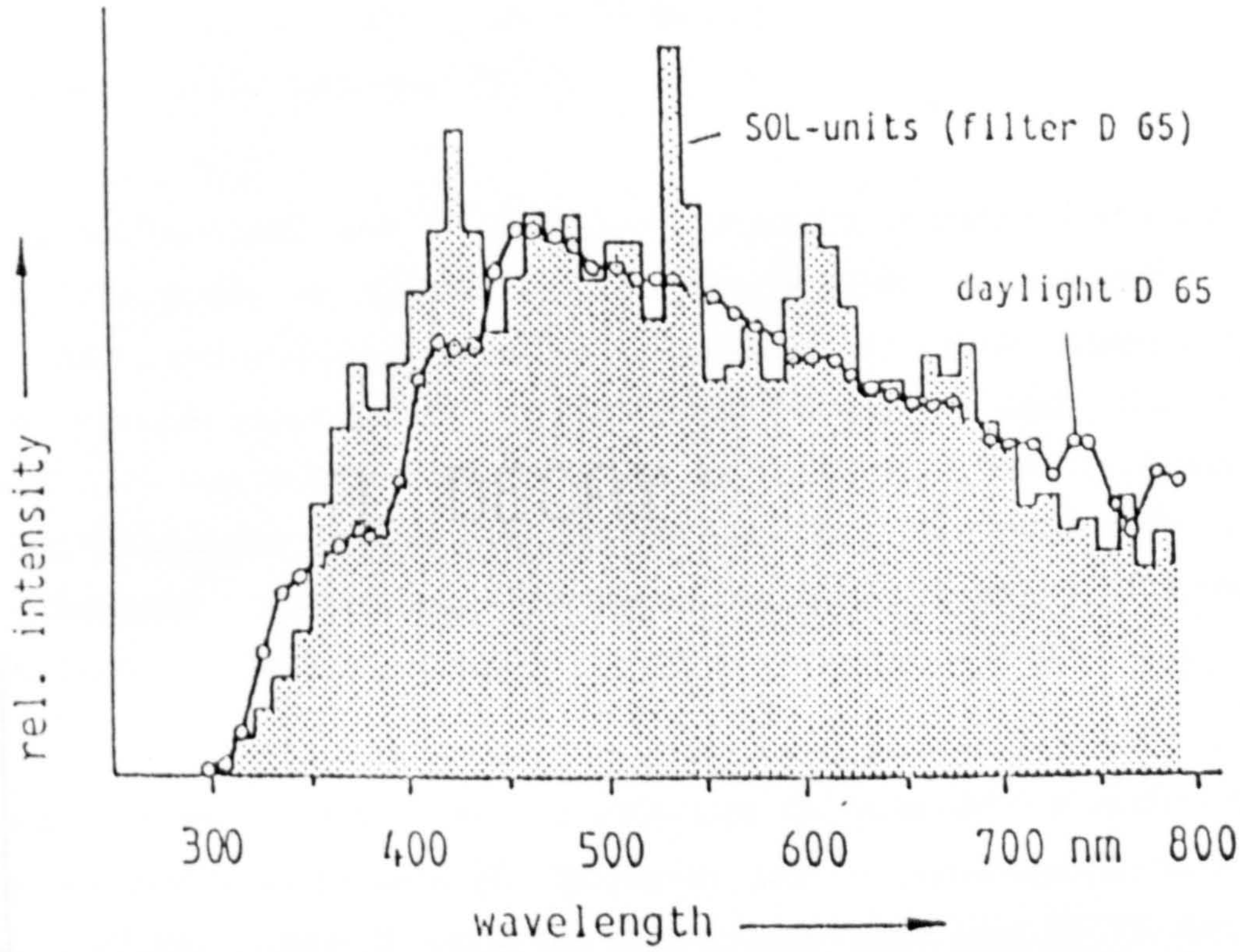

FIG 4.4 SPECTRAL DISTRIBUTION COMPARISON OF SOL2 AND DAYLIGHT.

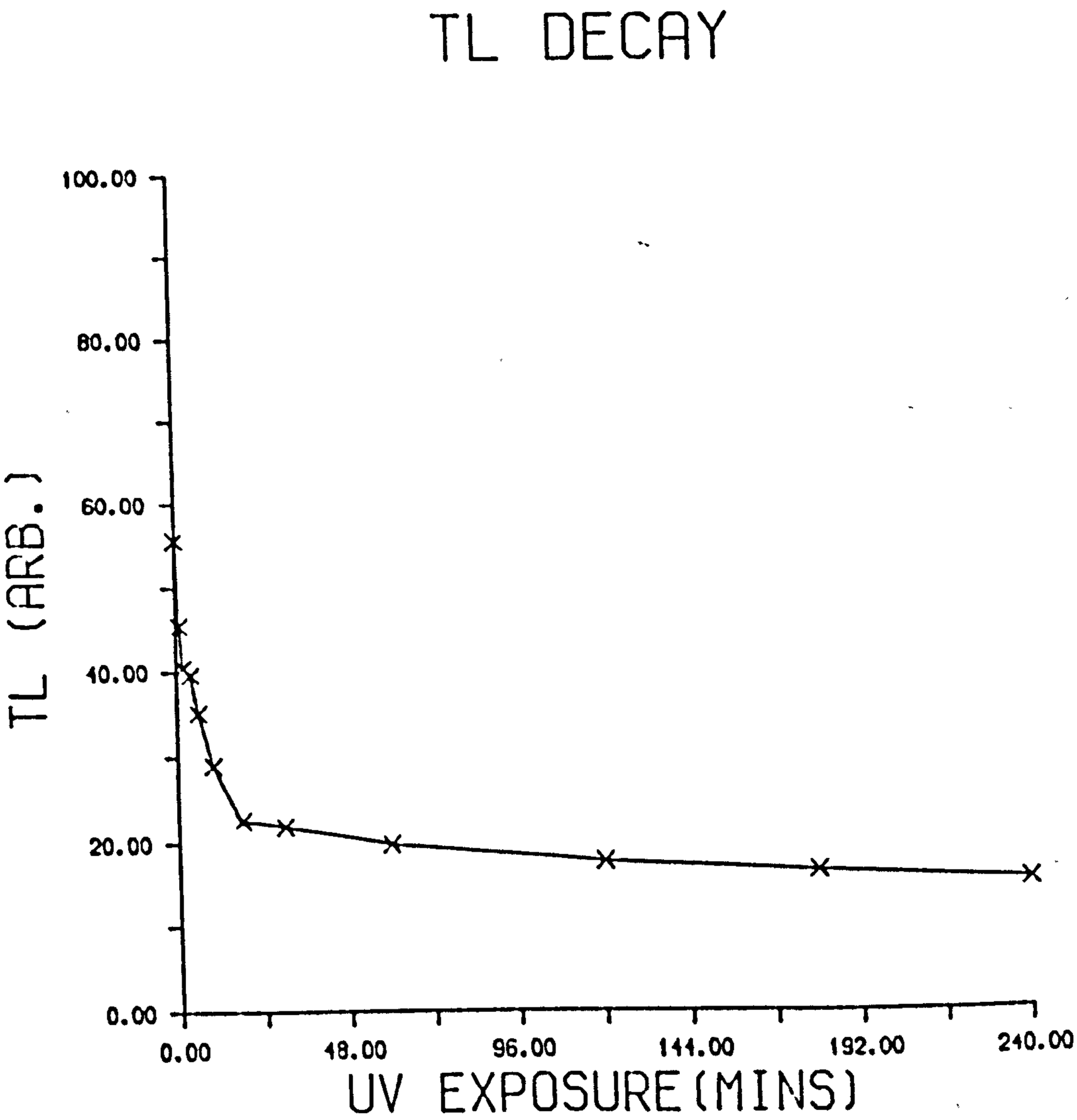

FIG 4.5 TL DECAY UNDER SOL2 SOLAR SIMULATOR

by side, one for palaeodose measurements the other for dose rate determination. The sub-samples were contained in plastic boxes and wrapped in aluminium foil for transportation to the Edinburgh TL lab.

To enhance the TL signal from the dosimeters a sequence of chemical treatment was devised to isolate the quartz fraction. This consisted of elimination of carbonates with hydrochloric acid, allowing digestion of organic material by soaking in hydrogen peroxide then removal of iron oxides with oxalic acid and aluminium. This was followed by treatment in hydrofluoric acid to remove felspars and by repeated flushing with distilled water to expel soluble salts. The remaining sediment, dispersed using 10% calgon, was sieved through a 90 micron mesh. The complete chemical preparation procedure is detailed in Appendix B.

The choice of grain size from which to determine the palaeodose is limited by alpha particle attenuation between 20 - 90 microns and the occurrence of spurious TL below 2 microns (WINTLE 1987). The most common grain sizes for TL dating are therefore greater than 90 microns and 4 - 11 microns. In MFM the greater than 90 micron fraction is extremely scarce and so the 4 - 11 micron fraction was selected for dating.

To separate the 4 - 11 micron fraction the sediment was dispersed in 1 litre measuring cylinders and allowed to settle for 29 mins 14 s to remove the greater than 11 micron fraction and again for 3 hrs 41 mins 8 s to collect the greater than 4 micron fraction. The settling times were calculated using STOKES LAW. The final stage of sample preparation is to resettle the treated sediment onto 10 mm diameter stainless steel discs as required.

Details of sediment treatment procedure were compiled and adapted from CARVER (1971) and PIPER (1974), application of STOKES LAW from WINTLE (1987).

4.7 TL METHODOLOGY

There are three main methods for determining palaeodose, (WINTLE and PROSZYNSKA 1983):

A. regeneration

B. total bleach

C. R-β

The technique adopted has been the R-β method developed by WINTLE and HUNTLEY (1980). It has the advantages of not introducing errors from dosimeter sensitivity changes on reheating and being capable of adaption to dating incompletely bleached sediments (MEJDAHL 1985).

Two suites of samples are prepared and each given a range of radiation doses from 5 mins to 1 hr, one suite is then bleached in the SOL2 for an hour. The following stages then apply to both suites:

1. Preheat individual samples to 250 ^{o}C. This is to empty non-geologically stable traps (MEJDAHL 1986).

2. Measure the TL output between 250 ^{o}C and 500 ^{o}C.

3. Redose sample for 5mins (26.8 Gy), preheat and measure TL again. This measurement was used as a 'normalising' value for the NTL + dose, It was found to give more consistent results as variations in the dosimeter efficiency between samples are taken into consideration.

4. Integrate glow curves (TL v's T ^{o}C) between 280 ^{o}C and 380 ^{o}C. These values were chosen as representing the zone of geologically stable TL determined from

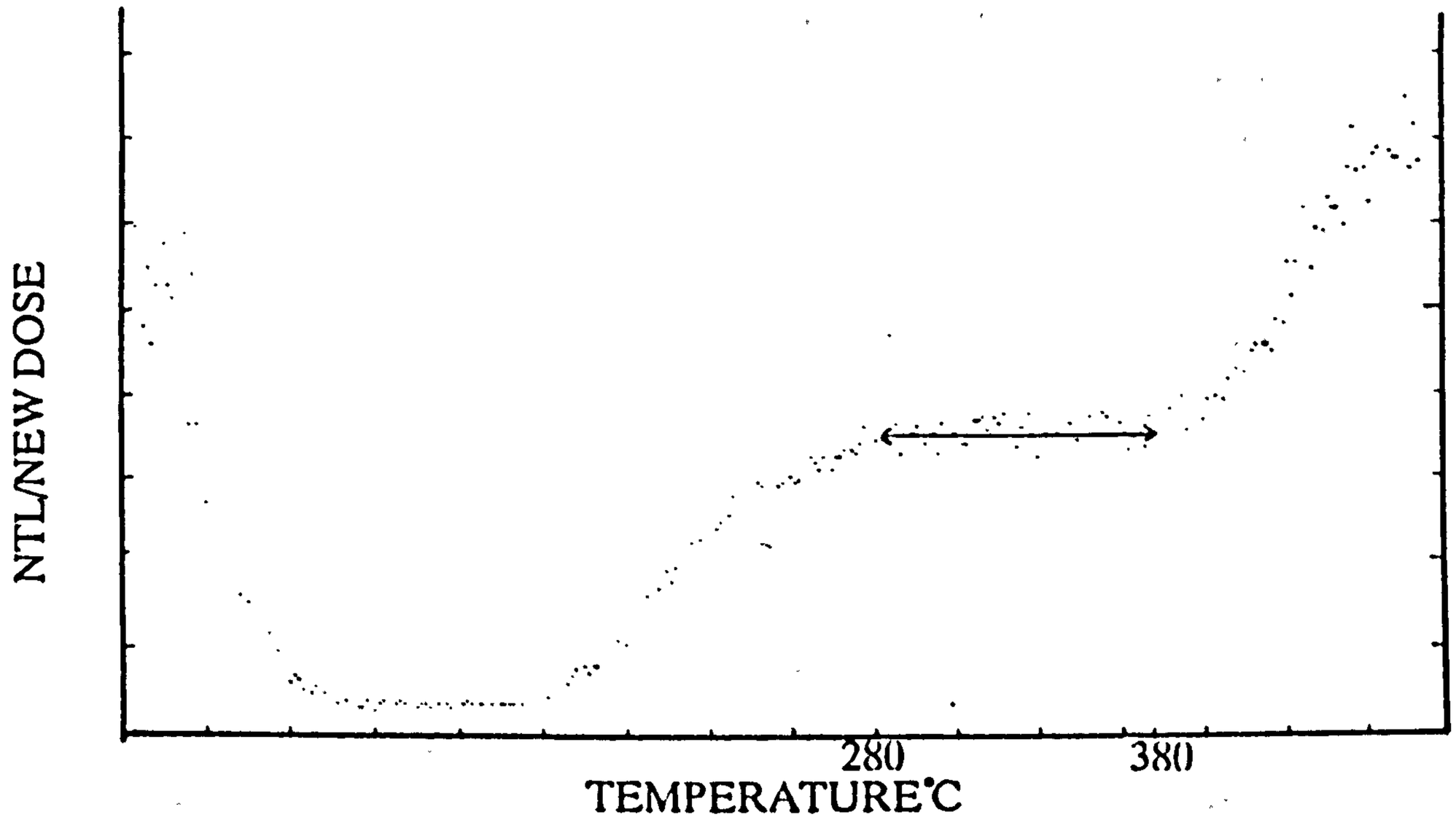

FIG 4.6 PLATEAU TEST SHOWING GEOLOGICALLY STABLE TL BETWEEN 280 AND 380°C. THESE VALUES WERE THEN CHOSEN AS THE LIMITS OF INTEGRATION FOR CALCULATING TL INTENSITY.

the results of a plateau test (FIG 4.6) where the glow curve for the full spectrum of a natural sample is divided by the full spectrum from the redosed drained sample. A plateau forms where there has been no loss of NTL (WINTLE and HUNTLEY 1982). Below 280 ^{o}C TL is unstable over a geological timescale and the NTL/NEW DOSE is low, NTL will also be lost in the sample preparation procedure. Above 380 ^{o}C NTL/NEW DOSE rises slightly, probably due to a decrease in sensitivity on the second heating. Luminescence at these temperatures is mainly black-body radiation.

5. Plot the normalised TL values for both sample suites (FIG 4.7) from which the equivalent dose (ED) can be determined by fitting regression lines extrapolated to intersection.

Prior to attempting routine TL measurement, tests for anomalous fading (WINTLE 1985, TEMPLAR 1986) were carried out. Two identical samples were given a 56.3 Gy β dose, the first was measured immediately as a control sample, the second stored in darkness for two weeks before measurment. Results: control TL = 66.9, after two weeks TL = 67.3, this is a 0.6% increase in TL indicating no significant difference beween TL levels in the two samples.

4.8 DOSE RATE METHODOLOGY

As previously discussed in section 4.4, the chosen method of dose rate determination was gamma spectrometry. Output is in the form of counts v's energy up to 8000 channels. Counting time was 24 hours and the resulting spectra were analysed by integrating below selected peaks (TABLE 4.1) to determine the activity. In the uranium-238 series five activity determinations were made on separate peaks which should, if the uranium series in in equilibrium, give the same result. Where results were variable, the highest and lowest were discarded and an average of the remaining three calculated. For thorium-232 and potassium-40 only one peak was analysed.

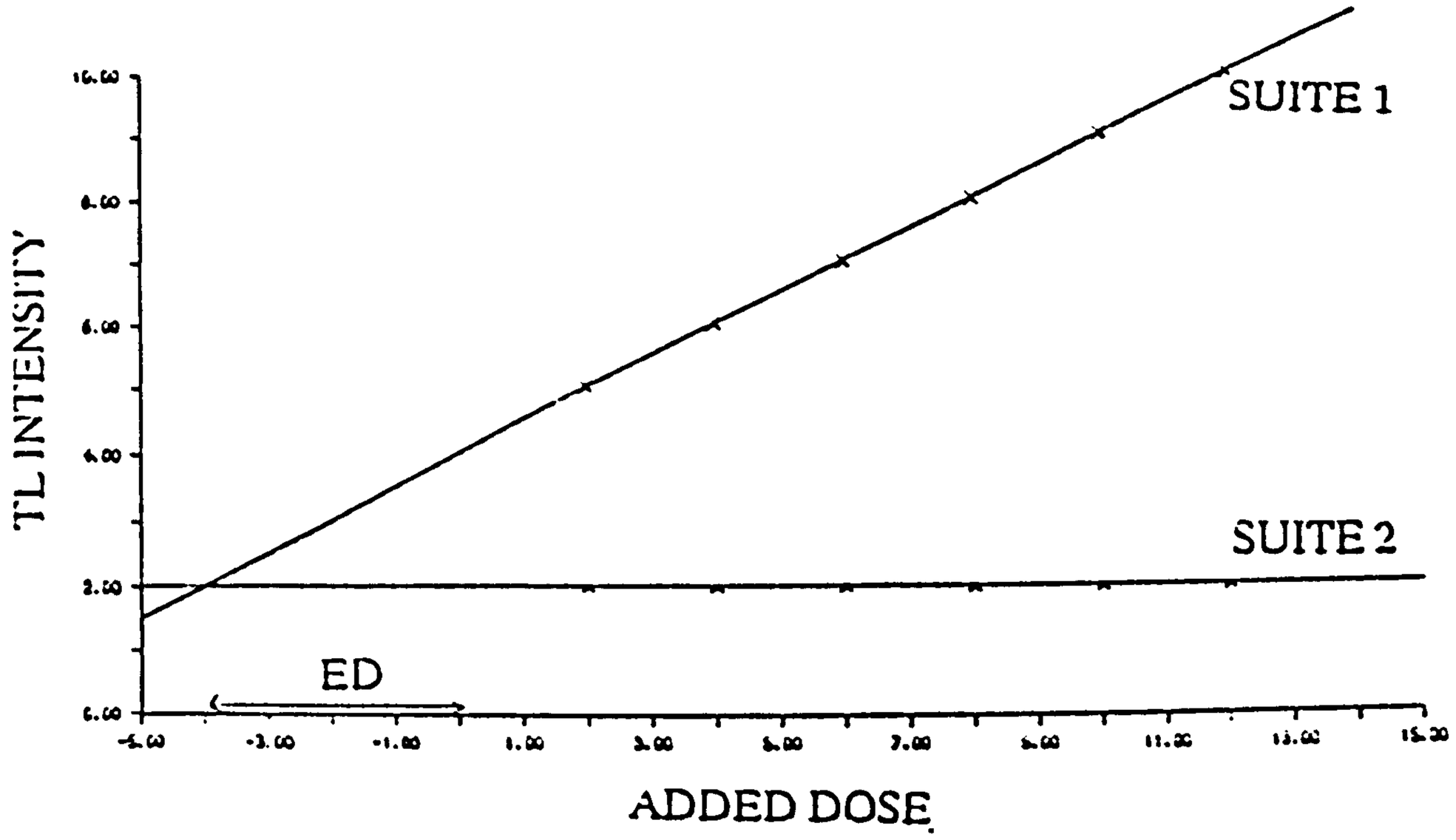

FIG 4.7 R-β METHOD OF DETERMINING THE EQUIVALENT DOSE (ED)
SUITE 1 = NATURAL TL + DOSE
SUITE 2 = NATURAL TL + DOSE, FOLLOWED BY A 1 HOUR BLEACH

TABLE 4.1 ENERGY PEAKS USED IN THE CALCULATION OF DOSE RATES FROM MFM SEDIMENT.

URANIUM-238 SERIES:

LEAD-210 46.5 keV

THORIUM-234 63.3 keV

RADIUM-226 186.2keV

LEAD-214 295.2 keV, 351.9 keV

BISMUTH-214 609 keV

THORIUM-232 SERIES:

LEAD-212 238.6 keV

POTASSIUM-40 :

POTASSIUM-40 1461 keV

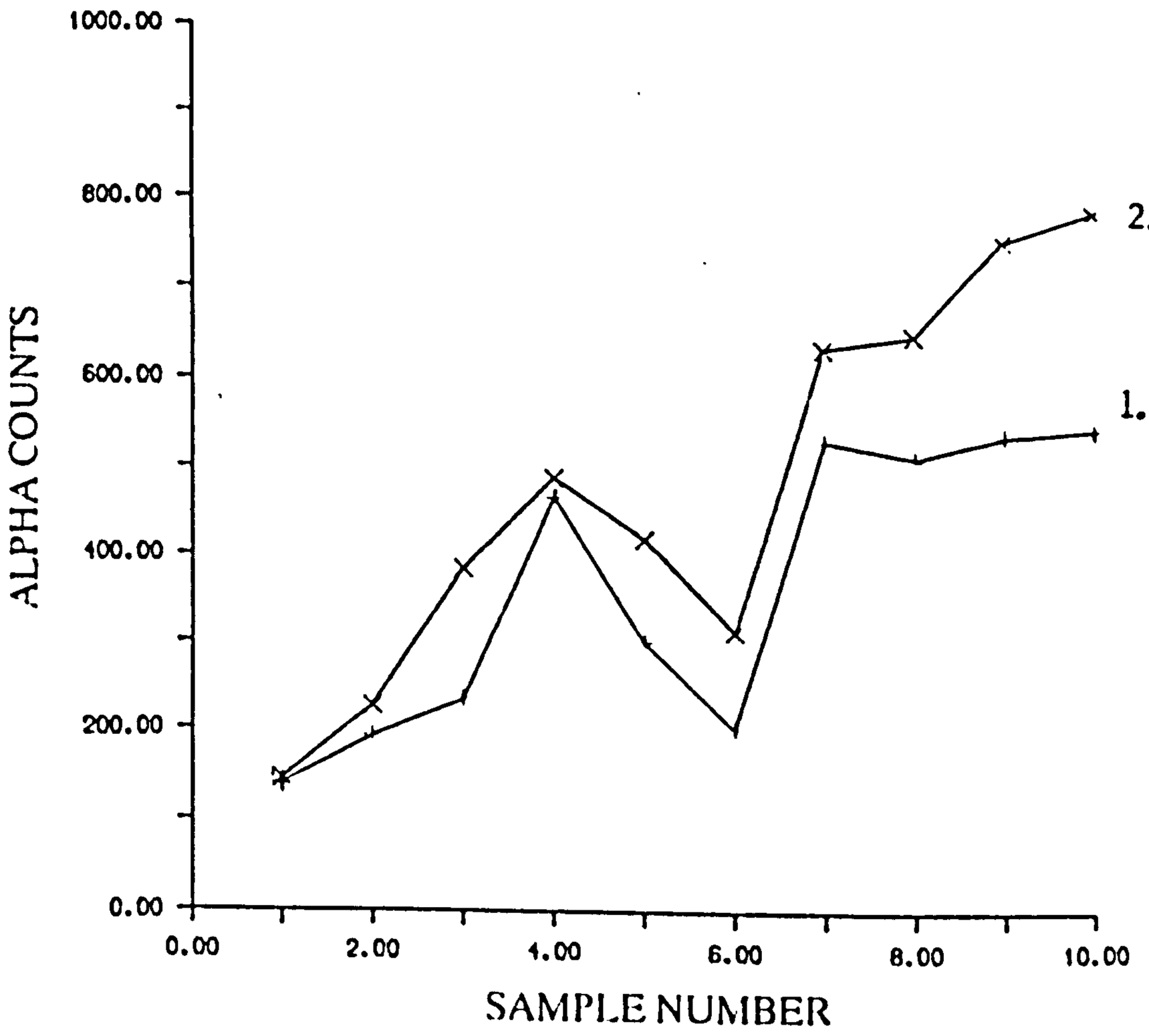

FIG 4.8 COMPARISON OF THE ALPHA COMPONENT CALCULATED FROM 1.GAMMA SPECTROMETRY WITH 2.THE RESULTS OF DIRECT COUNTING.

Calculation of dose rates (Gy/yr) from specific activities (Bq/kg) of U, Th and K was based on information in AITKEN (1985) assuming full-chain reactions and a homogeneous environment. Alpha ionising efficiency was assumed as 15%.

As an independent check on the gamma spectrometer results and calculations, the samples were subjected to direct alpha counting with silver doped ZnS scintillation screens for comparison. The results match well (FIG 4.8) although the counts calculated from the gamma spectrometer were consistently lower by up to 31%. ZOLLER and PERNICKA (1989) suggest direct alpha counting to over estimate true activity.

The instruments and methods described in this chapter were then applied to the preparation and dating of sediment samples. Chapter five covers the results and their discussion including estimates of accuracy.

CHAPTER FIVE.

THERMOLUMINESCENCE RESULTS FROM MEERFELDER MAAR.

5.1 TL RESULTS CORE F

Thermoluminescence measurements were carried out as described in section 4.7, on ten samples from MFM F core (F1 to F10). The results plotted as normalised TL values, from both the irradiated and bleached suites of samples (determined independently for each sample) are presented in FIGS 5.1a to 5.1h. The equivalent doses (ED) determined from these figures are listed in TABLE 5.1. A correction for laboratory light bleaching is included (section 5.3.5). Results for samples F1 and F3 are absent because insufficient material was produced in the preparation process.

5.2 DOSE RATE RESULTS CORE F

Dose rate determinations by gamma spectrometer as described in section 4.8, were carried out on ten samples from MFM F core (F1a to F10a). The results are presented as activity (Bq/kg) for the uranium and thorium series and for potassium. Dose rates (Gy/ka) were then calculated according to AITKEN (1985), assuming full decay chains, a homogeneous environment and an alpha ionising efficiency of 15%. Specific parent activity and the calculated dose rates are listed in TABLE 5.2.

5.3 SOURCES OF ERROR IN TL DATING

The four most important sources of error in TL sediment dating (MEJDAHL 1986) are considered:

FIG 5.1A MFM F2 TL

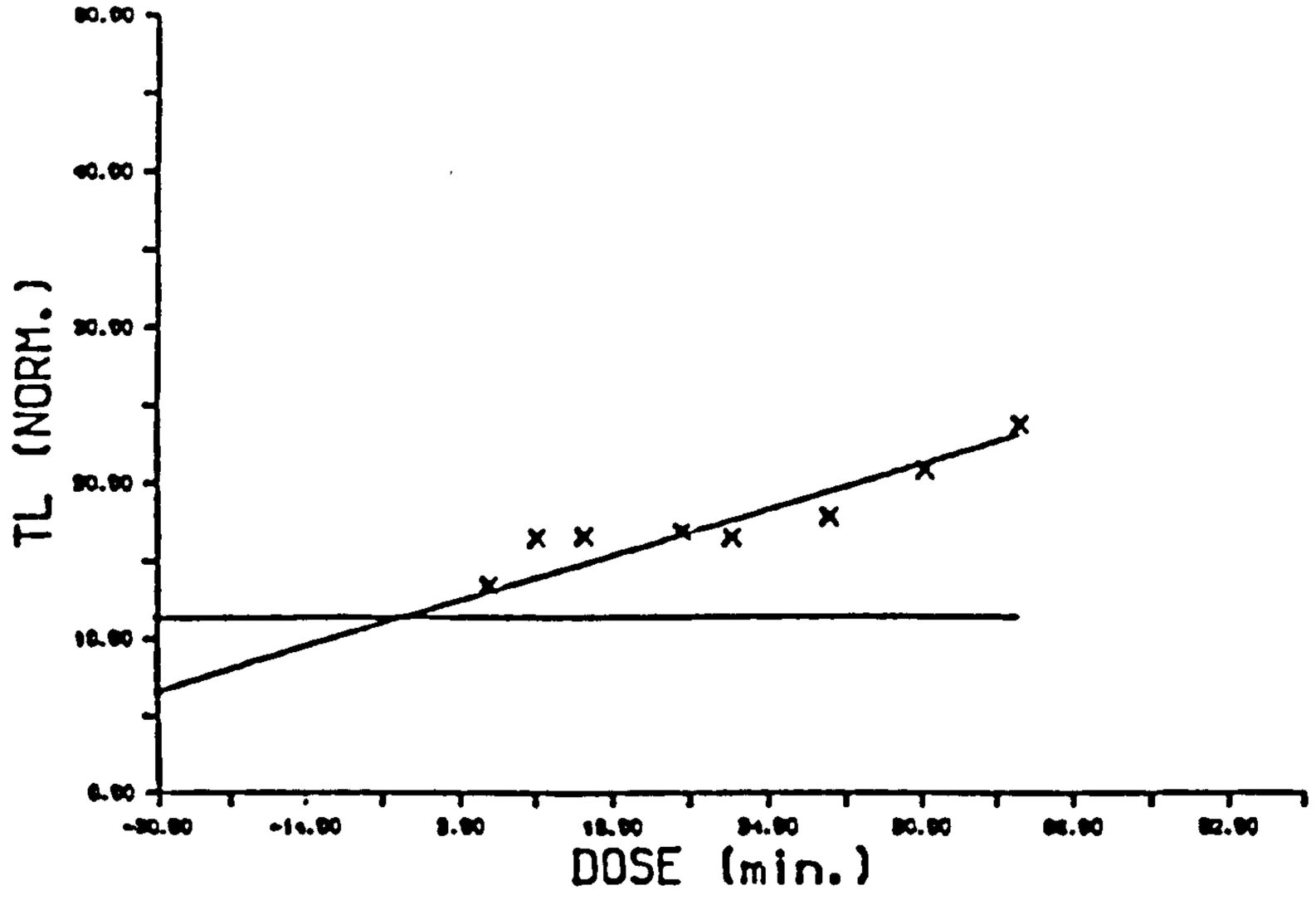

FIG 5.1B MFM F4 TL

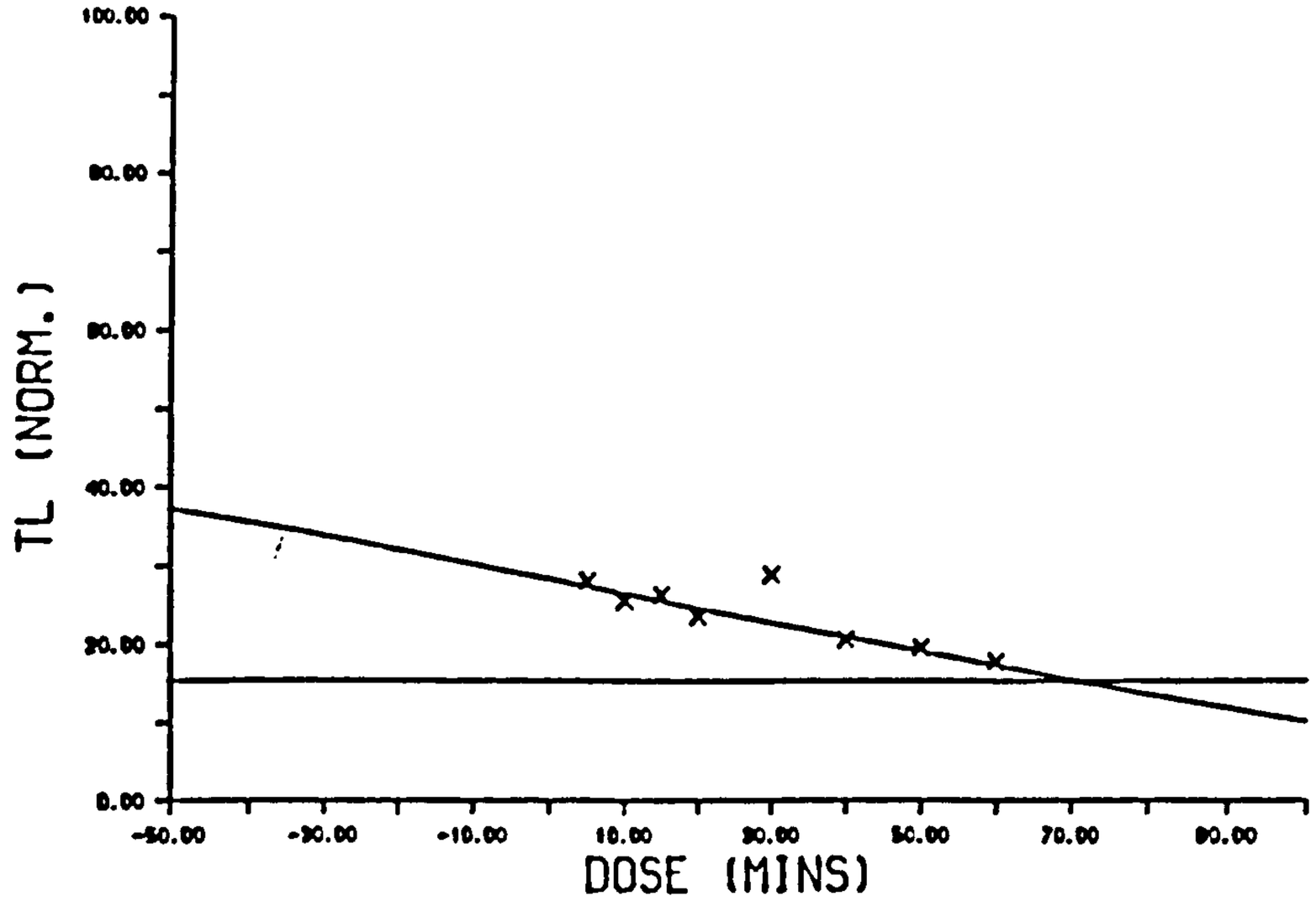

FIG 5.1a-h, THERMOLUMINESCENCE RESULTS FOR MFM F CORE SAMPLES. THE UPPER SLOPED LINE IS A LEAST SQUARES BEST FIT THROUGH THE IRRADIATED SAMPLE SUITE. THE LOWER HORIZONTAL LINE REPRESENTS THE UNBLEACHABLE TL COMPONENT CALCULATED INDEPENDENTLY FOR EACH SAMPLE AND CALCULATED FROM AN AVERAGE OF EIGHT SUBSAMPLES GIVEN A RANGE OF ADDED DOSES PRIOR TO BLEACHING.

FIG 5.1C MFM F5 TL

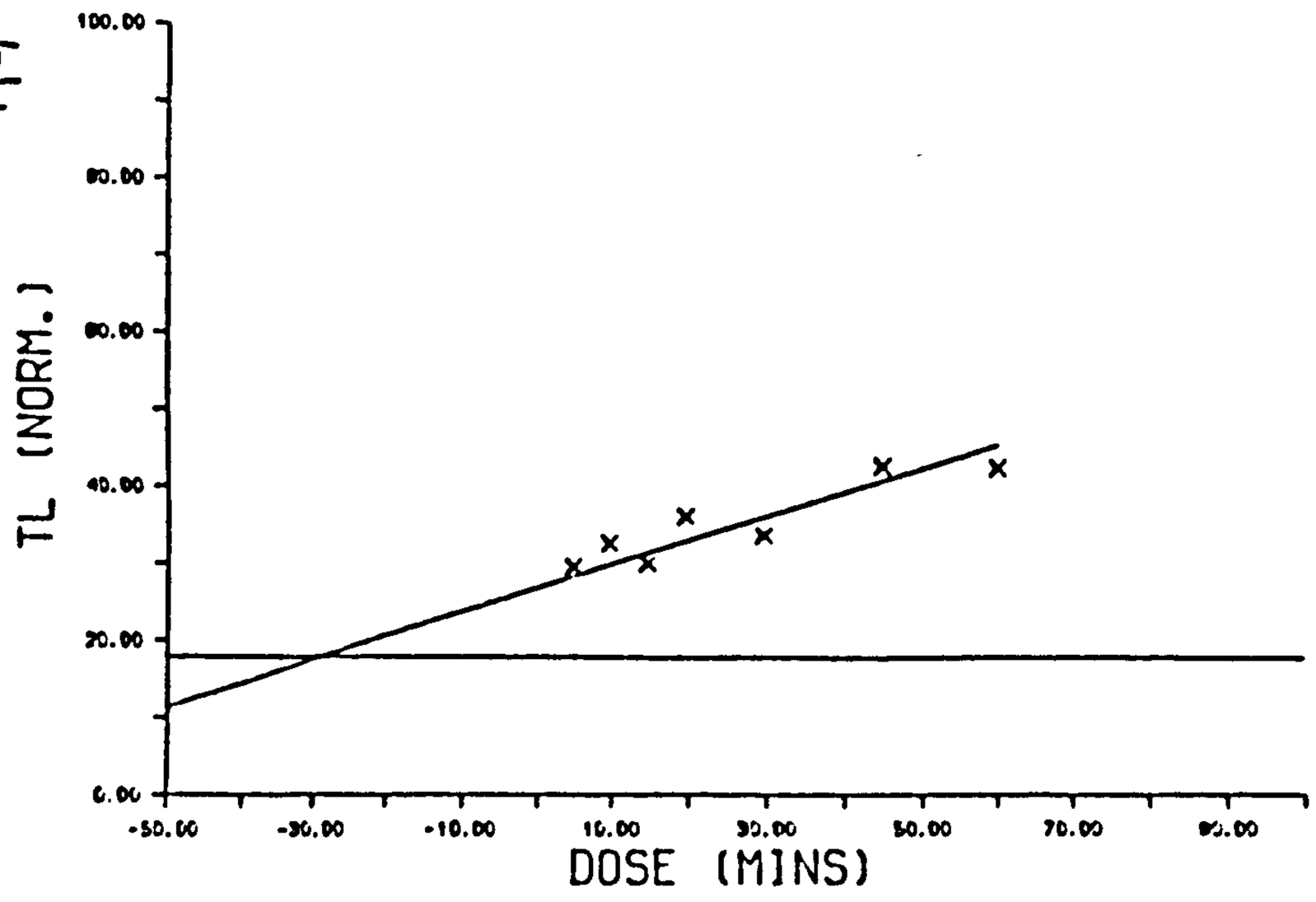

FIG 5.1D MFM F6 TL

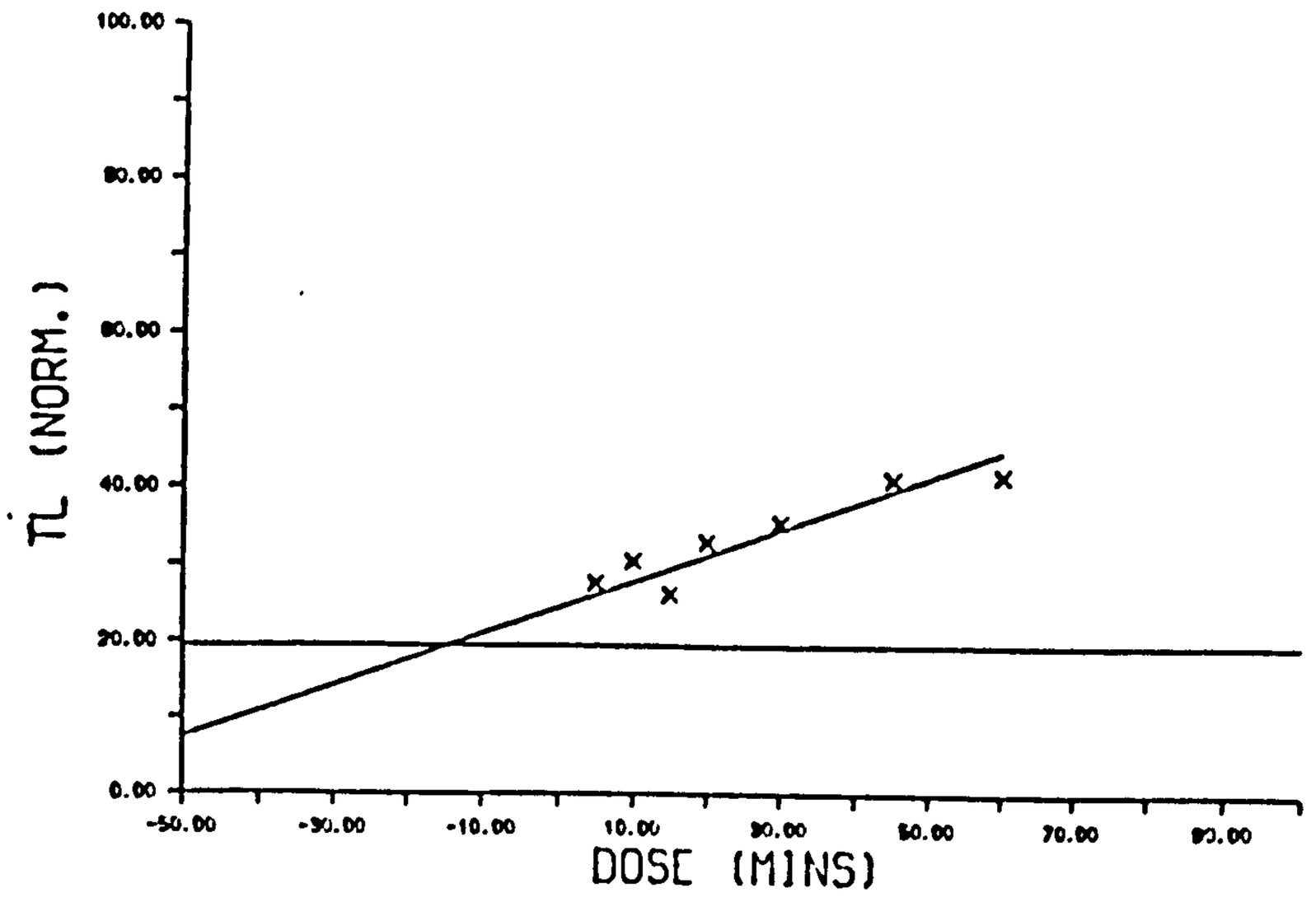

FIG 5.1E MFM F7 TL

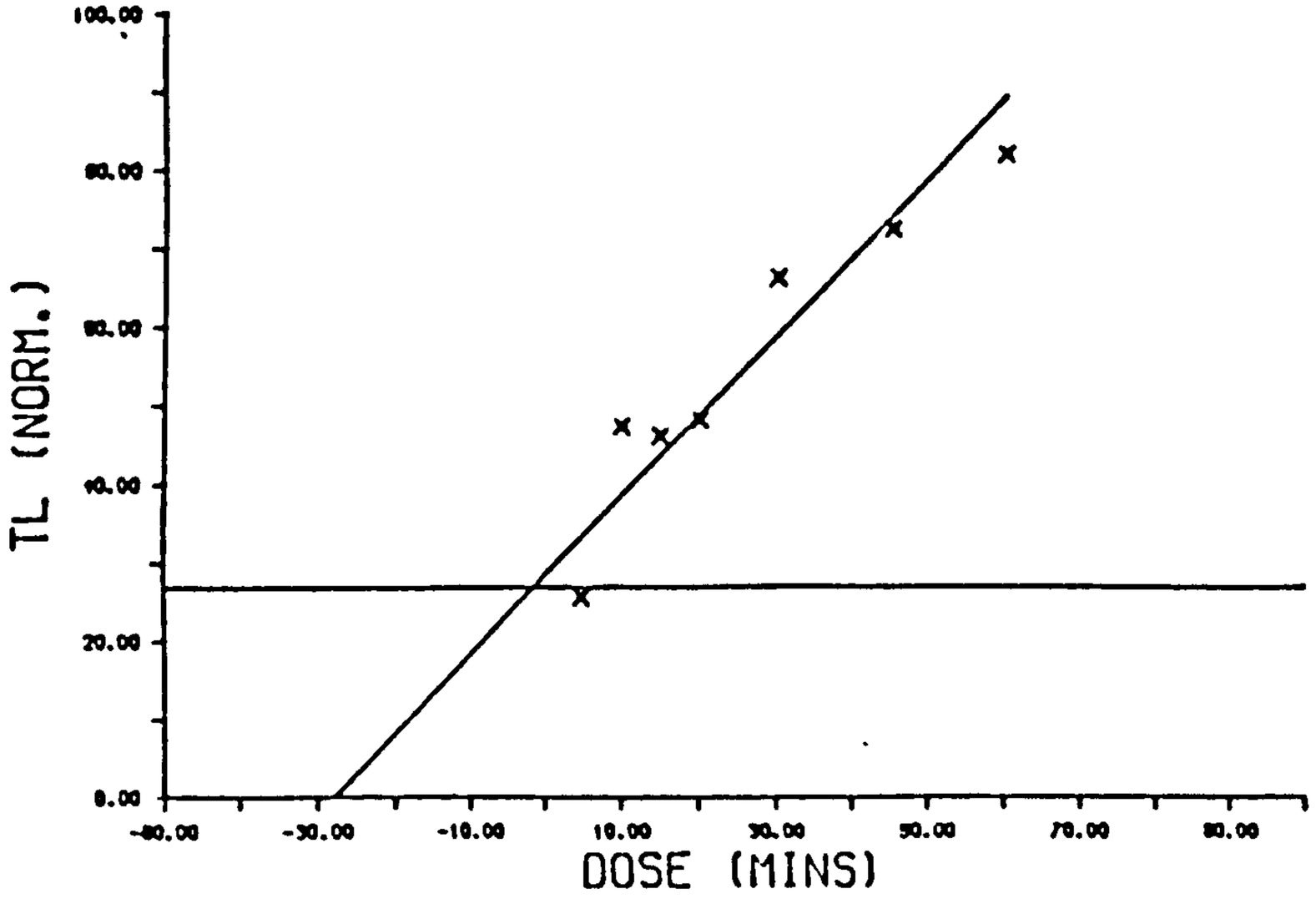

FIG 5.1F MFM F8 TL

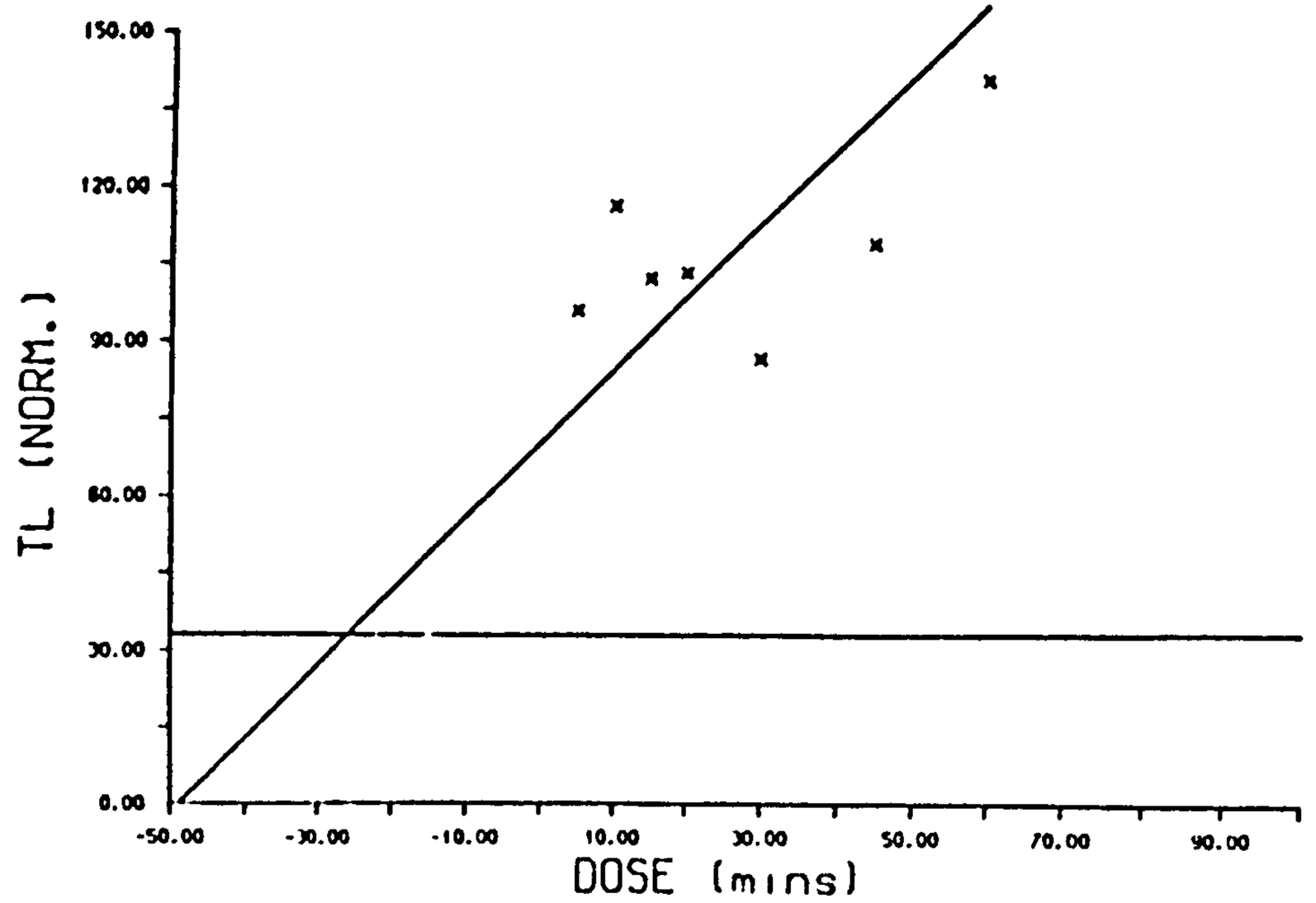

FIG 5.1G MFM F9 TL

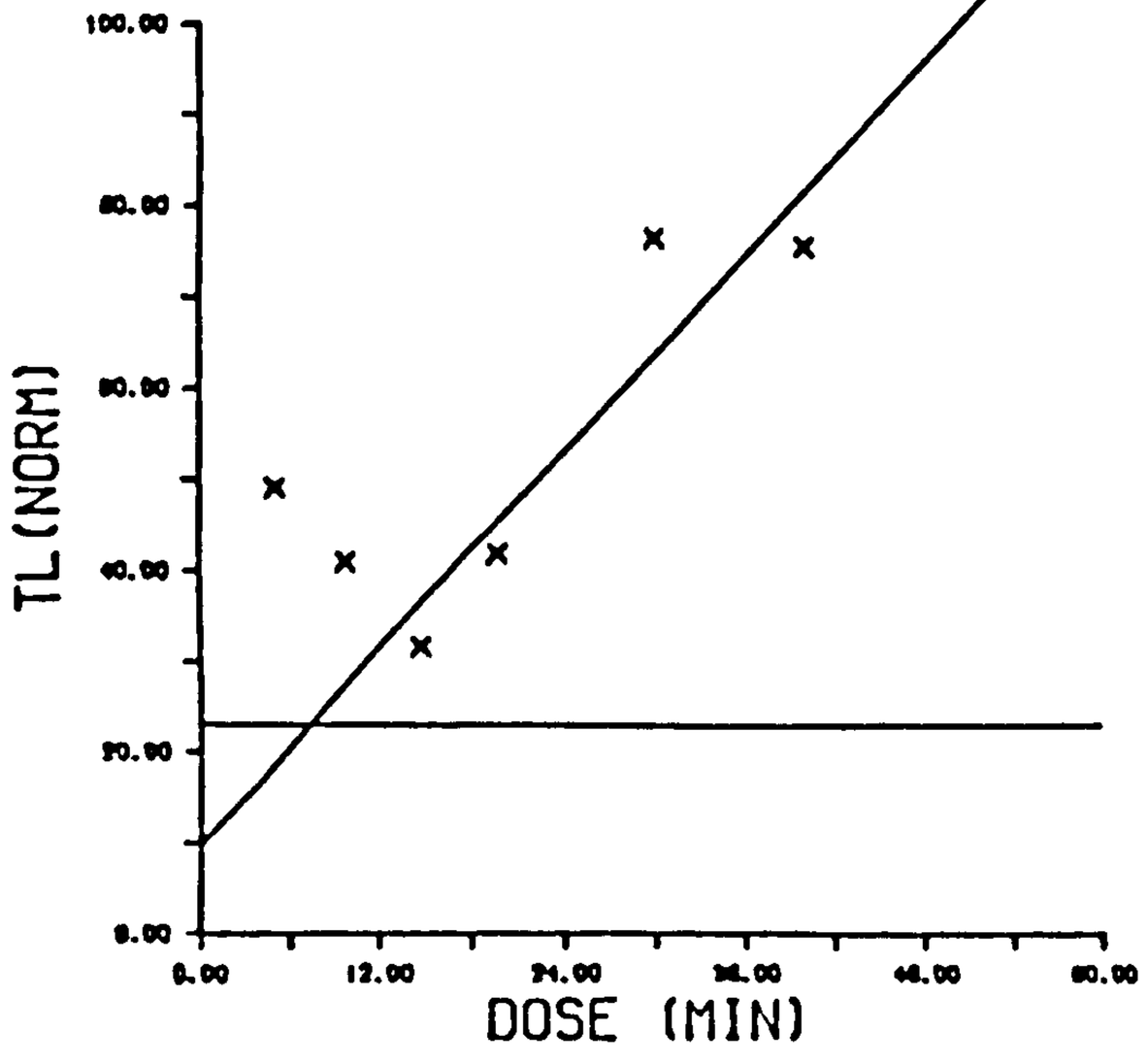

FIG 5.1H MFM F10 TL

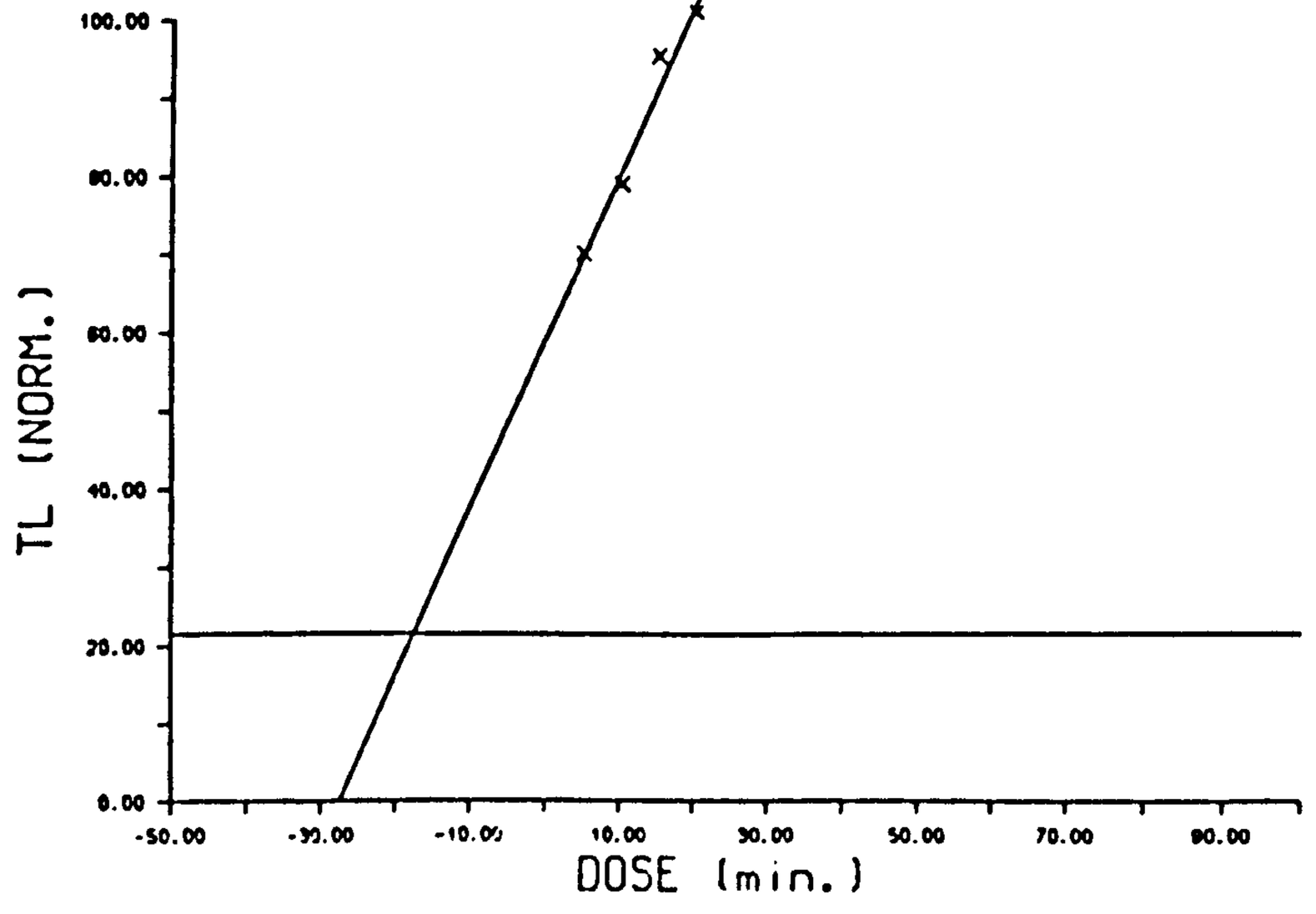

TABLE 5.1 EQUIVALENT DOSES CALCULATED FROM FIGS 5.1 EXPRESSED AS MINUTES OF Sr90 SOURCE EXPOSURE AND IN GRAYS. ERRORS ARE THE STANDARD DEVIATION OF THE LEAST SQUARES BEST FIT.

	MINUTES	Gy	ERROR (Gy)
F2.	7.1	37.8	27.3
F4.	-62.3	-333.9	42.9
F5.	32.8	175.8	28.9
F6.	16.6	89.0	25.2
F7.	1.5	8.0	22.5
F8.	26.0	139.4	84.2
F9.	-3.6	-19.3	25.7
F10.	17.2	92.2	13.9

TABLE 5.2 SPECIFIC PARENT ACTIVITY (Bq/kg) AND DOSE RATES (Gy/kg) DETERMINED BY GAMMA SPECTROMETER.

	URANIUM	THORIUM	POTASSIUM	DOSE RATES	+ ERROR
F1.	14.3	5.5	0.423	1.267	0.36
F2.	18.8	10	0.793	2.326	0.30
F3.	19.3	17	0.921	2.817	0.13
F4.	40.2	31	1.547	5.273	0.19
F5.	21.2	26	1.468	3.935	0.20
F6.	18.5	12	0.661	2.264	0.11
F7.	37.6	45	2.594	6.913	0.12
F8.	32.0	49	2.662	6.874	0.20
F9.	35.4	49	2.966	7.383	0.20
F10.	34.8	51	2.323	6.756	0.12

5.3.1 SHORT TERM STABILITY OF THE TL SIGNAL

Otherwise known as anomalous fading (WINTLE 1985, TEMPLAR 1986). This is not a problem for the MFM sediments as outlined in section 4.7.

5.3.2 LONG TERM STABILITY OF THE TL SIGNAL

Various estimates have been suggested for an upper limit to TL dating, (WINTLE 1985, DEBENHAM 1985). The upper limit is dependent on the saturation level of the minerals and time controlled loss of luminescence centres. DEBENHAM (1985) discovered that TL ages for polymineral fine grains (less than 11 microns) from loess, were accurate up to 50 ka without adjustment. 50 ka is the most pessimistic estimate of an upper limit with estimates in the order of 1 ma (WINTLE and HUNTLEY 1982, SINGHVI and MEJDAHL 1985) more common. The worst case approximation of 50 ka is more than adequate for dating MFM.

5.3.3 WATER CONTENT

Water acts as an absorber of radiation and as such will inhibit TL energy accumulation in the mineral grains. Accurate water contents were measured for each sample F1a to F10a and are listed in TABLE 5.3a. Using the results of ZIMMERMAN (1971) and AITKEN (1985), (equations 1) the corrected values of dose rate could be calculated (TABLE 5.3b). It is reasonable to assume that MFM samples have been 100% water saturated (F=1) since deposition. The case of negligible influence on the alpha activity, due to their short range was also assumed (AITKEN 1985).

$$D_\beta = \frac{D_{\beta\,dry}}{1+(1.25WF)} \qquad D_\gamma = \frac{D_{\gamma dry}}{1+(1.14WF)} \qquad W = \frac{\text{water wt.}}{\text{sediment wt.}} \qquad (1)$$

TABLE 5.3a WATER CONTENTS FOR MFM CORE F SAMPLES F1a TO F10a.

	SEDIMENT WT.(g)	WATER WT. (g)
F1.	6.7	43.6
F2.	7.5	41.5
F3.	11.2	43.2
F4.	14.6	44.7
F5.	12.8	38.5
F6.	13.4	44.5
F7.	25.9	38.5
F8.	35.1	34.4
F9.	44.5	29.9
F10.	61.9	32.1

TABLE 5.3b DOSE RATE VALUES FOR MFM CORE F, SAMPLES F1a TO F10a, WITH A MOISTURE CORRECTION APPLIED. THE alpha, beta AND gamma COMPONENTS OF THE APPLIED DOSE RATE ARE ALSO SHOWN.

	alpha	beta	gamma	DOSE RATE + ERROR(Gy/ka)	
F1.	0.93	0.07	0.04	1.04	0.17
F2.	0.88	0.12	0.07	1.07	0.12
F3.	1.09	0.19	0.11	1.39	0.05
F4.	2.15	0.41	0.25	2.81	0.09
F5.	1.40	0.32	0.18	1.90	0.09
F6.	0.93	0.17	0.10	1.20	0.05
F7.	2.45	1.02	0.57	4.04	0.11
F8.	2.37	1.30	0.73	4.40	0.12
F9.	2.48	1.72	0.93	5.17	0.13
F10.	2.52	1.66	0.98	5.16	0.16

5.3.4 DISEQUILIBRIUM OF THE URANIUM SERIES

Disequilibrium can arise from the diffusion of radon or from inherent de-ficiencies or surpluses of uranium relative to its daughters in the depositional environment. Disequilibrium as a result of radon diffusion is not usually a problem in lake sediments due to the homogeneous nature of the medium. Some indication of present day disequilibrium is possible from the results of gamma spectrometry (MURRAY and AITKEN 1982).

We might expect thorium-234 and lead-210 to produce the least reliable results by reason of their low energy and associated attenuation problems. Radium-226 overlaps in energy terms with uranium-235 which may potentially affect the accuracy of activity calculated from the radium-226 peak. The best results should be obtained from lead-214 and bismuth-214 which have relatively high energies reducing attenuation effects in the samples. The best statistical accuracy is also available from Pb-214 and Bi-214 due to the relatively high probability of emission and their separation from neighbouring peaks.

The measured activity of five radioisotopes from the uranium series are shown in FIG 5.2. If the MFM sediment is in secular equilibrium then we would expect the same calculated activity from each of the five radioisotopes, and this is apparently not so, however, when considering the activities we must also consider the relative reliabilities of each. The most reliable radioisotopes (lead-214 and bismuth-214), give similar levels of activity, they also display very similar downcore profiles. These facts point to a sediment with secular equilibrium already established at deposition.

5.3.5 LABORATORY LIGHT BLEACHING

In addition to the four main sources of TL dating error (MEJDAHL 1986), tests were carried out to asses the possible TL loss from bleaching by the laboratory 'safe' lighting.

FIG 5.2 URANIUM SERIES ACTIVIY OF THE FIVE RADIOISOTOPES: THORIUM-234, RADIUM-226,LEAD-214, BISMUTH-214 AND LEAD-210.

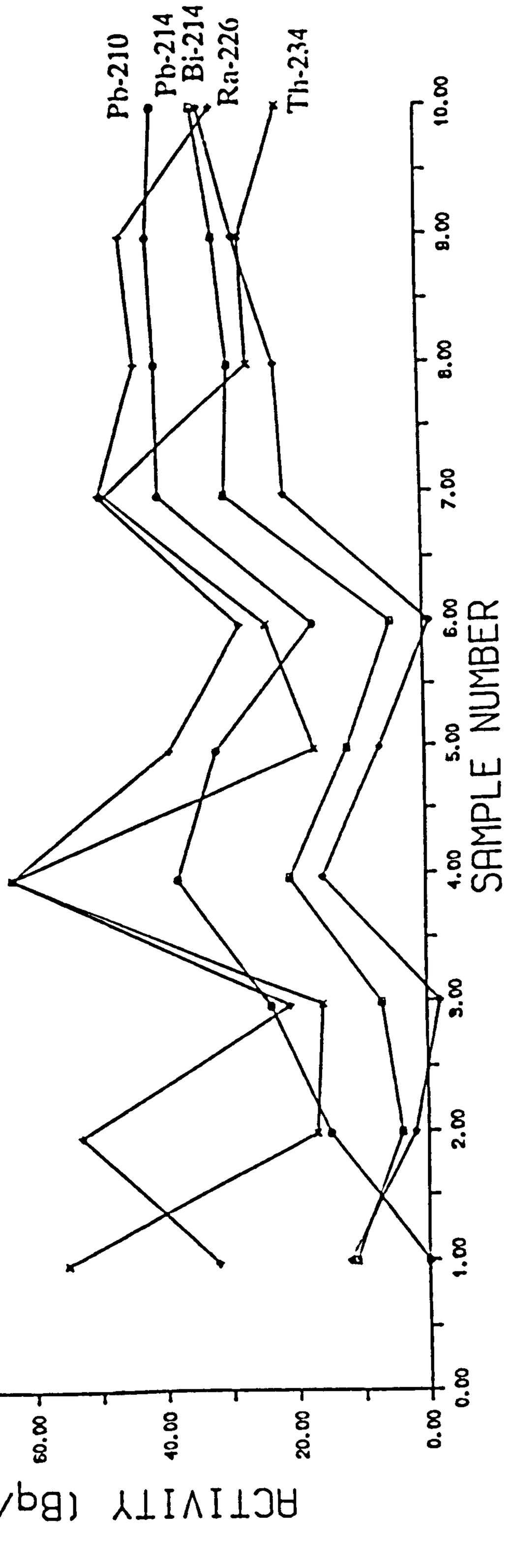

Two identical samples were given a 56.3 Gy beta dose, the first was measured immediately as a control sample, the second remaining under the laboratory lights for two weeks before measurement. RESULTS: control sample TL = 66.9, TL of the sample left in the lab = 57.8. This represents a 13.6% decrease in TL. Further tests of this type indicate 13% to be an approximately constant value for TL loss due to lab light exposure.

Initial tests of the lab lights did not reveal this problem when using pure quartz samples. It is now suggested that for fine grained polymineral samples, work should be carried out under enhanced light control procedures including: storing samples permanently in black boxes and using only photographic 'safe' lights.

For the results already obtained here, it was decided to add a 13% correction to each TL value in an attempt to counteract the effect of bleaching through laboratory light exposure.

5.4 DISCUSSION OF THERMOLUMINESCENCE RESULTS

The sources of error in determining TL values, long and short term fading, would theoretically appear not to influence these TL results. However, the statistical errors involved in the calculation of the equivalent dose, 13% at best, are extremely large. This is probably almost entirely the result of inadvertant bleaching due to periods of exposure to the laboratory lighting.

The sources of error in determining dose rates, water content and uranium series disequilibrium, have a substantial influence on the TL results. It has been suggested that uranium series disequilibrium is not a problem in the MFM sediments (section 5.3.4) but the moisture correction alters the calculated dose rate by up to 54% in the wettest samples, to 27% for the dryest. The moisture corrections were derived by ZIMMERMAN (1971) for working with pottery and soil involving weight changes in the order of 10 and 20% respectively. It is

TABLE 5.4 AGES OF SAMPLES F1 TO F10 AS CALCULATED FROM AGE EQUATION. VARVOMETRIC AGES ARE ALSO SHOWN. THE NEGATIVE AGES REPRESENT FUTURISTIC DATES.

	TL AGE (ka)	VARVE AGE (ka)	ΔAGES	SAMPLE DEPTH (cm)
F1.	-	3.5	—	265
F2.	35.3	4.2	31·2	365
F3.	-	4.8	—	465
F4.	-118.8	5.4	124·2	565
F5.	92.5	8.8	83·7	665
F6.	74.1	10.1	64·0	765
F7.	2.0	10.7	8·7	865
F8.	31.7	11.2	20·5	965
F9.	-3.7	11.7	15·4	1065
F10.	17.9	12.2	5·5	1165

unclear whether, when working with sediments of such high water contents as those from MFM, the same corrections remain applicable.

5.5 CONCLUSIONS

Thermoluminescence ages calculated from the results of this study and compared to the varvometric dates of ZOLITSCHKA (1988), (TABLE 5.4), have too large an error associated with them to allow construction of a new depth to time transform function. The primary source of this large error is from the TL measurements the result of a bleaching effect from the lab lighting. The other potential source of error is the moisture correction used to determine the dose rate. It is uncertain whether samples of such high water content fall within the scope of application of the correction.

Recommendations emerging from this TL study include: the permanent storage of TL samples in black boxes with exposure only to photographic 'safe' lights whilst working and that the moisture correction should be investigated for its applicability to samples with high water contents.

The thermoluminescence dating technique certainly has the potential to date MFM sediments in terms of range, also, uranium is probably in secular equilibrium with its daughter isotopes in the depositional environment, however, residual TL levels (FIGS 5.1) possibly indicate an incomplete zeroing process at deposition although the full effect of this cannot be assesed until the more major problems are resolved. The most promising samples to date next, might be older samples whose ages may be more easily resolved by the technique; they will also have a lower water content due to greater compaction.

CHAPTER SIX.

TIME SERIES ANALYSIS OF MEERFELDER MAAR PALAEOMAGNETIC RESULTS AND COMPARISON WITH LAC DU BOUCHET.

6.1 INTRODUCTION

Due to the problems encountered with TL dating, the varve chronology according to ZOLITSCHKA (1990 pers comm.) provides the main control for the depth time transform applied to the MFM palaeomagnetic results for their comparison with the LDB results and also for time series analysis. This chapter covers the additional data processing involved for correlation between the two lake records and details relating to analysis of the nature of the palaeomagnetic signal.

The processing sequence adopted was: stacking, transforming to time scale then smoothing. These have been accomplished utilising the STACK, TRANSFORM and FSMOOTH programs from the PALAEOMAG library package developed by SMITH (1985) for the Edinburgh Multi Access System (EMAS). These have been sucessfully applied to several palaeomagnetic studies, (CREER 1988,1989, CREER et al 1990, MORRIS 1990).

6.2 STACKING

Single core records are no longer considered a basis for interpreting geomagnetic field behaviour. Stacking of up to 12 individual core records (THOUVENY et al 1990) is necessary to eliminate the small scale sedimentological variations and to verify the intra-maar consistency of the records. It has also been suggested that a 'type' record can be constructed by patching together the best directional data for different depth windows (CREER 1991 pers.com.). Stacking produces composite palaeomagnetic curves with optimum characterisation of the maar as a whole although some resolution may be removed by this process. Since the individual cores from MFM were converted to a common depth scale based on intensity

This difference can be attributed to the effect of inclination error caused by magnetic mineral imbrication. This is due to the adoption of prefered orientations related to mineral shape, with a tendancy for the long axes to lie horizontally. This has the greatest influence on larger grains and explains some of the variations in directional data quality observed in FIGS 3.4 and 3.5 . Another possible contributer to the difference in inclination between the average value of the MFM data stack and the calculated value is inclination error, shallowing of the preserved inclination value, due to compaction.

correlations, without reference to the directional data, then if a consistent palaeomagnetic record exists within the lake, stacking will emphasise the common features besides acting destructively on noise.

The order of processing ie. stack, transform, smooth, was adopted to optimise the available data. It is important that stacking is carried out on near to original data to preserve as much detail as possible. It was decided on the basis of the intra-maar correlations (CHAPTER 3), to use only cores MFMA and MFMB for stacking. Cores MFMD and MFME cover only the post glacial period for which intra-maar correlation proved to be extremely poor.

Declination and inclination data from cores A and B were evenly spaced (EVENSPACE, SMITH 1985) with a spacing of 30mm to generate approximately the same number of data points as the original sub-samples ensuring the minimum level of interpolation and avoiding the creation of artefacts in the data set. The actual stacking process was accomplished by averaging the evenly spaced data at each depth (FIG 6.1). Errors are obtained as standard deviations from the mean at each level. The average inclination value for the stack was 58.8^{o} with error of 5.3^{o}. This compares with an inclination of 66.5^{o} expected from the MFM latitude of 49^{o} assuming an axial dipole field.

6.3 TRANSFORMING

TRANSFORM (SMITH 1985) performs the operation of converting the depth scale to a time scale. It uses a function constructed from a number of transformations between the common depth scale and a time scale. Interpolation between these known points is linear. At Meerfelder Maar the time scale is based on positive correlations between the log(susceptibility) profile of MFM B core and the core on which the varve chronology was based (CHAPTER 4).

6.4 SMOOTHING

The final stage of processing for the composite data was smoothing. This was to

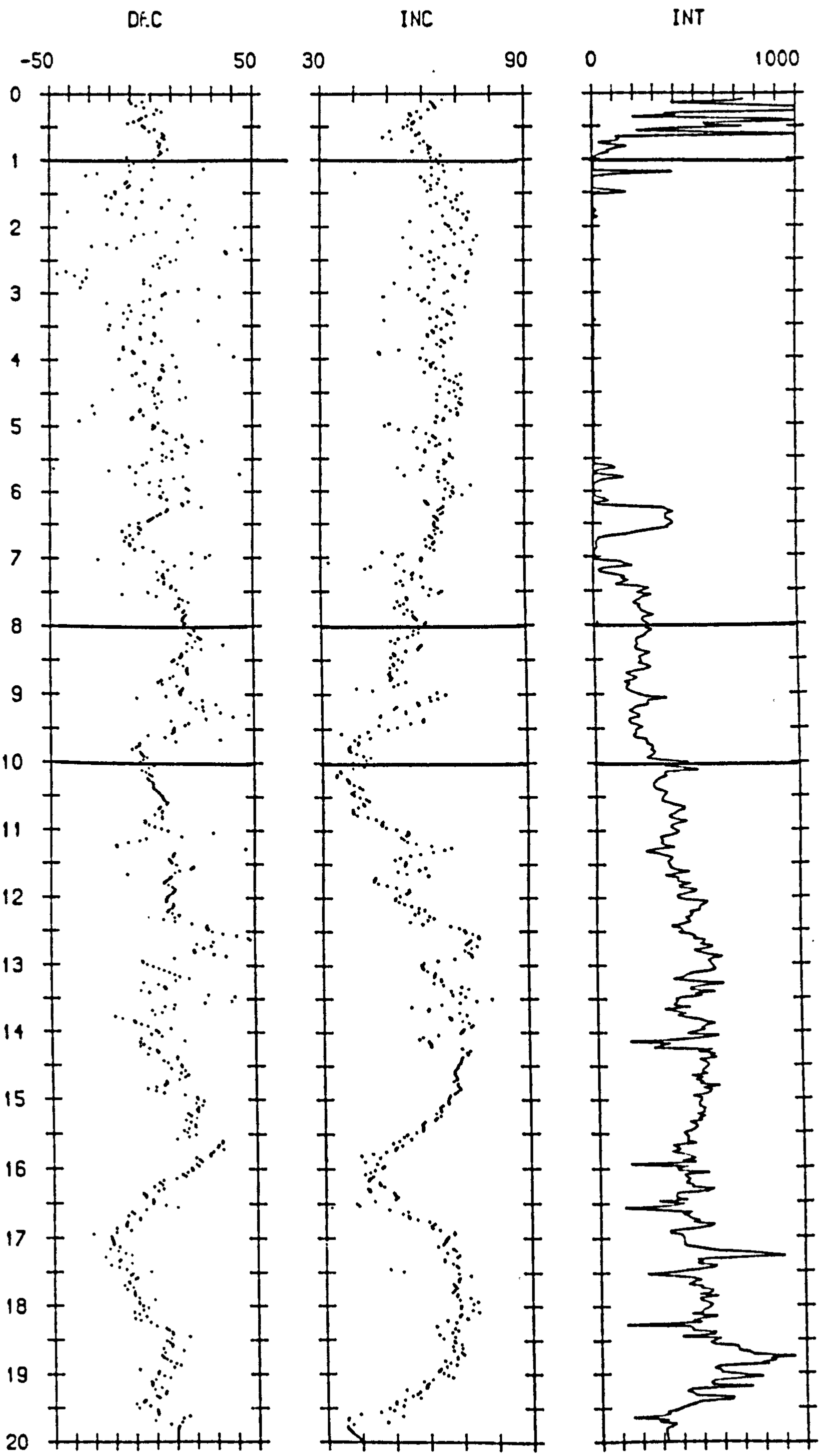

FIG 6.1 THE STACK OF CORES MFMA AND MFMB. CONSTRUCTED BY AVERAGING THE EVENLY SPACED DATA POINTS AT EACH DEPTH.
(with sedimentary units marked on)

eliminate some of the noise and clarify major secular variations. Two methods of smoothing were tried: CSSMOOTH (SMITH 1985), using a specified number of equally spaced cubic splines, and FSMOOTH (SMITH 1985), frequency filtering with smoothed curves fitted to the discrete data using low pass FFT based filters to leave periods greater than a specified value. Defining variations of the order of thousands of years is one of the major objectives of lake sediment palaeomagnetic research and it was decided to filter out wavelengths below 1000 years to 'clean' the signal of the higher frequency events which are superimposed on the secular variation (FIG 6.2). Various cubic spline fits were experimented with, the 50 knot cubic spline which exhibits much the same detail as the 1000 year frequency filter is shown in FIG 6.3 .

6.5 DISCUSSION AND INTERPRETATION

Comparison of the palaeomagnetic curve derived for MFM with that from LDB could now be made. One of the remarkable features of the LDB master-curve is the intra-maar consistency of the data from individual cores (FIG 6.4a,b). This data from LDB (CREER 1989) was stacked, transformed and smoothed in the same way as that from MFM to evaluate the degree of correlation between the composite palaeomagnetic curves for the two localities. It is this correlation which could indicate the validity of accepting the LDB W. European master curve (CREER et al. 1986) as a record of secular variation from the geomagnetic field. Other sites, including Lac de Joux, the Black Sea and even North America have been compared to LDB and it has been suggested that some of the same palaeomagnetic features are exhibited, (CREER 1985).

The individual declination and inclination, profiles from MFM, do not exhibit the strong coherence of the LDB results. The declinations fare worst in comparison. This may be because of reorientation errors in the rotating the 2m core sections on the horizontal plane which is a necessary part of Livingston coring and not involved in the Mackereth coring technique used to acquire these Lac du Bouchet cores.

These MFM declination and inclination results were a little disappointing, for

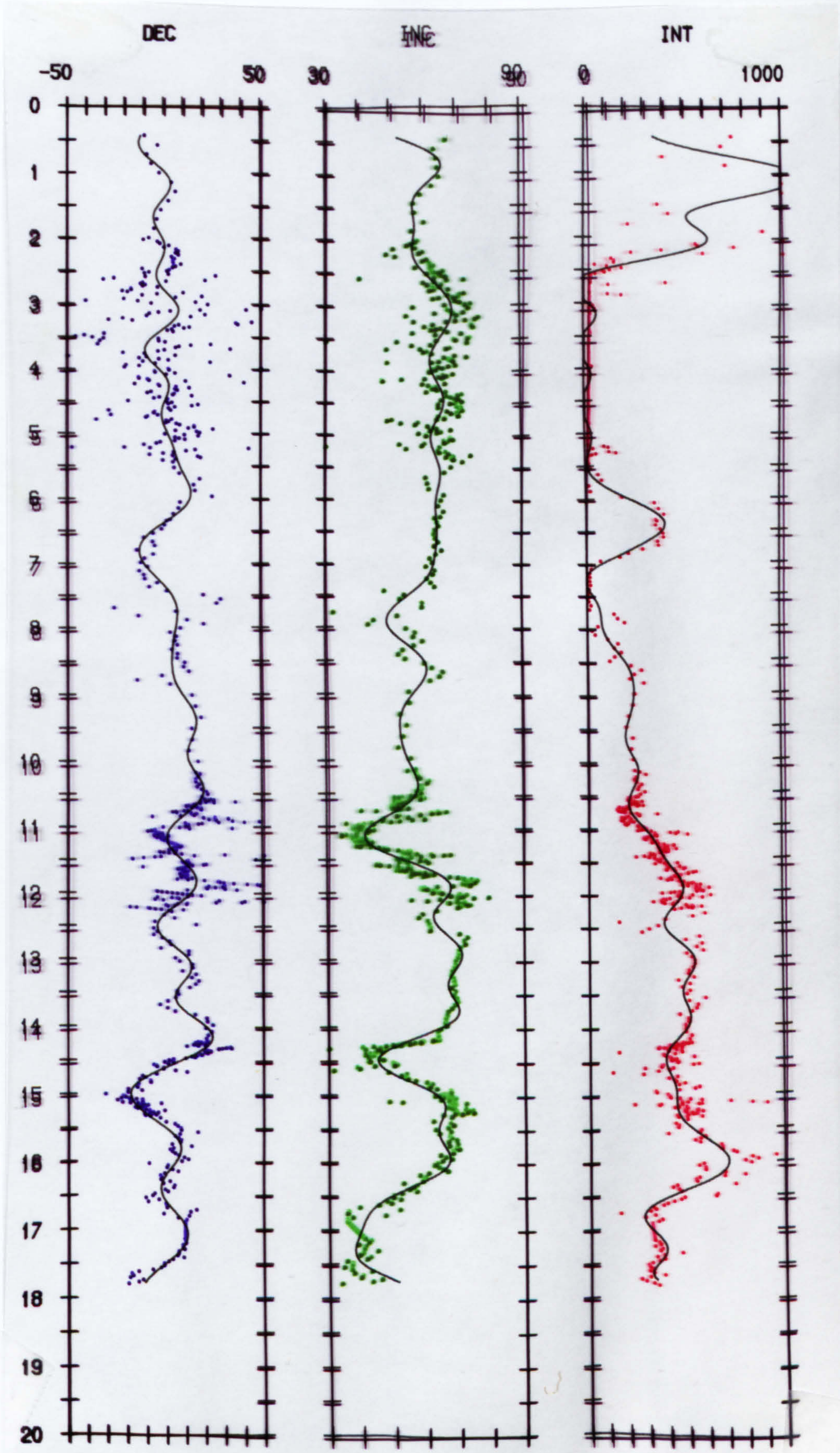

FIG 6.2 THE MFM STACK SMOOTHED BY A 1000 YEAR FREQUENCY FILTER WITH THE ORIGINAL STACKED DATA OVERLAYED.

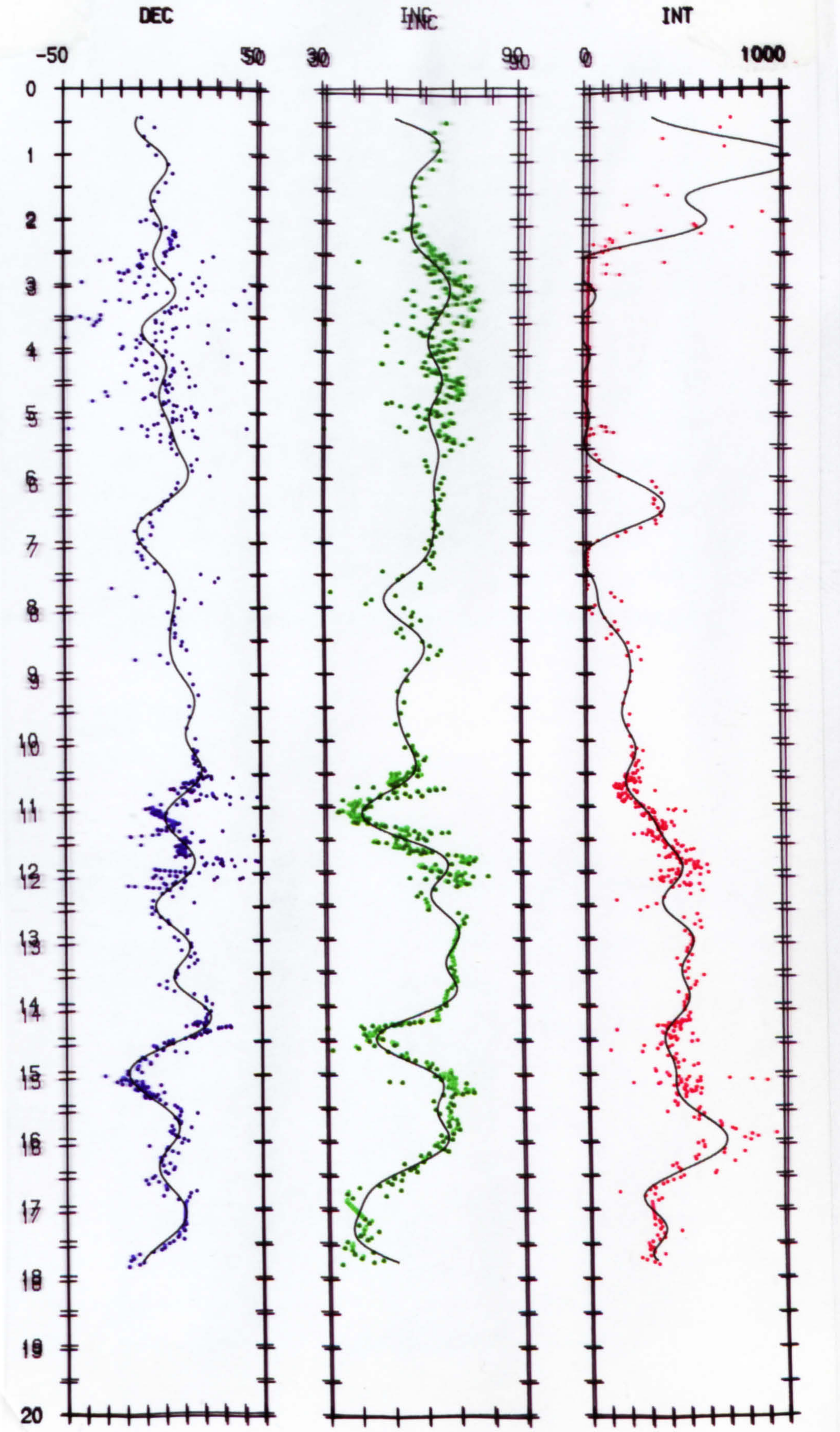

FIG 6.3 THE MFM STACK SMOOTHED BY A 50 KNOT CUBIC SPLINE WITH THE ORIGINAL STACKED DATA OVERLAYED.

a LDB DEC

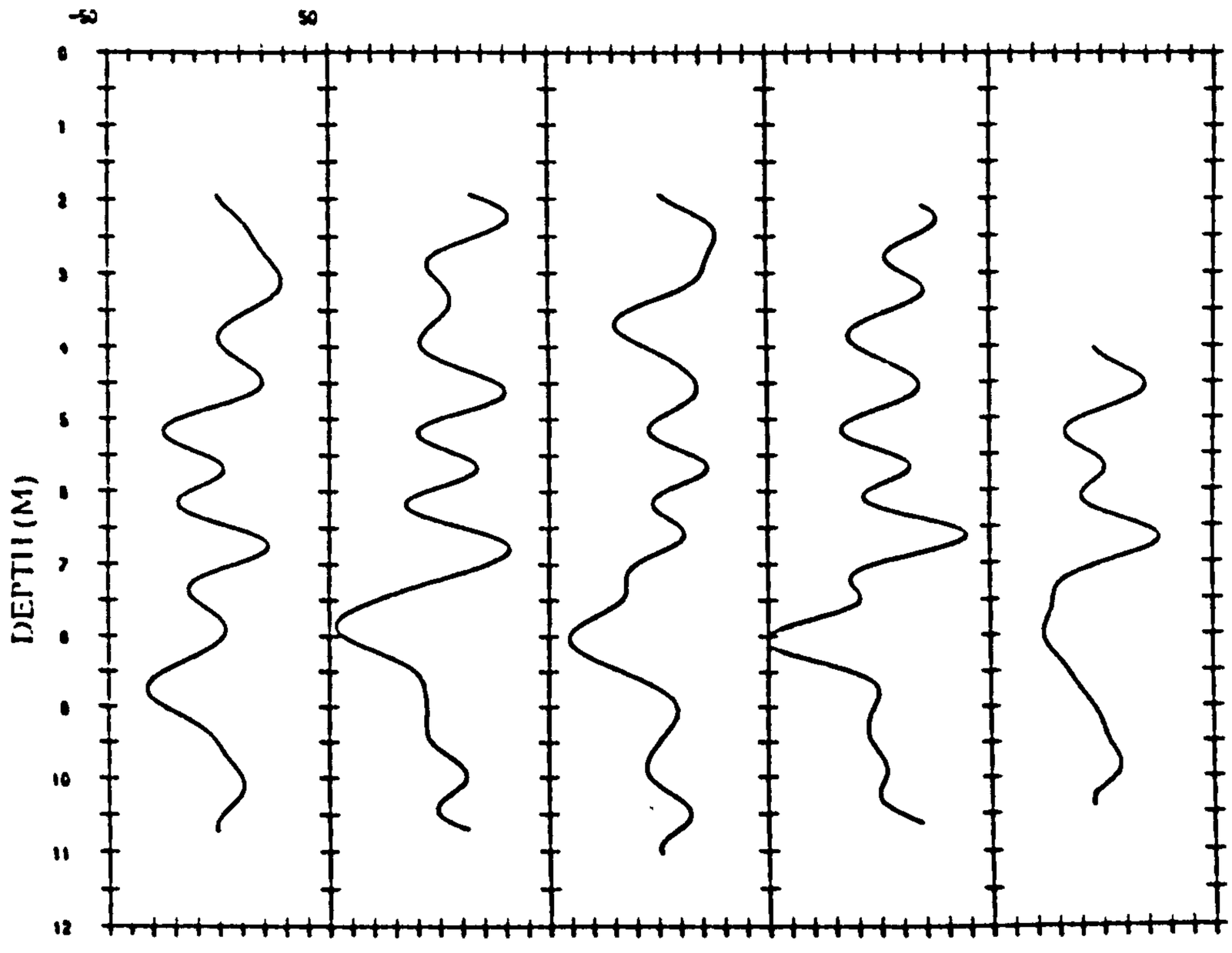

b LDB INC

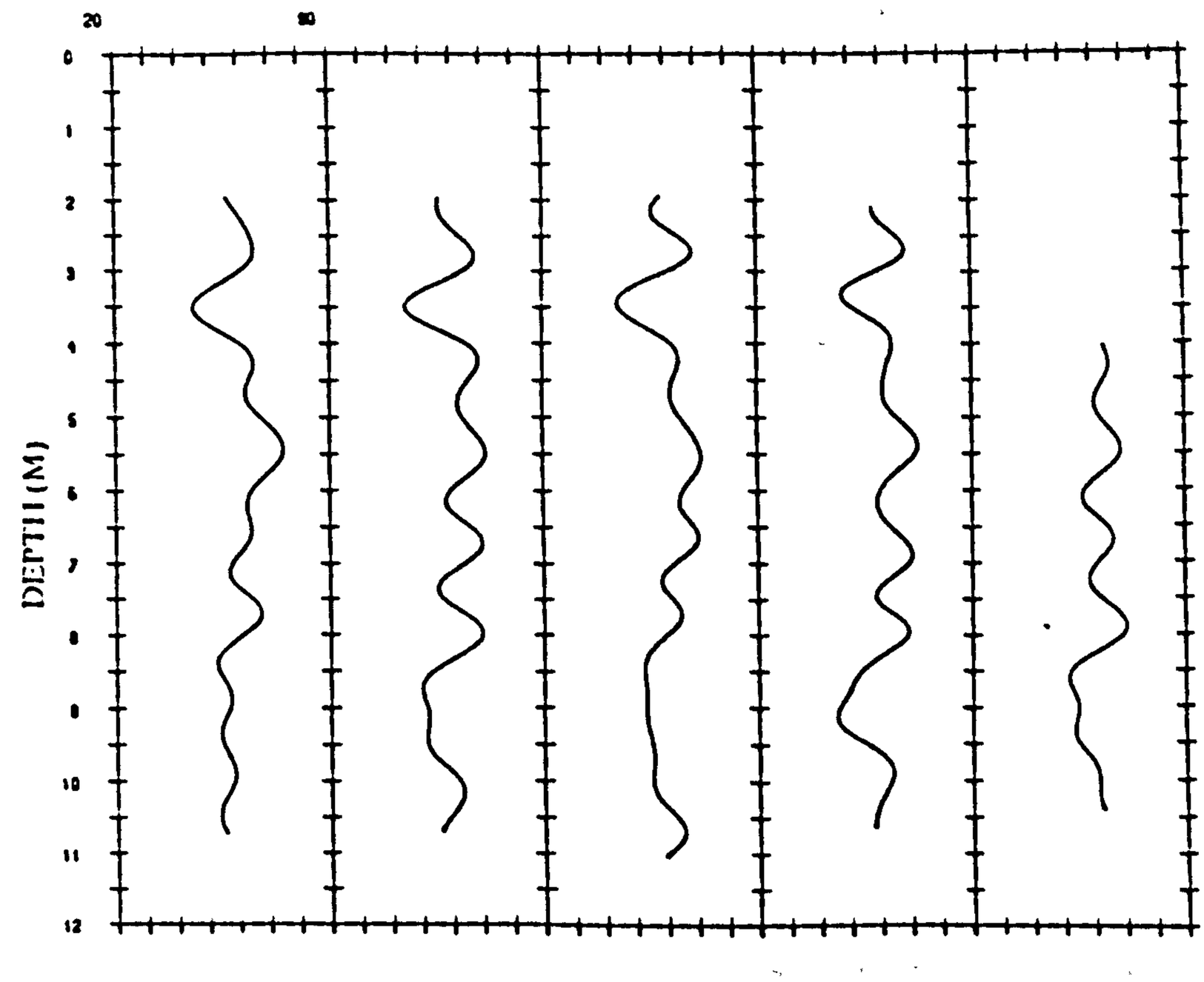

FIG 6.4 PALAEOMAGNETIC CURVES FROM LAC DU BOUCHET EXHIBITING EXCELLENT INTRA-MAAR CONSISTENCY IN a.DECLINATION AND b.INCLINATION.

despite the carefully chosen site and recovery techniques, these records have not the quality of the LDB record. Potentially the directional data suffers from poor definition in the Post Glacial span by reason of the increased abundance of organic matter during this time, both reducing the magnetic intensity of the record and causing possible distortion to the magnetic fabric. An isotopic and elemental analysis investigation of the organic material is detailed in CHAPTER 7, where an attempt to identify the changing sources and quantities of organic carbon has been made.

Comparison of stacked and smoothed curves for MFM and LDB are made in FIG 6.5 by overlaying LDBFS1000 on MFMFS1000. The area of most interest lies between 11 and 19,000 years BP. Above 11,000 yrs BP, the MFM record is inconsistent between cores, consequently most detail is lost in the stacking process and the LDB record is uniform with a value of approximately 60^{o} inclination by reason of the sparse sample frequency due to the very slow sedimentation rate (CREER et al. 1986).

6.6 CROSSCORRELATION OF LDB AND MFM RESULTS

Cross correlations between MFM declinations and LDB declinations (FIG 6.6a) and between MFM inclinations and LDB inclinations (FIG 6.6b) were used to find the best fit for the two records. Cross-correlating in this way enabled the point, or zone of positive correlation to be detected, (since by evenly spacing the datapoints in each profile and applying the individual time transform functions, it is unlikely that all equivalent parts of the two series would move into correspondence at the same lag).

The zone of overlap of the MFM and LDB series between 11 and 19 kyrs BP, with data evenly spaced at 30cm intervals, was used for cross-correlation analysis. The cross-correlation allowed calculation of match positions up to +-1750 years lag, that is n/4, where n is the number of data points in each series. In this case n=214.

Positive correlations between the two series are shown in the declination data at

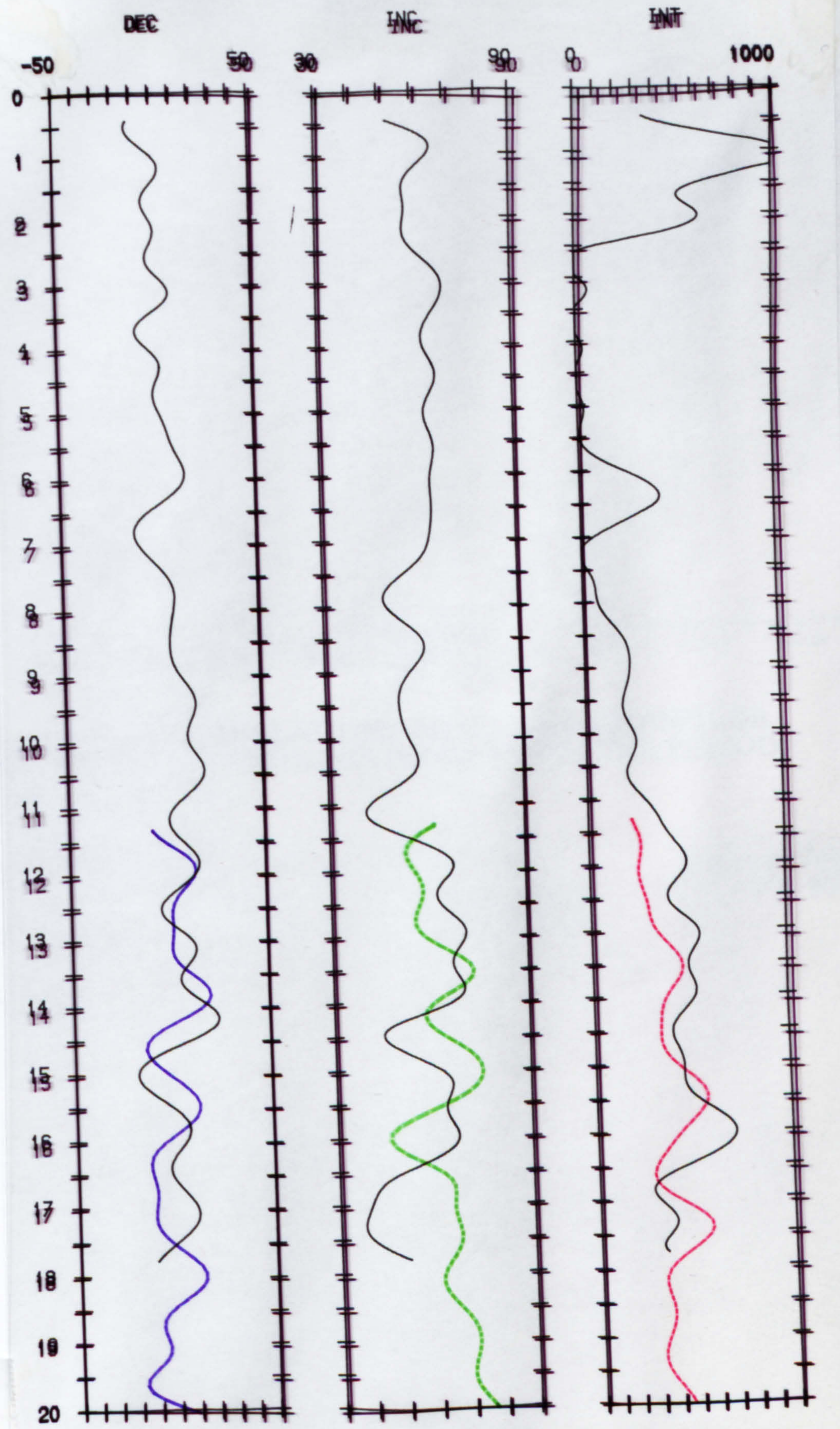

FIG 6.5 A COMPARISON OF STACKED AND SMOOTHED PALAEOMAGNETIC CURVES FROM MFM AND LDB (OVERLAY).

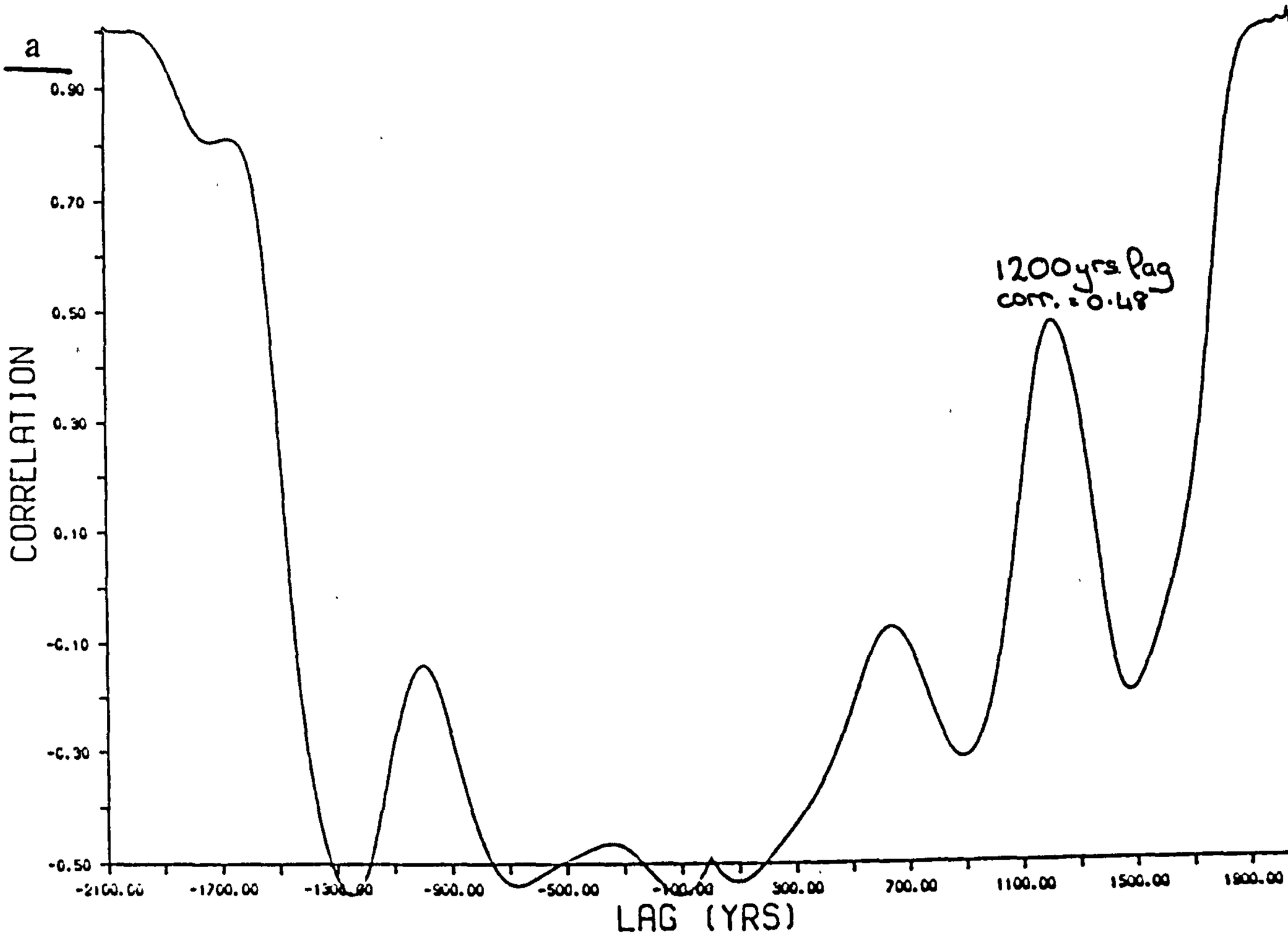

FIG 6.6 CROSS CORRELATIONS BETWEEN MFM AND LDB
a.DECLINATIONS AND b.INCLINATIONS FOR THE PERIOD.
11 TO 19 KYRS BP.

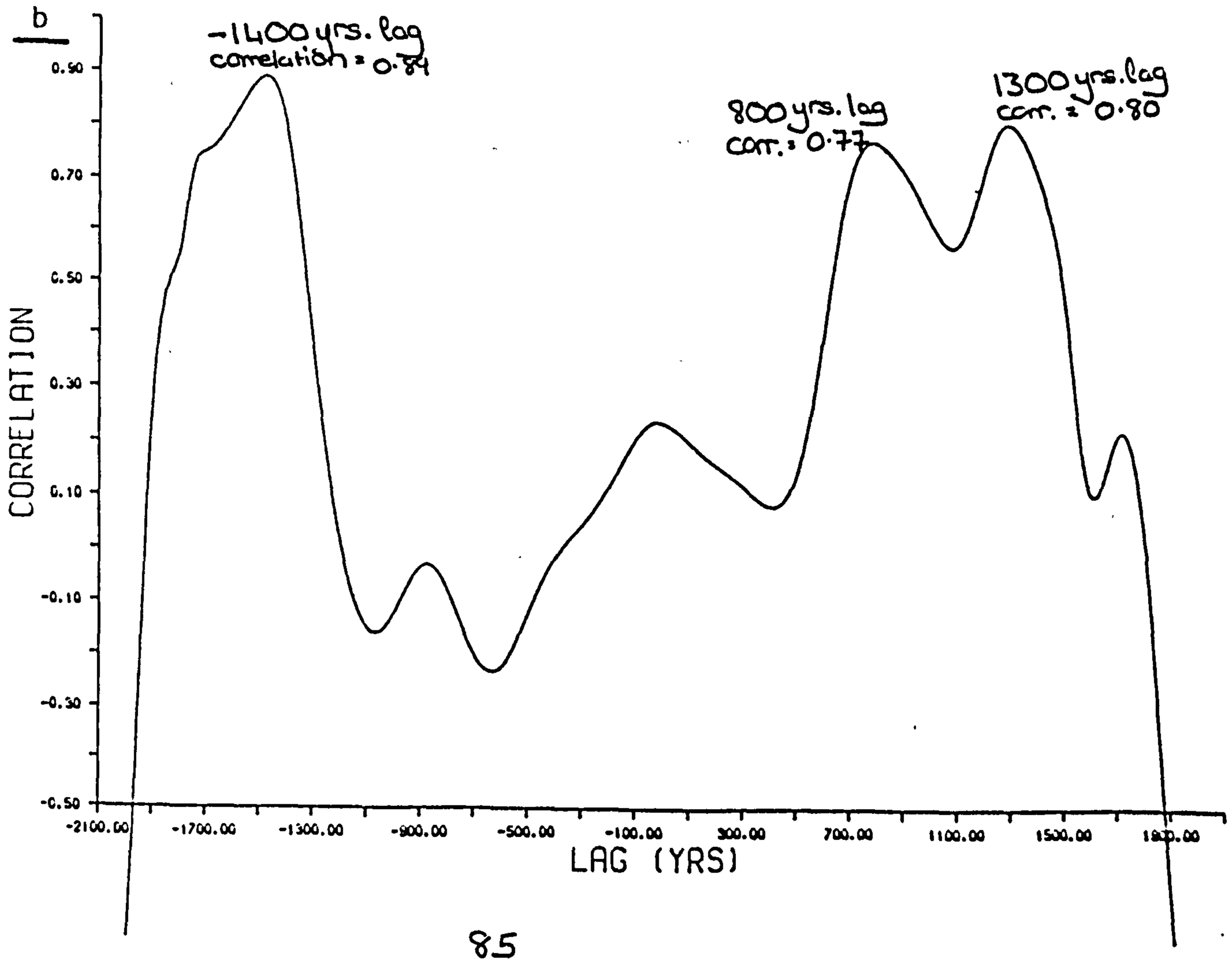

1200 years lag with a correlation coefficient of 0.48 and in the inclination data at -1400, 800, and 1300 years lag with respective correlation coefficients of 0.89, 0.77 and 0.80.

Little significance can be attributed to high correlations at long lags since the variance of the correlation will be high and the number of observations on which the correlation is based, will be low (DAVIES 1973).

Considering the cross-correlation results, the best option is a fit based on the inclination correlation where the MFM series lags the LDB series by 800 years. This is not considered to be a real lag but an adjustment to be applied to the two time series producing the best correlation. The adjustment (800 years) is a product of the dissimilarity of the respective time transform functions of MFM and LDB. It may be possible to adjust the LDB transform by bestowing ages to the maxima and minima from the more accurately dated MFM sequence.

6.7 TIME-SERIES ANALYSIS

Analysis of the MFM palaeomagnetic time-series was attempted in an effort to elucidate significant periodicities in the time domain by autocorrelation and to resolve power spectra for MFM using Fourier analysis.

6.7.1 AUTOCORRELATION

Autocorrelation is a simple and effective method of spectral analysis where a data sequence is progressively offset against a copy of itself and the correlation coefficient of successive lag positions calculated (DAVIES 1973). Dominant periodicities appear as a succession of maxima and minima along the autocorrelation curve of correlation coefficient versus lag with the periodicity defined by the lag between consecutive maxima or minima.

Autocorrelation was carried out on declination, inclination and intensity from

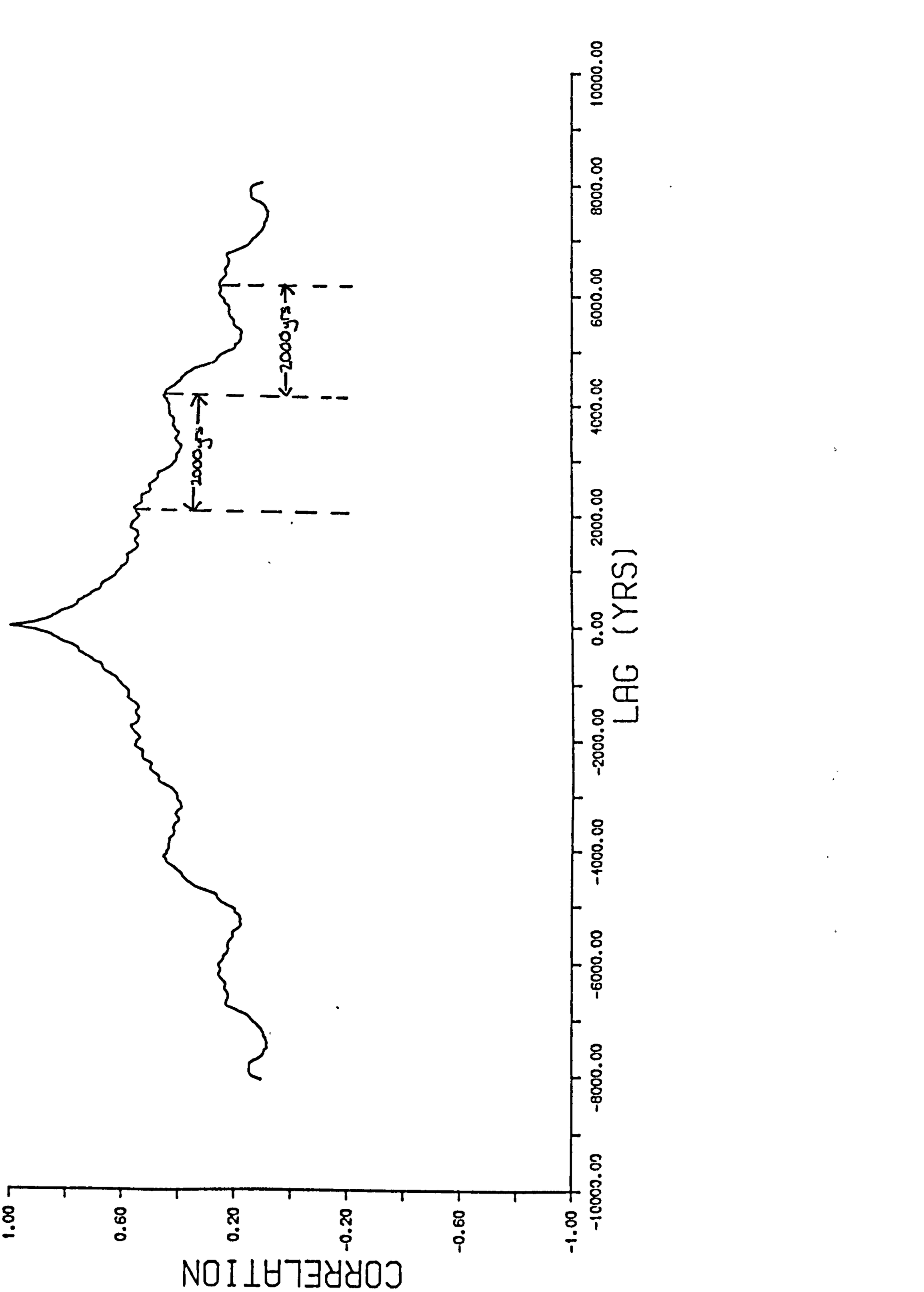

FIG 6.7 THE AUTO CORRELATION OF DECLINATION FROM MFMB CORE. THIS EXHIBITS A WEAK 2000 YEAR PERIODICITY.

MFM B core and the combined stack of MFM cores A and B. The only result emerging from this was a 2000 year periodicity for the autocorrelation of MFM B core declination profile, (FIG 6.7).

6.7.2 FOURIER ANALYSIS

Fourier analysis is a method of describing a signal eg. a palaeomagnetic signal, in terms of its harmonic constituents and their relative power or dominance. A signal is composed of a trend plus periodic and random components. Data should be detrended before Fourier analysis, usually by fitting linear regression lines, although in the case of MFM there is no requirement for this as the data exhibits no overall trend.

The evenly spaced data stack from MFM cores A and B was analysed using the FOURIER program developed by SMITH (1985). This relies on the number of data points being factorisable by a prime number, if the initial attempt fails then the last data point is discarded and a new attempt made. The program has the option of tapering the data set using a half cosine bell on the first and last 10% of data points to prevent leakage. The dominant periods revealed by Fourier analysis are listed in TABLE 6.1 and shown graphically in FIG 6.8 .

Periodicities consistently appearing in MFM at various data window lengths were compared to the results of SMITH (1985) based on the Fourier analysis of LDB. This revealed several periodicities common to both lakes, declination 1.8 and 2.7 kyrs, inclination 2.0 and intensity 2.0 kyrs.

In addition other similarities between the MFM and the LDB analyses (SMITH 1985) were noted, namely: declination and inclination are out of phase with the declination leading the inclination, an indication of westward drift. The VGP path for MFM (FIG 6.9) was observed to possess a predominantly clockwise looping sense also indicative of a westward drifting nondipole field source (RUNCORN 1959), although not uniquely (CREER 1983). Secondly, the inclination and

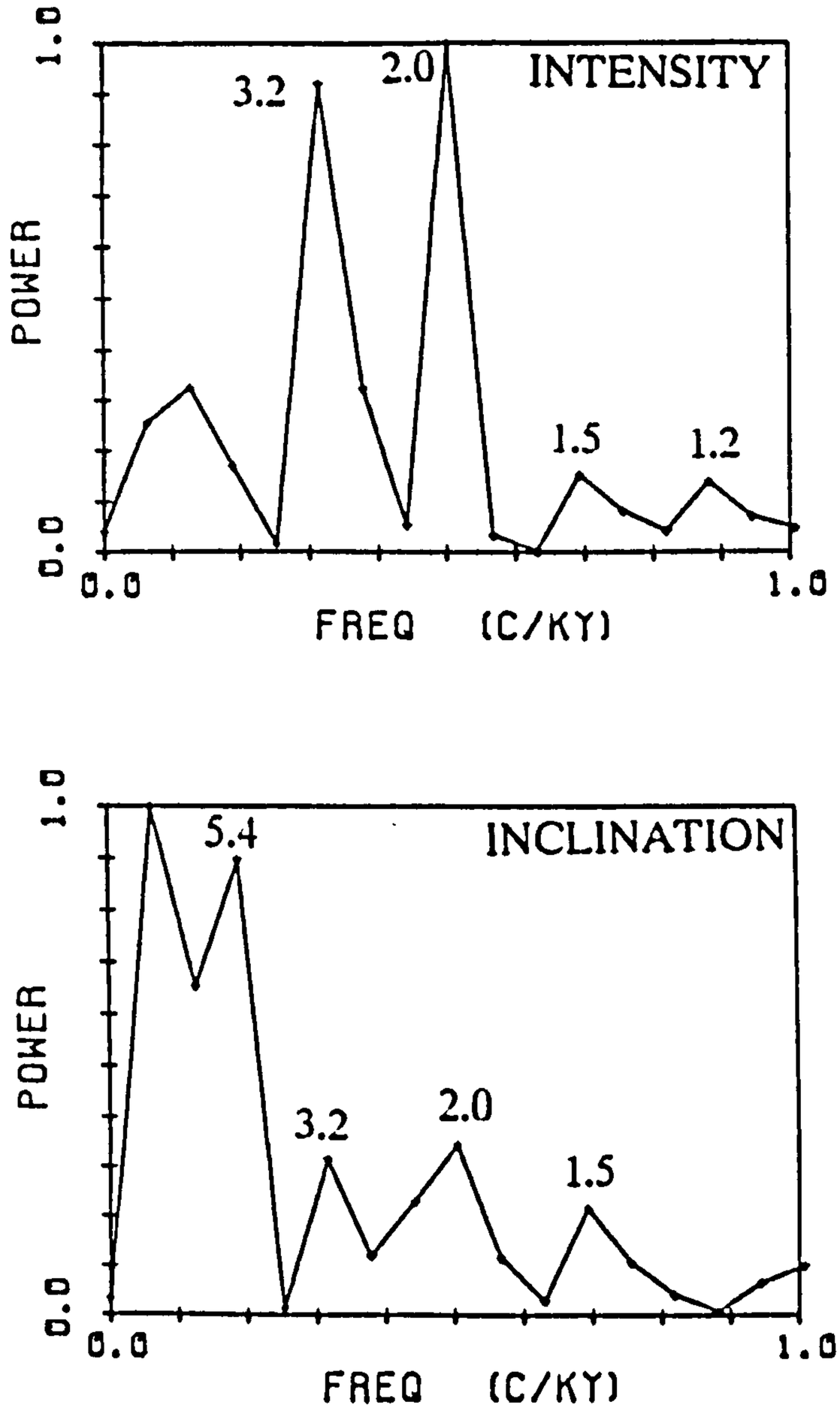

FIG 6.8 THE FOURIER ANALYSIS RESULTS FOR THE MFM STACK. THESE ARE CONSISTENT OVER A VARIETY OF TIME WINDOWS. SEVERAL PERIODICITES ARE COMMON TO LDB, DECLINATION 1.8 AND 2.7 KYRS. INCLINATION AND INTENSITY 2.0 KYRS.

mfm fs1000

46 % anticlockwise rotn

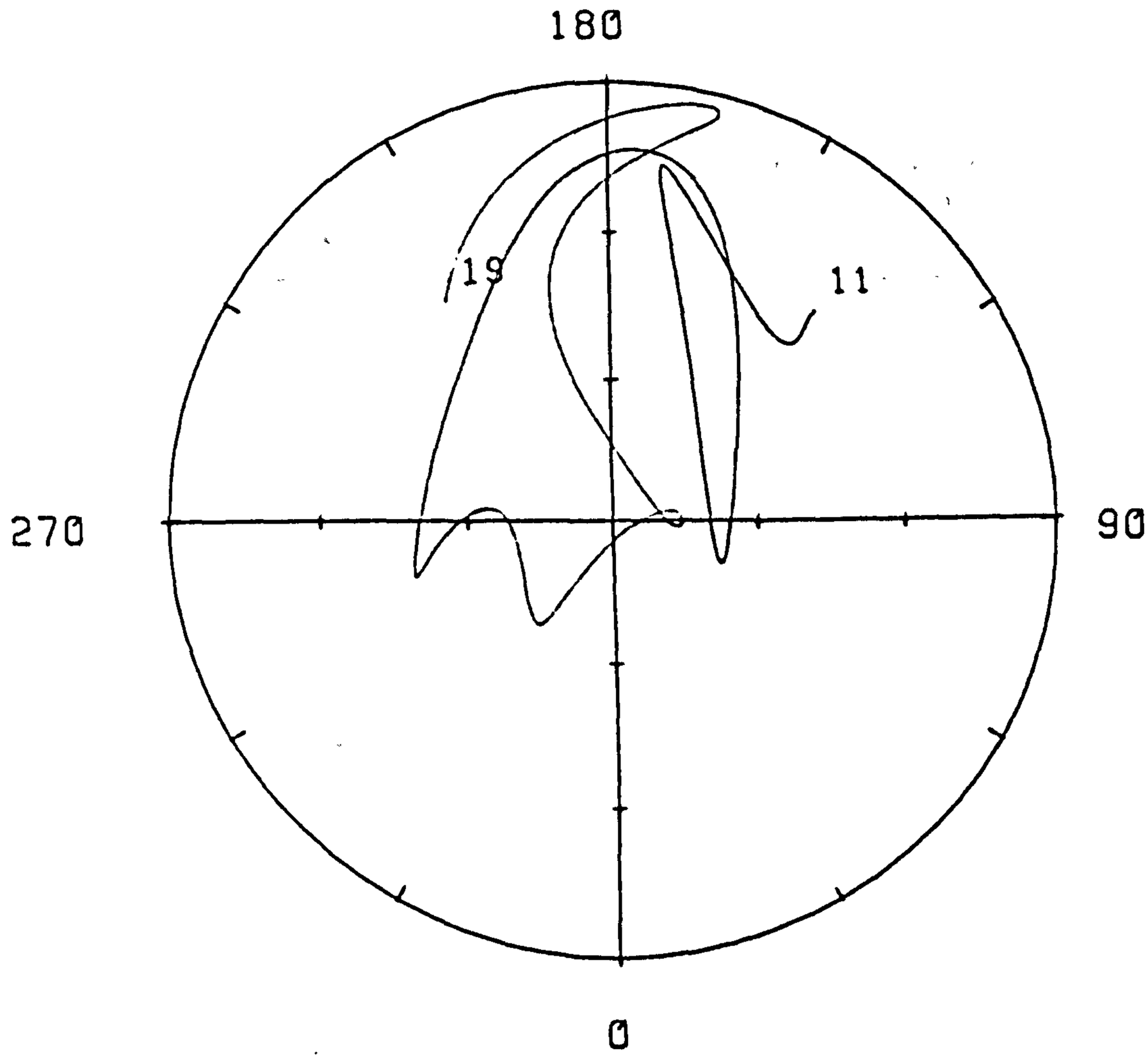

FIG 6.9 THE VGP PATH FOR MFM STACK BETWEEN 19 AND 11 KYRS BP, THE PATTERN IS PREDOMINANTLY ONE OF CLOCKWISE LOOPING SIMILAR TO LDB.

TABLE 6.1 RESULTS OF FOURIER ANALYSIS ON MFM STACKED DATA, THE DOMINANT PERIODICITIES IN (kyrs) ARE LISTED:

DECLINATION	INCLINATION	INTENSITY
4.1	5.4	8.1
2.7	3.2	3.2
1.8	2.0	2.0
1.2	1.5	1.5
		1.2

intensity are in phase at the 2000 year harmonic.

It is an assumption of Fourier analysis that the time series we analyse is a periodic stationary one. This may be seriously flawed. It may be that spectral analysis is not appropriate and that we should attempt other methods of interpreting geomagnetic secular variations such as fractal analysis (MANDELBROT and WALLIS 1969, FEDER 1988), this has been suggested by TRITTON (1988) in the interpretation of the geomagnetic reversal sequence.

It must also be considered that the 'time series' itself contains a degree of error as the time transform is based on only 2% of the data points being assigned ages which will themselves have an associated error.

6.7.3 A COMPARISON OF TIME TRANSFORMS

The outstanding positive feature of lake sediment palaeomagnetic secular variation records is the distinct sequence of inclination maxima and minima (ξπρστ) which are not only clearly found in MFM and LDB, but may also feature as part of the palaeomagnetic records of Lac de Joux (CREER et al 1980) and the varved clays of Soviet Karelia (BAKHMUTOV and ZAGNIY 1990). Assuming a geomagnetic source for this widespread feature, then the discrepancies between the various time transforms for each location can be resolved by matching the palaeomagnetic markers from each record to a chosen master curve with the best time control. Meerfelder Maar probably provides the best time control with its combination of palynological (USINGER 1984) and continuous varve chronology (ZOLITSCHKA 1988). Dating for Lac de Joux was on the basis of palynological analysis and for LDB, palynology plus radiocarbon. The Soviet Karelia palaeomagnetic records have been dated by a combination of palynology, radiocarbon and varvometric methods although the latter is not continuous.

Lacs de Joux and du Bouchet have been compared by CREER (1985) where it was noted that discrepancies exist between the biochronozones for the two records. Table 6.2 shows the various ages assigned to the palaeomagnetic features (ξπρστ) for the locations MFM, LDB, LDJ and Soviet Karelia (KAR) where they are

TABLE 6.2 THE VARIOUS AGES ASSIGNED TO THE PALAEOMAGNETIC FEATURES [illegible] FROM THE LOCATIONS MFM, LDB, LDJ, AND SOVIET KARELIA.

	MFM	LDB	LDJ	KAR.
ε	11.8	13.0	12.7	-
κ	12.6	13.8	13.4	13.2
ρ	13.3	14.2	15.0	14.7
σ	15.3	15.0	-	16.0
τ	18.1	16.2	-	-

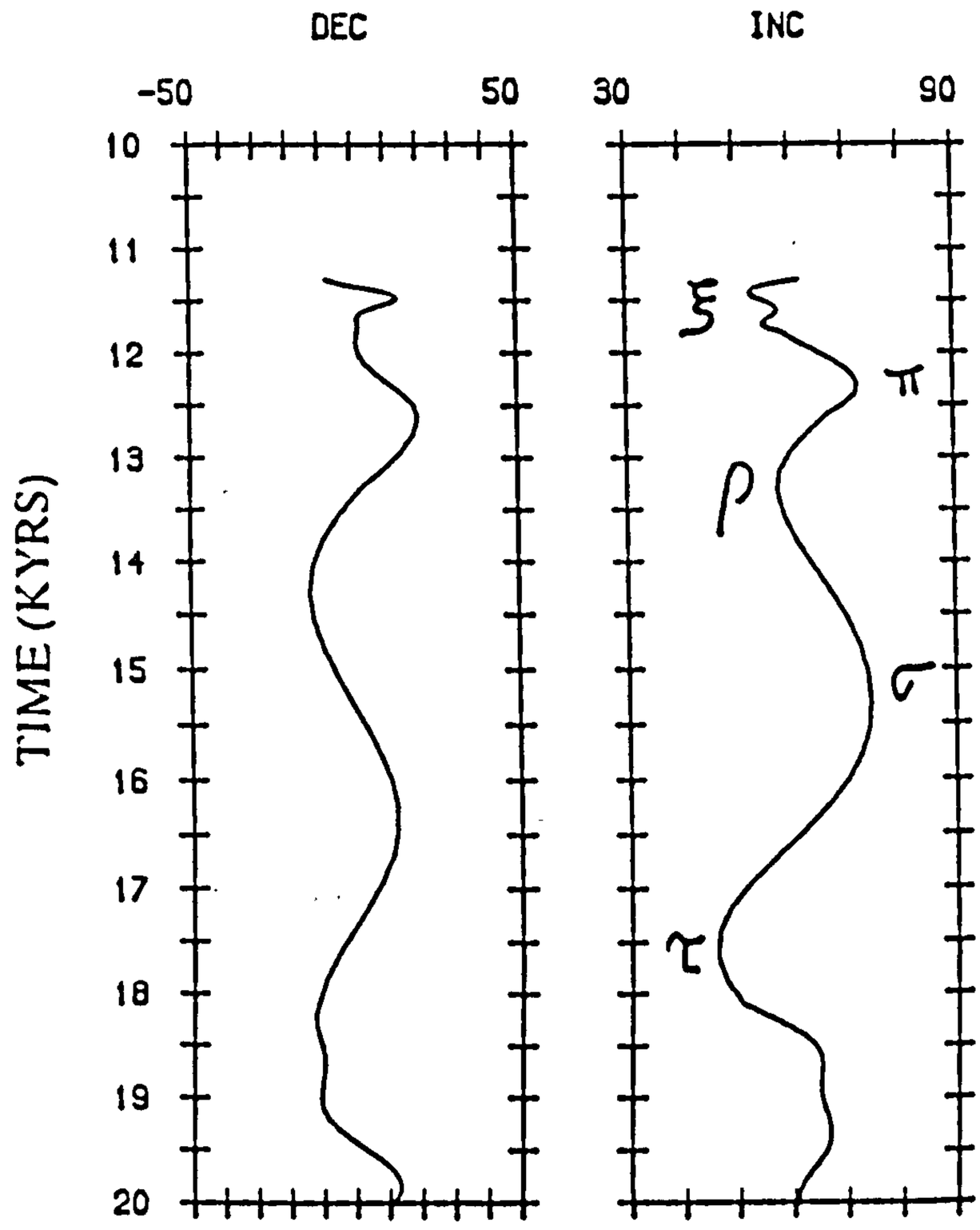

FIG 6.10 LAC DU BOUCHET DECLINATION AND INCLINATION CURVES TRANSFORMED TO A TIMESCALE BASED ON CORRELATION OF PALAEOMAGNETIC FEATURES WITH THE VARVOMETRICALLY DATED MEERFELDER MAAR RECORD.

known. It is suggested that MFM timescale be used as a master to which the other palaeomagnetic curves be fitted. This would have the benefit of improving time control over the various palaeomagnetic records and is especially useful for LDB which is by far the best quality curve in terms of intra-maar consistency, timespan (although not for the Post Glacial) and magnetic intensity. Using these individual palaeomagnetic features (ξπβ⌐τ) to transform the LDB time series further improves the suggested blanket adjustment of 800 years (section 6.6). The results of this transform are shown in FIG 6.10 .

6.8 SUMMARY

The MFM palaeomagnetic record does not exhibit the same degree of intra-maar consistency as the LDB record, however, below 11 kyrs BP the quality is improved considerably. Crosscorrelation between MFM and LDB from 11-19 kyrs reveals a significant correlation where the MFM series lags the LDB series by 800 years. This is not a real effect but a result of the differences in the time transform functions for the two lakes. It is suggested that part of the LDB palaeomagnetic master curve could be dated magnetically by attributing ages, from the more accurately dated MFM series, to the maxima and minima common to the two records.

Further similarities between the palaeomagnetic records are revealed by time series analysis. The periodicities of 2.7 kyrs and 1.8 kyrs in the declination, and 2.0 kyrs in the inclination and intensity records are common to both data sets. In addition a similar phase relationship exists between inclination and declination, the declination leading the inclination. One interpretation of this is that westward drift of the non-dipole field is a feature of geomagnetic secular variation. A comparison of VGP paths reveals the same predominantly clockwise sense of rotation in MFM and LDB records between 11 and 19,000 years BP.

These similarities give credence to the hypothesis of accepting the palaeomagnetic curves as a true product of geomagnetic control and not the result of local sedimentological processes.

CHAPTER SEVEN.

CARBON ISOTOPE GEOCHEMISTRY: CHANGES IN SEDIMENTARY ORGANIC MATTER ASSOCIATED WITH MAJOR CLIMATIC CHANGE.

7.1 INTRODUCTION

It is thought probable that palaeomagnetic signal incoherence in the Post Glacial period could be a consequence of either the type or concentration of organic material found in those samples, (chapter 3). An extreme example of the influence of organic material on the ability of a sediment to record a palaeomagnetic signal is the 'B' horizon of Lac du Bouchet (SMITH 1985) where the preserved fibrous organic matter inhibits sub-sampling; it is unlikely that a sedimentary fabric so constrained could record a geomagnetic signal, (TUCKER 1980). Some indication of the type of extraneous vegetation, which could contribute both soluble and detrital organic matter to MFM is available from spore and pollen data (USINGER I984) indicating a cycle of tundra grassland with shrubs followed by afforestation on climatic amelioration around 12 ka BP. A return to tundra grassland is indicated at around 11 ka BP, the Dryas 111 climatic deterioration, before final afforestation. The other potentially major source of organic matter, the indigenous seasonally sedimenting algal bloom (ZOLITSCHKA 1989) used to construct the varve chronology (chapter 4), is undefined.

We have measured $\delta^{13}C$ and N/C ratios down MFM B core to gain information on the nature of past organic deposition, and total organic carbon (TOC) to indicate relative quantity. Results show large (20‰) $\delta^{13}C$ variations reflecting at least two distinct regimes of organic deposition.

7.2 FACTORS INFLUENCING ISOTOPIC COMPOSITION OF ORGANIC CARBON

Stable carbon isotope compositions of organic matter are dependent on the

pathway of the constituents through the carbon cycle (O'LEARY 1981, DE NIRO 1983). Important factors influencing the isotopic composition are:

A. Original carbon source, ie. atmospheric CO_2 (-7‰) or inorganic carbon derived from carbonate bearing rocks (0‰).

B. The pathway of carbon fixation from source into organisms contributing to the organic matter of the maar sediment, strongly influences the isotopic composition of organic matter (BENDER 1971, DE NIRO 1983). The different types of organism, ie. algae, aquatic and terrestrial vegetation, will modify the reservoir isotopic signature by varying degrees. The method of carbon fixation adopted by an organism during the uptake of carbon from the local reservoir, strongly influences the isotopic composition of organic matter deposited. There are two different methods by which photosynthesising plants take up carbon. These are refered to as the C3 (CALVIN) and C4 (HATCH-SLACK) pathways. C3 photosynthesis includes the carboxylation of ribulose biphosphate (RuBP), this process preferentially utilises ^{12}C resulting in organic carbon isotopic values ranging from -32‰ to -22‰. C4 photosynthetic reactions include carboxylation of phosphoenol pyruvate (PEP). The ^{13}C depletion is not as great as for C3 plants, resulting in organic carbon isotopic values ranging from -23‰ to -9‰. CAM (crassulacean acid metabolism) plants fix atmospheric carbon by both C3 and C4 routes, shifting between pathways in response to environmental conditions, such plants therefore have isotopic compositions indicative of both C3 and C4 types, (O'LEARY 1981, ROUNICK and WINTERBOURNE 1986). Aquatic plants generally follow a C3 pathway although high isotopic values can be found due to the slow diffusion of CO_2 in water, this limits supply hence reducing the fractionation effect (O'LEARY 1981). Aquatic plants are also very sensitive to changes in the water hardness (OANA and DEEVEY 1960, SMITH and EPSTEIN 1971), organic carbon is enriched in ^{13}C in proportion to the hardness of the water. This can lead to a wide range of isotopic values, for example OSMOND et al (1981) report isolated environments resulting in carbon isotope compositions for aquatic plants as low as -50‰ and as high as -16‰.

C. Diagenetic effects: Any post depositional reaction involving the biased

elimination or preservation of a compound group differing from the average isotopic value of the whole organism, will shift the bulk isotopic composition (DEINES 1980), for example, bacterial degradation and decarboxylation reactions.

7.3 METHODOLOGY

Twelve representative samples from MFM B core were subjected to XRD analysis to determine the abundance or absence of carbonate. Any contribution from carbonate carbon would lead to inaccuracies during the determination of the isotopic composition of the organic carbon. (It was also hoped to investigate the possible use of carbonate carbon isotope ratios as a palaeoenvironmental proxy (WALKER and HARKNESS in press.). XRD analyses were performed on a Philips PW 1800 scanning between 5^{o} and 60^{o}. In each case, carbonate concentrations were found to be below the detection level of 3%. However, it was still considered necessary to acid wash all samples to remove traces of carbonate.

The MFM B core was sampled at 30cm intervals between 1m and 21m. A few grammes of sediment were washed in 10% CH_3 COOH to remove carbonate then rinsed with distilled water. Reaction to acid is indicated in TABLE 7.2. Approximately 50mg of sediment was combusted at 850 ^{o}C under vacuum with with 2g of CuO in a sealed quartz tube for five hours, promoting the reaction:

$$C_xH_y + (2x+y/2)CuO \rightarrow xCO_2 + (y/2)H_2O + (2x+y/2)Cu \quad (1)$$

Water generated by reaction with hydrogen bearing organic matter was removed by passing the gaseous reaction products through acetone/dry ice slush trap at -78^{o}C, after which the CO_2 was condensed in a liquid nitrogen trap at -196^{o}C and the noncondensing gases removed under vacuum. The isotopic composition of this purified CO_2 was then determined on a VG ISOGAS SIRA 10 gas source mass spectrometer. The resultant raw data was computed relative to the Pee Dee Belemnite standard (PDB) using equation 2:

$$\delta^{13}C_{PDB} = \frac{(^{13}C/^{12}C)sample - (^{13}C/^{12}C)^{PDB}}{(^{13}C/^{12}C)^{PDB}} X10^3 \quad (2)$$

Repeated measurements of an internal laboratory standard indicated accuracies of 0.07% and precision better than 0.2% . Included were two measurements where the carbon standard was subjected to the same preparative techniques as the sediment to detect fractionation in the sample preparation. It was concluded that a minor shift (0.23%) was induced by acid washing. The NBS21 graphite standard indicated accuracies of 0.01% with precision better than 0.12% , (TABLE 7.1).

A second aliquot of acid washed sediment was subjected to elemental analysis on a CARLO ERBA CNS ANALYSER (model 1500) to measure total organic carbon (TOC) and nitrogen levels. Approximately 5mg of dried sediment was crushed and ground before being sealed within a foil capsule and combusted; elements are distinguished by their retention time which shifts marginally with the build up of ash during a run; acetanilide standards run every five samples allows automatic recalibration for this effect. Percentage error on the standard was calculated at 3.2% for TOC, 1.5% for nitrogen and 2.8% for N/C although repeat measurements on samples of the lowest C,N concentrations, gave a worst case error of 18% where either N or C fell below the detection level.

7.4 RESULTS

$\delta^{13}C_{org}$ values for MFM B core (TABLE 7.2) range from -33.89‰ to -13.85‰, between 21m and 18.5m values rise unsteadily from -30.48‰ to -16.61‰ (FIG 7.1), where upon variation around approximately -19‰ occurs for 2m before an abrupt decline at 16.5m to approximately -28‰. In order to detail this major isotopic shift, the section between 16m and 17.5m was sampled with increased sample

TABLE 7.1 ISOTOPIC COMPOSITIONS OF INTERNAL AND INTERNATIONAL STANDARDS DETERMINED DURING INVESTIGATION OF MFM SEDIMENT.

INTERNAL SURRC C LAB STD. (CALCULATED ACCURACY = -25.65‰)
-25.69
-25.69
-25.67
-25.75
-25.23
-25.44
MEAN = -25.58‰, PRECISION = 0.20‰
-25.79*
-25.84*
*- ACID WASHED SAMPLE
INTERNATIONAL STD. NBS21 (CALCULATED ACCURACY = -28.16‰)
-28.16
-28.24
-28.01
-28.06
-28.28
-28.28
MEAN = -28.17‰, PRECISION = 0.12‰

TABLE 7.2 MFM B CORE GEOCHEMICAL AND CARBON ISOTOPE DATA

DEPTH (cm)	δ13C (‰)	TOC (%)	N\C
129.75	-30.22	18.3	0.076
159.25	-30.94	15.8	0.078
184.25	-31.36	18.7	0.078
213.00	-31.60	21.0	0.085
240.25	-32.17	19.0	0.062
269.50	-32.52	13.2	0.074
297.00	-31.95	13.7	0.089
330.00	-32.17	16.4	0.067
368.00	-28.64	9.8	0.079
402.00	-30.46	8.7	0.080
427.75	-29.41	9.4	0.081
457.75	-31.66	11.3	0.101
486.75	-29.74	10.4	0.071
522.25	-33.31	8.6	0.059
549.50	-32.50	12.4	0.065
576.50	-33.89	6.9	0.132
619.25	-29.31	4.8	0.097
649.50	-30.92	2.9	0.117
674.25	-30.32	5.2	0.065
707.50	-33.18	10.9	0.075
737.50	-32.82	7.1	0.110
764.50	-30.08	2.3	0.043
791.00	-29.61	1.1	0.089
843.00	-28.58	2.3	0.179 +
915.25	-29.23	1.9	0.102 +
974.50	-28.83	0.7	0.210
1023.75	-24.49	0.5	0.103
1077.50	-28.18	0.7	0.126

DEPTH (cm)	δ13C (‰)	TOC (%)	N\C
1138.25	-27.50	0.6	0.000
1192.25	-27.58	0.7	0.000
1246.50	-26.31	0.4	0.000
1319.50	-27.68	0.4	0.000
1355.50	-27.57	0.3	0.000
1383.00	-27.53	0.5	0.000
1415.75	-20.83	0.6	0.000 +
1443.50	-28.50	0.4	0.000
1470.50	-26.47	0.5	0.000
1499.00	-26.95	0.5	0.000
1543.75	-28.35	0.5	0.000
1572.75	-29.10	0.6	0.000
1613.00	-28.11	0.5	0.000
1642.25	-29.68	0.6	0.000
1653.25	-16.65	0.3	0.000
1664.50	-15.54	0.2	0.000
1666.75	-27.53	0.4	0.000
1676.00	-13.85	0.5	0.000
1687.25	-20.39	0.4	0.000
1694.25	-27.21	0.9	0.000
1711.75	-17.91	0.6	0.000
1723.25	-15.70	0.6	0.000
1735.00	-20.19	0.8	0.000
1746.25	-16.48	0.6	0.000
1762.50	-18.85	0.2	0.000
1790.50	-24.49	0.8	0.000
1820.50	-20.74	0.8	0.000
1856.75	-16.61	0.6	0.000 +

TABLE 7.2 CONTD.

1886.00	-20.89	0.7	0.000
1918.50	-28.27	0.5	0.000
1945.75	-22.39	0.5	0.000
1973.75	-29.38	0.5	0.000
2024.75	-25.89	0.7	0.000
2052.00	-26.92	0.6	0.000
2079.00	-30.48	0.7	0.000 +

ADDITIONAL $\delta^{13}C$ VALUES COVERING THE DRYAS III PERIOD

760.00	-30.88
771.25	-30.24
782.50	-29.88
816.00	-28.86
860.50	-28.34
883.00	-27.67
906.00	-27.38 +
928.75	-29.45
952.25	-28.66

+ DENOTES POSITIVE REACTION TO 0.1M ACETIC ACID.

density. Two excursions at 14.2m and 10.2m have been confirmed by repeat analysis. Above 8m a series of skewed but regular fluctuations occurs within a narrow (5‰) range about a mean of approximately -31‰.

TOC results (FIG 7.2) indicate the levels of organic carbon to be below 2% in the bottom 11m of core, however, this increases to 20% at 1m depth. The increase is erratic although some of this small scale detail must be interpreted as within the noise spectrum of 3%.

N/C plot (FIG 7.3) shows erratic variation below 10m with a range of between 0.01 and 0.38. Above 10m, the values are generally lower, (less than 0.12). The coincidence of increased variation of N/C below 10m with the decrease in TOC prompted the set of repeat analyses on samples of low N and C concentrations since at such low carbon concentrations the possibility of large experimental errors in the determinations of nitrogen concentrations could not be ruled out. The repeat analyses indicated precision to only 18% for N/C, thus the N/C fluctuations below 10m are considered inaccurate and unreliable.

Interpretation of the data is based on time curves derived from the depth to time transform function constructed from a varve chronology (ZOLITSCHKA pers comm 1988). This transform has already been discussed in chapter 4.

7.5 QUANTITY OF ORGANIC CARBON

The TOC profile (FIG.7.4) could should reflect both organic productivity in the lake and lake-shore environment and degree of preservation of organic matter in the lake sediment. The marked increase of TOC after 12 ka BP coincides with the end of the Late Glacial period when a climatic amelioration resulted in a decrease in the clastic to organic ratio of deposited material. This trend is not constant suggesting that the primary control over TOC levels is productivity rather than preservation. Further, the preservation of laminations down to millimeter scale in the lake sediment indicates the sediments to have been undisturbed by bioturbation. The absence of reworking is conducive to enhanced preservation of organic matter (TISSOT and WELTE 1984) as consumption by organisms is

FIG 7.1 ORGANIC CARBON ISOTOPE DATA MFM B CORE.

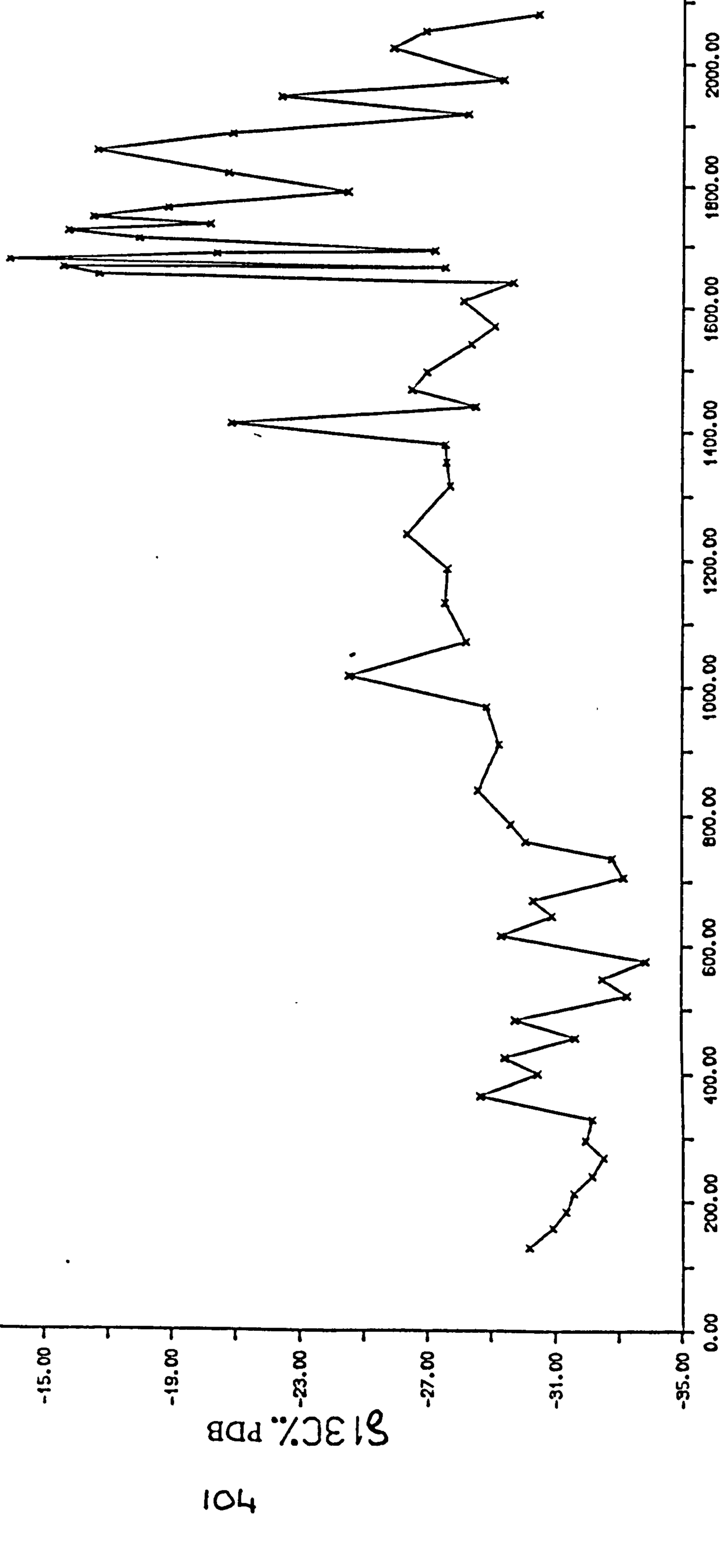

FIG 7.2 TOTAL ORGANIC CARBON DATA MFM B CORE.

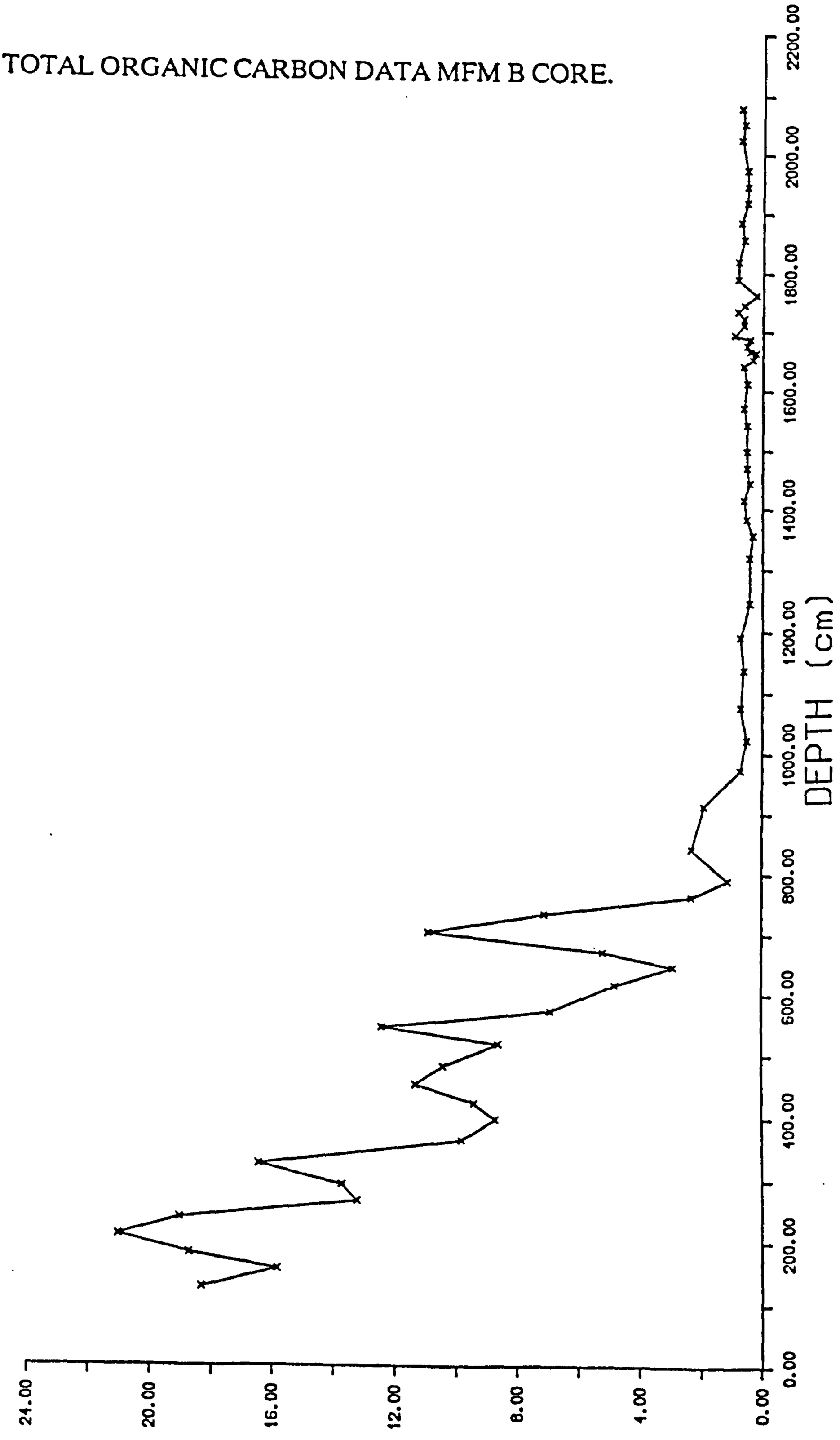

FIG 7.3 NITROGEN, CARBON RATIOS FOR MFM B CORE.

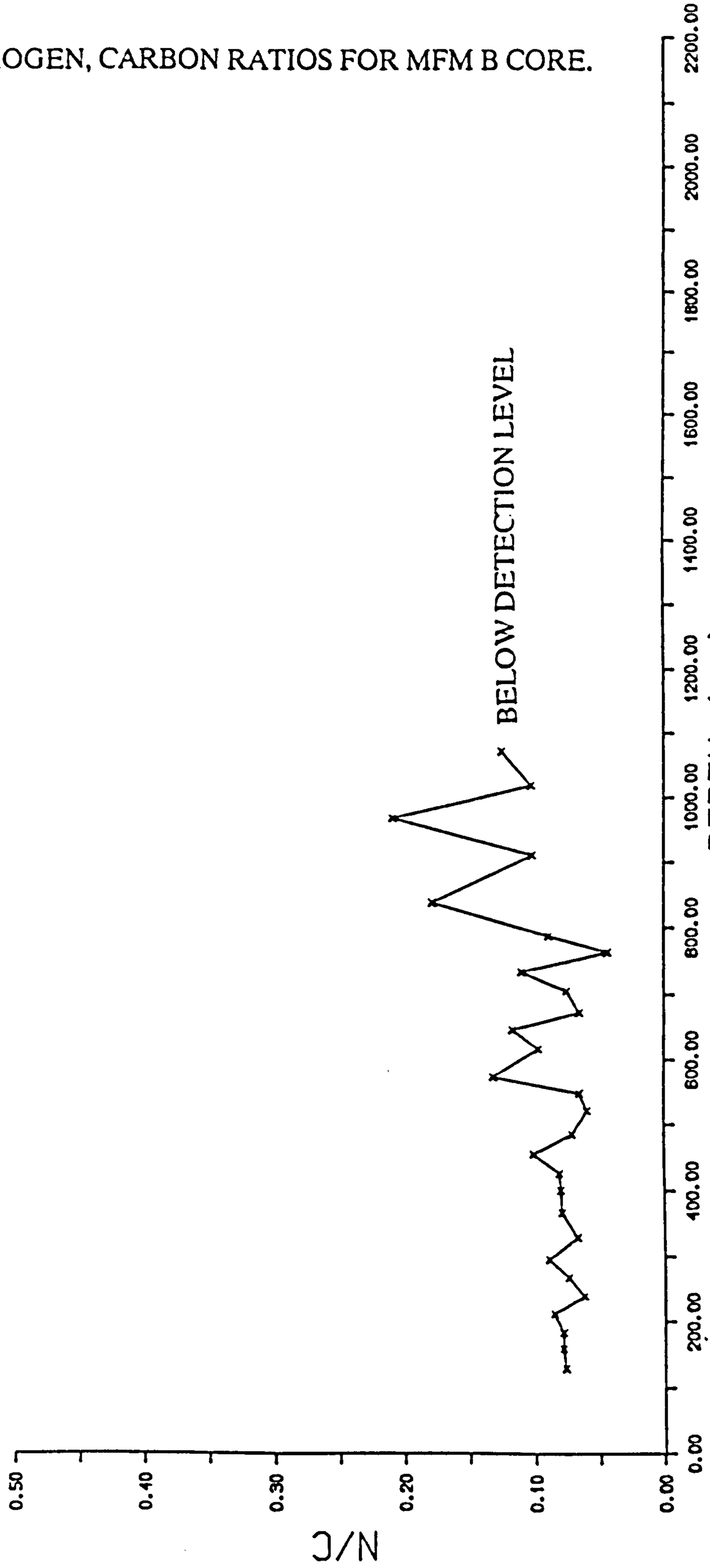

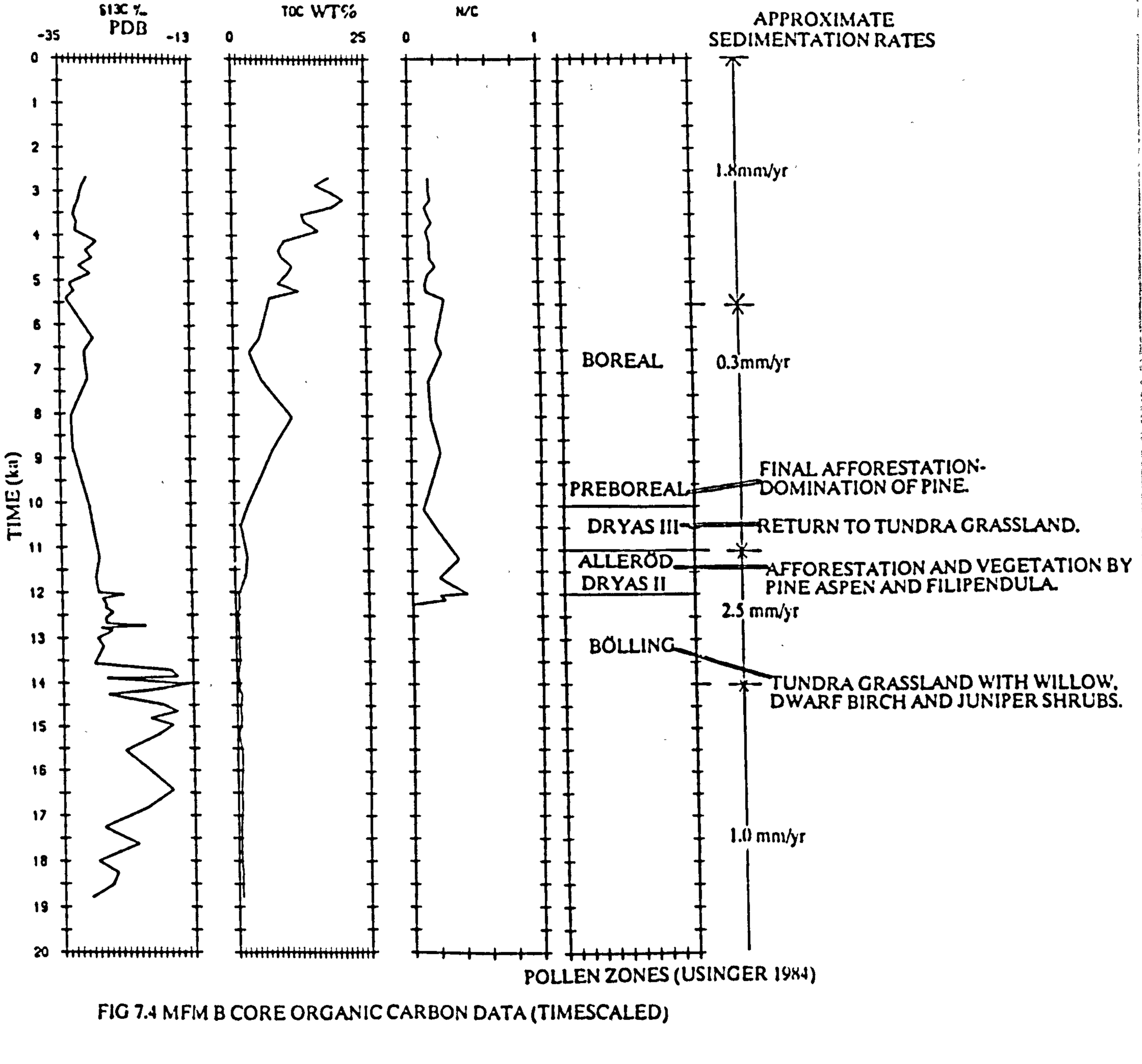

FIG 7.4 MFM B CORE ORGANIC CARBON DATA (TIMESCALED)

minimised and the sediment is not oxygenated by contact with oxygen-rich bottom waters, thus reducing the extent of the aerobic oxidation zone where maximum destruction occurs. In addition, MFM will have a limited aerobic zone by reason of the fine grain sizes of the sediments which reduces permeability and therefore the penetration of oxygenated water (FIG 7.5).

7.6 NATURE OF ORGANIC CARBON

The organic carbon pote ntially comprises; internally a seasonally sedimenting algal bloom plus various submersed macrophytes, and externally vegetation from the maar catchment zone. We could expect the inorganic component to have remained fairly constant in terms of composition because of the restricted sediment source of the maar crater, however, the organic component composition will have varied in response to the environmental changes of this period.

7.6.1 PALYNOLOGICAL EVIDENCE

The nature of the terrestrial organic input to MFM has been defined by palynological analysis, (USINGER 1984). Pollen and spore data indicate a cycle of treeless tundra grassland with willow, dwarf birch and juniper shrubs followed by vigorous afforestation and vegetation on climatic amelioration around 12 ka BP by juniper and downy birch followed by pine, aspen and filipendula. A return to tundra grassland is indicated during the Dryas III (11 ka BP) climatic deterioration before final afforestation and domination of pine from Preboreal times, about 10 ka BP.

7.6.2 EVIDENCE FROM ELEMENTAL ANALYSIS

In addition to determining the quantity of organic carbon (TOC), elemental analysis can also assist in defining the nature of organic carbon through calculation of N/C ratios (JASPER and GAGOSIAN 1989). The more protein rich matter such as algae have higher N/C values than plant material which is relatively protein poor (STUERMER 1978). The N/C value may therefore reflect the relative

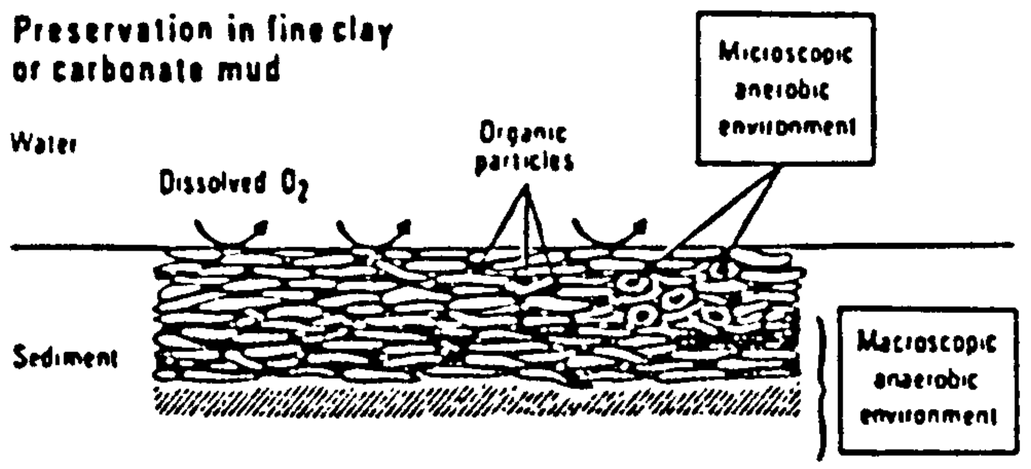

FIG 7.5 PRESERVATION OR DESTRUCTION OF ORGANIC MATTER IN FINE GRAINED SEDIMENTS (TOP) WHERE THERE IS NO REPLENISHMENT OF OXYGEN AND ANAEROBIC CONDITIONS ARE RAPIDLY ESTABLISHED. IN COARSE GRAINED SEDIMENTS, (BOTTOM) FREE CICULATION OF WATER CONTAINING DISSOLVED OXYGEN RESULTS IN DESTRUCTION OF THE ORGANIC MATTER. (after TISSOT and WELTE 1984).

contribution of the algal material to the total organic carbon of the lake sediment. Work by ZOLITSCHKA (1988) studying the varve structures suggests an increased algal component from about 12.5 ka BP.

After 12 ka BP, the N/C profile (FIG 7.4) exhibits values consistently in the range of higher plants (less than 0.1). Deeper in the zone of low organic productivity, results are unreliable. It is apparent that N/C elemental analysis is inconclusive in the task of further constraining relative sources of organic matter and despite the known algal contribution after 12.5 ka BP, N/C ratios have a higher plant signature. This suggests that the major organic constituent of the varves is the autumnal maximum of vegetation deposition.

7.6.3 ISOTOPIC EVIDENCE

The organic composition of MFM B core sediment will have varied in response to changing environmental conditions. The $\delta^{13}C$ profile may then reflect these variations if changes in the carbon reservoir and fractionation induced by diagenesis can be constrained.

A. ORGANIC CARBON SOURCE VARIATION AS δC^{13} CONTROL

It is suggested that the carbon isotopic signature from the sedimentary organic material reflects variations in the source organic carbon contributing to the sediment a product of the changing environmental conditions at MFM. In the Late Glacial, up until 13.5 ka BP, the pollen record (USINGER 1984) indicates a grass dominated tundra environment, the low TOC presumably reflecting the low organic productivity at that time. The isotopic record exhibits the heaviest values here, which drop sharply in synchronisation with the change in vegetation indicated by the pollen record. It is possible that these heavy isotopic values are the result of a contribution of C4 photosynthesising grasses (O'LEARY 1981) or are a signature of the indigenous algal bloom (ZOLITSCHKA 1989). C4 grasses most commonly occur in water stressed environments such as salt-marsh or desert, it is not known whether the environment of MFM during the late glacial was capable of allowing such specialised species to flourish.

Between 13.5 and 9 ka BP, the period covering the Pleistocene to Holocene temporal boundary and much climatic, hence vegetational fluctuation, isotopic values remain relatively steady at around -28‰. The distinct drop at 9 ka BP has no associated vegetational change or emergence of a new source of isotopically distinct carbon within the lake. However, HAAKANSSON (1986) has described similar shifts (approximately -8‰) in the isotopic composition of several southern Swedish lakes, indicating that a large regional if not global, effect is responsible for the changes in $\delta^{13}C$.

From 9 ka BP to present the dramatic increase of TOC and the N/C levels, indicating higher plant material, suggests the primary source of organic matter to the lake to be plant material from the catchment zone. The light isotopic values suggest C3 photosynthesising plants dominate.

The cyclicity of this section is difficult to explain but may be the result of variations in the dominance of different pollen types with various $\delta^{13}C$ values within the broad C3 range.

B. RESERVOIR AS $\delta^{13}C$ CONTROL

The main choices of reservoir from which organisms may fix carbon are: 1. atmospheric carbon dioxide and 2. bicarbonate generated by dissolution of limestone from the local groundwater regime. The latter option can be ruled out as a significant contributer in the case of MFM since carbonate is almost non-existent in the sediments analysed in this study. The isotopic value of atmospheric carbon has not varied significantly over the period of MFMB deposition (STUIVER 1975), the major controls on the isotopic composition of atmospheric carbon being temperature and pollution. Although the results of HAAKANSSON (1986) suggest a global excursion in $\delta^{13}C$ which may be related to a variation in atmospheric carbon isotope composition.

C. DIAGENESIS AS $\delta^{13}C$ CONTROL

The isotopic signature is susceptible to change via diagenesis by reason that most

diagenetic processes induce a fractionation effect. Early alteration of biospheric carbon during conversion to geospheric carbon, is in the form bacterial degradation. This would normally occur in three stages (TISSOT and WELTE 1984): 1. oxidation, 2. anaerobic sulphate reduction, although dissolved sulphate concentration in fresh water is usually very low, and 3. anaerobic methane generation.

At MFM any oxidising zone is extremely limited due to the eutrophic nature of the water column (ZOLITSCHKA 1988), the lack of bioturbation and the fine grain size which reduces permeability (section 7.5). We can therefore assume that anaerobic sulphate reducing conditions are established very close to the sediment-water interface and within a few centimetres of the sediment surface. The bacterial degradation occuring under these conditions preferentially utilises ^{12}C leading to an increase in $\delta^{13}C$ of the residual material. However, incorporation of the resultant ^{12}C rich bacteria into the sediment will oppose this trend.

If diagenesis has progressed onto anaerobic methane generation, then isotopic values might increase as the methane is very ^{12} C rich, however, this is balanced by the action of methane oxidising bacteria which generate ^{13}C rich CO_2.

With the balancing of bacterial degradation by bacterial incorporation and of methane generation by methane oxidation, the expected trend is ^{13}C increase due to preferential consumption of ^{12}C components. The abrupt $\delta^{13}C$ changes in MFM B (12 and 20 ka BP) are inconsistent with these anticipated effects of diagenetic fractionation, unless imbalance exists in the diagenetic behaviour with for instance the loss to the system of an isotopically light or heavy fraction.

D. OTHER INFLUENCES

A study by HAAKANSSON (1986) of sediment from nine Swedish lakes, revealed a drop in $\delta^{13}C$ in eight out of nine cases, over the Pleistocene/Holocene boundary. A similar feature is evident in the data from MFM although much more detail is available as HAAKANSSON's results were based on an average of less than six isotopic determinations per lake. No conclusions were reached by HAAKANSSON

(1986) as to the specific cause of this widespread drop. The MFM results not only show the same drop over the Pleistocene/Holocene boundary but also an equally dramatic increase around 17 ka BP.

7.7 CONCLUSIONS

The quantity of organic material deposited in MFM is accurately reflected in the TOC profile for MFM B core. This indicates that organic productivity increased dramatically above 10m. Variation in the type of organic material deposited in MFM is indicated by the carbon isotope signature. Distinct regimes of organic deposition have been defined isotopically with boundaries at 16.5m and around 8m.

Concerning the change in quality of palaeomagnetic signal, this seems most closely related to the quantity of organic matter being deposited. The accompanying decrease in concentration of magnetic minerals substantially reducing the intensity of the palaeomagnetic signal.

It is difficult to quantify the effect of variations in the type of organic material on the palaeomagnetic signal. It is possible that the C3 higher plant material dominant in the upper 8m of core is less degradable and therefore might be disruptive to the sedimentary fabric to a depth beyond the magnetic 'locking depth' (TUCKER 1983) thus preventing the recording of a geomagnetic signal.

The carbon isotope data itself and its relation to the other organic indicators (pollen, TOC, N/C) is extremely interesting in that they reveal major shifts in the $^{13}C/^{12}C$ ratio of organic matter deposited over the last 20,000 years. This 20‰ variation is vast, covering a considerable portion of the reported range of isotopic C_{org} values (DEINES 1980). The variation appears to be mostly dependent on the composition of organic material entering the lake from the catchment zone.

During the Pleistocene it is possible that the isotopic signature is controlled by variation in the dominance of C3 or C4 photosynthesising plants from the

catchment zone, although around the Pleistocene to Holocene transition there appears to be a regional or possibly global control. The flourishing of the annual algal bloom through the Holocene has neither caused a dramatic shift in isotopic compositions, nor buffered the sedimentary organic matter compositions from vegetational changes occuring in the catchment zone where some of the cyclic smaller scale variations may represent changes in the dominance of specific plant types.

CHAPTER EIGHT.

CONCLUSIONS

8.1 IDENTIFICATION AND STABILITY OF THE MAGNETIC MINERALS

The magnetic mineralogy of MFM has been shown to consist mainly of original detrital grains from the titanomagnetite series, predominantly multidomaim magnetite. A small amount of hematite is also present. There is no significant change in magnetic mineralogy downcore, reflecting the isolated catchment of MFM, although a marked increase in the magnetic intensity in the uppermost 1m of sediment has been attributed to changes in the magnetic mineralogy related to anthropogenic activity. The magnetic remanence carried is most likely to be a post depositional remanent magnetisation, It is a stable primary remanence with a weak (<10mT) viscous or drilling overprint.

8.2 PALAEOMAGNETIC SECULAR VARIATION AND ANALYSIS

There is no evidence of sedimentary control over magnetic directions at MFM, nor any indications of diagenetic alteration to the magnetic minerals to produce a CRM. It is therefore probable that the palaeomagnetic secular variations recorded in MFM sediment are a product of the geomagnetic field. This is supported when analysis of the processed palaeomagnetic data from MFM is compared with results from the established type curve from LDB, where-upon many similarities are revealed: peroidicities of 2.7 and 1.8 kyrs in the declination record and of 2.0 kyrs in the inclination and intensity records, a similar phase relationship where the declination leads the inclination, and dominantly clockwise looping VGP paths. These similarities indicate that the palaeomagnetic signal recorded in these lake sediments exhibit a regional control especially when considering the palaeoinclination record where the features (ξ π ρ σ τ) are distinctive and observable in many lake sediment palaeomagnetic records. However, the quality of the MFM palaeodirectional data is not of the same high standard as that from LDB: the intra-maar correlation is inferior and we might also have expected better inter-

Magnetic mineral dissolution may be indicated in the top 8.5m of MFM by the link between their downcore reduction in grainsize and the simultaneous reduction in preserved organic carbon (FIGS 2.3, 7.2). Further study should include using the improved chronology of NEGENDANK et al (1990) to asses the association of carbon flux with these diagenetic reactions and other parameters discussed in this work.

The reduction in magnetic mineral grainsize (0-8.5m) may also provide a link with the quality of palaeomagnetic directional data. Further work might include investigation of the relationship between grainsize and inclination data quality since the level of inclination error associated with an individual magnetic particle is directly related to its grainsize.

maar correlation between palaeomagnetic signals recorded in such analogous environments. It can be concluded, because of the similarities between records, that we are measuring a geomagnetic signal; but also that it is only the unique environment of LDB that has produced a palaeomagnetic signal of suitable quality for analysis on aspects of the geomagnetic field.

Correlation between the palaeoinclination features (ξ πρσ τ) from MFM and LDB has enabled some improvements to the LDB timescale between 11 and 19 ka BP to be made, since these features have been more reliably dated at MFM using the varve chronology according to ZOLITSCHKA (1988).

8.3 THERMOLUMINESCENCE DATING

Edinburgh University Physics Department thermoluminescence laboratory now has a working TL unit and gamma spectrometer capable of dating maar lake sediments. At present it is also being developed for optically stimulated luminescence dating to provide an alternative and/or support dating method for comparison to thermoluminescence. The large errors encountered during this study have been constrained to the bleaching effect of the laboratory lighting on the measured TL with the additional possibility of error contributed from incomplete zeroing and/or some doubt over the applicability of the moisture correction to the dose rate of such high water content samples.

8.4 ORGANIC CARBON ISOTOPE GEOCHEMISTRY

Palaeomagnetic signal degradation in the MFM record during the Post Glacial has been linked with the quantity of organic carbon being deposited and preserved at that time. Increased TOC both dilutes the magnetic content, hence reducing the magnetic intensity of the signal, and may physically disrupt the recording of a PDRM that relects past geomagnetic field directions.

The organic carbon isotopic signature from MFM reveals a variety of information on the changing nature of sedimentary organic matter through a major climatic

change. Significant shifts in the $^{13}C/^{12}C$ ratio appear mainly dependent on environmentally controlled shifts in vegetational carbon and fluctuations in isotopically distinct carbon within MFM, however, a major shift at the Pleistocene/Holocene temporal boundary is independent of such variations but correlates with reports of $\delta^{13}C$ change from other localities. This suggests the influence of a large regional if not global effect being responsible for the change in $\delta^{13}C$ of sedimentary organic matter deposited at that time. Thus a $\delta^{13}C_{org.}$ profile is not a simple geothermometer or palaeovegetational indicator but a much more integrated view of the carbon cycle of a lacustrine environment.

Further work in this field to resolve the questions arising from this study should include characterisation of the organic matter in MFM and a ^{13}C study of the individual species comprising the organic material.

8.5 OVERVIEW

Considering future developments in the area of Quaternary research around this work; firstly, there is great potential for application of the varve chronology of MFM to the independent continuous calibration of the radicarbon timescale. This could be achieved by a programme of accelerator dating the organic carbon from the yearly autumnal organic-rich layer of the MFM varves (ZOLITSCHKA 1989). This should also proceed within a broad multidisciplinary framework involving isotopic analyses of the organic carbon to monitor the potential problem of contamination by dead carbon from magmatic sources. This information would have application to evaluating the link between the variation of atmospheric ^{14}C and changes in the magnetic moment of the dipole field.

Secondly, the proposed regional / global $\delta^{13}C$ drop around the Pleistocene to Holocene transition (section 7.7) might be considered in the context of ice retreat from the lake environment. It is interesting to note that a current study (ROBINSON pers com 1991) of the $\delta^{13}C_{org}$ profile for Lago de Monticchio, Italy, which would have undoubtedly been well south of the last glaciation, does not reveal this shift towards lighter carbon. If this phenomena is asociated with the deglaciation then we have a tool to determine the extent and timing of ice sheet movements.

APPENDIX A.

OVERVIEW OF ANALYSES

MEERFELDER MAAR CORE A (MFMA) MEASUREMENTS

NATURAL REMANENT MAGNETISATION (NRM)

PILOT DEMAGNETISATIONS

BULK DEMAGNETISATION, 10mT

SUSCEPTIBILITY

SMEAR SLIDES

XRF ANALYSIS

EXTRACTION OF MAGNETIC MINERALS

XRD OF EXTRACTS

THERMOMAGNETIC ANALYSIS OF EXTRACTS

SEM VIEW OF EXTRACT

MEERFELDER MAAR CORE B (MFMB) MEASUREMENTS

NRM

PILOT DEMAGNETISATIONS

BULK DEMAGNETISATION, 10mT

SUSCEPTIBILITY

ARM PILOTS 40, 60, 80mT

DEMAGNETISATION OF ARM PILOTS

IRM AQUISITION

PARTIAL DEMAGNETISATION OF SIRM

XRD ISOTOPE GEOCHEMISTRY PILOTS

$\delta^{13}C$ (70 SAMPLES)

TOTAL ORGANIC CARBON (TOC)

ELEMENTAL ANALYSIS, N/C

MEERFELDER MAAR C CORE (MFMC) MEASUREMENTS

THERMOLUMINESCENCE PILOT SAMPLES

MEERFELDER MAAR D CORE (MFMD) MEASUREMENTS

NRM

PILOT DEMAGNETISATION

BULK DEMAGNETISATION

SUSCEPTIBILITY

MEERFELDER MAAR E CORE (MFME) MEASUREMENTS

NRM

PILOT DEMAGNETISATION

BULK DEMAGNETISATION

MEERFELDER MAAR F CORE (MFMF) MEASUREMENTS

THERMOLUMINESCENCE SAMPLES (X10)

LAC DU BOUCHET CORE Z (LDBZ) MEASUREMENTS

NRM

PILOT DEMAGNETISATION

BULK DEMAGNETISATION

SUSCEPTIBILITY

ALPHA COUNTING

THERMOLUMINESCENCE SAMPLES (X6)

APPENDIX B

CHEMICAL PREPARATION PROCEDURE FOR TL SAMPLES

1) Dry sediment at 40^{o}C overnight.

2) Crush gently to disaggregate.

3) Add 25ml of distiled water and 10% HCl to a ph of 3.5.

4) Heat to 80^{o}C and add drops of 10% HCl until effervescence ceases.

5) Carefully add 50ml of 30% hydrogen peroxide, allow to settle for 10mins.

6) Heat gently for 2mins to dissociate excess hydrogen peroxide.

7) Add 10ml 30% hydrogen peroxide and allow to digest by leaving for 2 hrs at 50^{o}C covered by a watch glass.

8) Heat briefly.

9) Add distilled water to make up to 300ml plus 15g of oxalic acid, stir well.

10) Add perforated aluminium sheet and leave on hotplate until colour changes brown to grey, (approx 10mins).

11) remove aluminium sheet.

12) Wash the sample in distilled water in a litre cylinder filled to 640ml, allowing sample to settle for 5hrs before siphoning off the liquid.

13) REPEAT (12) twice.

14) Transfer sample to a poly beaker and add 10% HF to 200ml for 3hrs.

15) Siphon off the HF, VERY CAREFULLY.

16) Add distilled water to 300ml.

17) Add 10ml of 10% calgon to disperse the sediment ready for grain size separation by settling.

REFERENCES

Aitken M.J., 1979, Dose rate evaluation : PACT v. 2, p. 18-33.

Aitken M.J., 1985, Thermoluminescence Dating : Academinc Press, New York.

As J.A., 1967, The a.c. demagnetisation technique: in: Methods in palaeomagnetism, Collinson D.W., K.M. Creer and S.K. Runcorn eds, Elsevier, Amsterdam.

Bakhmutov V.G. and G.F. Zagniy, 1990, Secular variation of the geomagnetic field : data from the varved clays of Soviet Karelia : Physics of the Earth and Planetary Interiors v. 63, p. 121-134.

Barraclough D.R., 1982, Historical observations of the geomagnetic field : Philosophical Transactions of the Royal Society of London v. A306, p. 71-78.

Bender M.M., 1971, Variation in the $^{13}C/^{12}C$ ratios of plants in relation to the pathway of photosynthetic carbon dioxide fixation : Phytochemistry v. 10, p. 1239-1244.

Berger G.W., 1988, Dating Quaternary events by luminescence : Geological Society of America, Special Paper 227.

Berger G.W., J.J. Clague and D.J. Huntley, 1987, TL dating applied to glaciolacustrine sediments from central British Columbia : Canadian Journal of Earth Sciences v. 24, p. 425-434.

Boyle R., 1663, Experiments and considerations upon colours with observations on a diamond that shines in the dark.

Bullard E.C., C. Freedman, H. Gellman and J. Nixon, 1950, The westward drift of the Earth's magnetic field : Philosophical Transactions of the Royal Society of London v. 243, p. 67-92.

Carver R.E., 1971, Procedures in Sedimentary Petrology : Wiley.

Collinson D.W., 1983, Methods in rock magnetism and palaeomagnetism, Chapman and Hall.

Craig R.F., 1984, Soil Mechanics 3rd edition : Van Nostrand Reinhold, UK.

Creer K.M., 1971, Geophysical interpretation of remanent magnetisation in oxidised basalts : Zeitschrift fur Geophysik, band 37, seite 383-407, Physica-Verlag, Wurzburg.

Creer K.M., 1983, Computer synthesis of geomagnetic palaeosecular variations : Nature v. 304, p. 695-699.

Creer K.M., 1985, Review of lake sediment palaeomagnetic data (part 1) : Geophysical Surveys 7 by D. Reidel publishing coy.

Creer K.M., 1988, Geomagnetic field and radiocarbon activity through Holocene time : in F.R. Stephenson and A.W. Wolfendale eds., Secular, solar and geomagnetic variations in the last 10000 years, Kluwer Academic Publishers, p. 381-397.

Creer K.M., 1989, The Lac du Bouchet palaeomagnetic record : its reliability and some inferences about the character of geomagnetic secular variations through the last 50000 years : in F.J. Lowes, D.W. Collinson, J.H. Parry, S.K. Runcorn, D.C. Tozer and A. Soward eds., Geomagnetism and Palaeomagnetism, Kluwer Academic Publishers, p. 71-89.

Creer K.M., G. Smith, P. Tucholka, E. Bonifay, N. Thouveny and E. Truze, 1986, A preliminary palaeomagnetic study of the Holocene and late Wurmian sediments of Lac du Bouchet (Haute-Loire, France) : Geophysical Journal of the Royal astronomical Society, v. 86, p. 943-964.

Creer K.M., N. Thouveny and I. Blunk, 1990, Climatic and geomagnetic influences on the Lac du Bouchet palaeomagnetic secular variation record through the last 10000 years : Physics of the Earth and Planetary Interiors v. 64, p. 314-341.

Davies J.C., 1973, Statistics and data analysis in geology, Wiley.

Debenham N.C., 1985, Use of UV emissions in TL dating of sediments : Nuclear Tracks and Radiation Measurements v. 10, p. 717-724.

Deines P., 1980, the isotopic composition of reduced organic carbon : in Fritz and Fontes eds., Handbook of Environmental Radiation Volume 1.

De Niro M.J., 1983, Distribution of the stable isotopes of carbon, nitrogen, oxygen and hydrogen among plants : in W,G, Meinschein ed., Organic Geochemistry of Contemporaneous and Ancient Sediments.

Dunlop D.J., 1981, The rock magnetism of fine particles : Physics of the Earth and Planetary Interiors, v. 26 p. 1-26.

Feder J., 1988, Fractal records in time : in Fractals, chapter 9, Plenum.

Fleming S. J., 1970, Thermoluminescent Dating: refinement of the quartz inclusion method: Archaeometry v. 12, p. 133-145

Galloway R.B., 1990, Notes on a recently constructed TL system : Ancient TL v. 8 no. 2, p. 10-11.

Gemmell A.M.D., 1985, Zeroing of the TL signal of sediment undergoing fluvial transportation : a laboratory experiment : Nuclear Tracks v. 10 nos. 4-6, p. 695-702.

Gilberte W., 1958, "De Magnete" (1600) ; reprinted by Dover, New York.

Gorce W.S. and M. Fuller, 1976, Magnetometers using RF-driven squids and their applications in rock magnetism and palaeomagnetism : Reviews of Geophysics and Space Physics v. 14 no. 4, p. 591-608.

Gubbins D., 1989, Historical secular variation and geomagnetic theory : in F.J. Lowes, D.W. Collinson, J.H. Parry, S.K. Runcorn, D.C. Tozer and A. Soward eds., Geomagnetism and Palaeomagnetism, Kluwer academic Press, p. 31-43.

Haakansson S., 1986, A marked change in the stable carbon isotope ratio at the Pleistocene-Holocene boundary in southern Sweden : Geol. Forens. Stockholm Forhandl v. 108 no. II, p. 155-158.

Housden J., A. De Sa and W. O'Reilly, 1988, The magnetic balance and its application to studying the magnetic mineralogy of igneous rocks : Journal of Geomagnetism and Geoelectricity v. 40, p. 63-75.

Irion G. and J.F.W. Negendank, 1984, Sediment sequences - Das Meerfelder Maar : Cour. Fourch. Inst. Senkenberg v. 65, p. 17-20, Frankfurt.

Jasper J.P. and R.B. Gagosian, 1989, Glacial-interglacial climatically forced $\delta^{13}C$ variations in sedimentary organic matter : Nature v. 342, p. 60-62.

Latham A., 1988, Current progress in studies of secular and palaeosecular variation of earth's magnetic field : EOS April 26.

Levi S. and S.K. Banerjee, 1976, On the possibility of obtaining relative palaeointensities from lake sediments : Earth and Planetary Science Letters v. 29, p. 219-226.

Lorenz V., 1973, On the formation of maars : Bulletin Volcanologique v. 37, p. 183-204.

Lowrie W. and M. Fuller, 1971, On the alternating field demagnetisation characteristics of multidomain thermoremanent magnetisation in magnetite : Journal of Geophysical Research v. 76, p. 6339-6349.

Magee G., 1982, "Popper", Collins, Glasgow, p. 44.

Mackereth F.J.H., 1971, On the variation in the direction of the horizontal component of the magnetisation in lake sediments : Earth and Planetary Science Letters v. 12, p. 332-338.

Mandelbrot B.B. and J.R. Wallis, 1969, Some long-run properties of geophysical records : Water Resources Research v. 5 no. 2, p. 321-334.

McKeever S.W.S., 1985, Thermoluminescence of Solids : Cambridge solid state science series, Cambridge University Press.

Mejdahl V., 1985, TL dating of partially bleached sediments : Nuclear Tracks v. 10 nos. 4-6, p. 711-715.

Mejdahl V., 1986, Thermoluminescence dating of sediments : Radiation Protection Dosimetry v. 17, p. 219-227, Nuclear Technology Publishing.

Moffatt H.K., 1978, Magnetic Field Generation in Electrically Conducting Fluids, Cambridge University Press.

Morris A., 1990, Palaeomagnetic studies of the Mesozoic-Tertiary tectonic evolution of Cyprus, Turkey and Greece : Ph.D. thesis, University of Edinburgh.

Murray A.S. and M. J. Aitken, 1982, The measurement and importance of radioactive disequilibria in TL samples : PACT v. 6, p. 53-60.

Neel L., 1955, Some theoretical aspects of rock magnetism : Advances in Physics v. 4, p. 191-243.

O'Leary M.H., 1981, Carbon isotope fractionation in plants (Review) : Phytochemistry v. 20 no. 4, p. 553-567.

Oana S. and E.S. Deevey, 1960, Carbon 13 in lake waters and its possible bearing on palaeolimnology : American Journal of Science v. 258A, p. 253-257.

Osmond C.B., N. Valaane, S.M. Haslam, P. U. Otila and Z. Roksandic, 1981, Comparisons of $\delta^{13}C$ values in leaves of aquatic macrophytes from different habitats in Britain and Finland : Oecologia v. 50, p. 117-124.

Peddie N.W.,1979, Current loop models of the Earth's magnetic field : Journal of Geophysical Research v. 84, B9, p. 4517-4523.

Pernika E. and G.A. Wagner, 1982, Radioactive equilibrium and dose rate determination in TL dating : PACT v. 6, p. 132-144.

Piper D.J.W., 1974, manual of sedimentological techniques : Dalhousie University, Halifax.

Popper K.R., 1963, Conjectures and Refutations : The Growth of Scientific Knowledge, RKP, London.

Rounick J.S. and M.J. Winterbourn, 1986, Stable carbon isotopes and carbon flow in ecosystems : Bioscience v. 36 no. 3. p. 171-177.

Runcorn S.K., 1959, On the theory of geomagnetic secular variation : Annals de Geophysics v. 15, p. 87-92.

Singhvi A.K. and V. Mejdahl, 1985, Thermoluminescence dating of sediments : Nuclear Tracks v. 10, p. 137-161.

Smith B. N. and S. Epstein, 1971, Two categories of $^{13}C/^{12}C$ ratios for higher plants : Plant Physiology v. 47, p. 380-384.

Smith G. and K.M. Creer, 1986, Analysis of geomagnetic secular variations, 1000-3000 years b.p., Lac du Bouchet, France : Physics of the Earth and Planetary Interiors v. 44, p. 1-14.

Smith G., 1985, Late glacial placomagnetic secular variations from France : Ph.D. thesis, Edinburgh University.

Smith P.J., 1981, The Earth as a magnet : in D.J. Smith ed., The Cambridge Encyclopedia of Earth Science, Cambridge.

Snowball I. and R. Thompson, 1988, The occurrence of greigite in sediments from Loch Lomond : Journal of Quaternary Science v. 3, p. 121-125.

Stuermer D.H., K.E. Peters and I.R. Kaplan, 1978, Source indicators of humic substances and proto-kerogen. Stable isotope ratios, elemental compositions and electron spin resonance spectra : Geochimica et Cosmochimica Acta v. 42, p. 989-997.

Stuiver M., 1975, Climate versus changes in ^{13}C content of the organic component of lake sediments during the late Quaternary : Quaternary Research v. 5, p. 251-262.

Templer R.H., 1986, The localized transition model of anomalous fading : Radiation Protection Dosimetry v. 17, p. 493-497.

Thompson R. and F. Oldfield, 1986, Environmental Magnetism : Allen and Unwin, London.

Thouveny N., 1987, Variations of the relative palaeointensity of the geomagnetic field in western Europe in the interval 25-10kyr b.p. as deduced from analyses of lake sediments : Geophysical Journal of the Royal astronomical Society v. 91, p. 123-142.

Thouveny N., K.M. Creer and I. Blunk, 1990, Extension of the Lac du Bouchet palaeomagnetic record over the last 120,000 years : Earth and Planetary Science Letters v. 97, p. 140-161.

Tissot B.P. and D.H. Welte, 1984, Petroleum Formation and Occurrence, Springer-Verlag, Berlin.

Tritton D.J. 1988, Deterministic chaos, Geomagnetic reversals and the Spherical pendulum : Proceedings of NATO ASI on Geomagnetism and Palaeomagnetism, University of Newcastle-upon-Tyne.

Tucker P., 1980, A grain mobility model of post-depositional realignment : Geophysical Journal of the Royal astronomical Society v. 63, p. 149-163.

Tucker P., 1981, Palaeointensities from sediments : normalization by laboratory redepositions : Earth and Planetary Science Letters v. 5b, p. 398-404.

Tucker P., 1983, Magnetization of unconsolidated sediments and theories of DRM : in K.M. Creer, P. Tucholka and C.E. Barton eds., Geomagnetism of baked clays and recent sediments, Elsevier Amsterdam, p. 9-19.

Usinger H., 1984, Pollen investigations on the age of Meerfelder Maar and on vegetational development in the western Eifel mountains during the declining ice age : Cour. Forsch - Inst. Senkenberg v. 65, p. 49-66, Frankfurt.

Walker J.C. and D.D. Harkness, (in press): The Devensian Late Glacial carbon isotope record from Llanilid, south Wales.

Wintle A.G. and D.J. Huntley, 1979, Thermoluminescence dating of a deep-sea sediment core : Nature v. 279, p. 710-712.

Wintle A.G. and D.J. Huntley, 1980, Thermoluminescence dating of ocean sediments : Canadian Journal of Earth Sciences v. 17, p. 348-360.

Wintle A.G. and D.J. Huntley, 1982, Thermoluminescence dating of sediments : in D.Q. Bowen ed., Quaternary Science Review v. 1, p. 31-53, Pergamon Press.

Wintle A.G. and H. Proszynska, 1983, TL dating of loess in Germany and Poland : PACT v. 9, p. 547-554.

Wintle A.G., 1981, Thermoluminescence dating of late Devensian loesses in southern England : Nature v. 289, p. 479-480.

Wintle A.G., 1985, Stability of TL signal in fine grains from loess : Nuclear Tracks v. 10 nos. 4-6, p. 725-730.

Wintle A.G., 1987, Experimental Tasks : SERC Short Course : on the applications of TL dating.

Zimmerman D.W., 1971, Thermoluminescent dating using fine grains from pottery : Archaeometry v. 13 no. 1, p. 29-52.

Zolitschka B., 1988, Spatquartare sedimentatiangeschichte des Meerfelder Maares (Westeifel) - Mikrostratigraphie jahreszeitlich geschichteter seesedimente : Eiszeitalter u gegenwart v. 38 p. 87-93.

Zolitschka B., 1989, Jahreszeit geschichtete seesedimente aus dem Holzmaar und dem Meerfelder maar : Z. dt. geol. Ges v. 140, p. 25-33.

Zoller L. and E. Pernicka, 1989, A note on overcounting in alpha-counters and its climination : Ancient TL v. 7 no. 1. p. 11-14.

ADDITIONAL REFERENCES

Bard E., B.Hamelin, R B.Fairbanks and A.Zindler, 1990, Calibration of the ^{14}C timescale over the past 30,000 years using mass spectrometric U-Th ages from Barbados corals. Nature v. 345, p.405-410.

Calvert S E., R E.Karlin, L J.Toolin, D J.Donahue, J R.Southons and J S.Vogel, 1991, Low organic carbon accumulation rates in Black Sea sediments. Nature v. 350, p.692-695.

Negendank J F W., A.Brauer and B.Zolitschka, 1990, Die Eifelmaare als erdgesschichtliche Fallen und Quellen zur Rekonstruktion des Palaeoenvironments. Mainzer geowiss. Mitt v.19, p.235-262, Mainz.